Annu. Rev. Earth Planet. Sci. 2000. 28:211–80

GEOLOGIC EVOLUTION OF THE HIMALAYAN-TIBETAN OROGEN

An Yin and T. Mark Harrison
Department of Earth and Space Sciences and Institute of Geophysics and Planetary Physics, University of California, Los Angeles, California 90095–1567; e-mail: yin@ess.ucla.edu, tmh@argon.ess.ucla.edu

Key Words orogenic development, continental collision, Himalaya, Tibetan plateau

■ **Abstract** A review of the geologic history of the Himalayan-Tibetan orogen suggests that at least 1400 km of north-south shortening has been absorbed by the orogen since the onset of the Indo-Asian collision at about 70 Ma. Significant crustal shortening, which leads to eventual construction of the Cenozoic Tibetan plateau, began more or less synchronously in the Eocene (50–40 Ma) in the Tethyan Himalaya in the south, and in the Kunlun Shan and the Qilian Shan some 1000–1400 km in the north. The Paleozoic and Mesozoic tectonic histories in the Himalayan-Tibetan orogen exerted a strong control over the Cenozoic strain history and strain distribution. The presence of widespread Triassic flysch complex in the Songpan-Ganzi-Hoh Xil and the Qiangtang terranes can be spatially correlated with Cenozoic volcanism and thrusting in central Tibet. The marked difference in seismic properties of the crust and the upper mantle between southern and central Tibet is a manifestation of both Mesozoic and Cenozoic tectonics. The former, however, has played a decisive role in localizing Tertiary contractional deformation, which in turn leads to the release of free water into the upper mantle and the lower crust of central Tibet, causing partial melting in the mantle lithosphere and the crust.

INTRODUCTION

Mountain belts created by continent-continent collision are perhaps the most dominant geologic features of the surface of the Earth (Dewey & Burke 1973). The Appalachian belt in North America, the Ural mountains in central Eurasia, and the Qinling-Dabie-Shandong belt in east-central Asia are some of the best examples, each extending for thousands of kilometers along strike. A great deal of attention has been paid to the genesis of these orogenic systems since the development of plate tectonics some 35 years ago, largely owing to the fact that continent-continent collision is the dominant and most efficient process in forming the supercontinents, which profoundly affect the geologic and biologic evolution

of the Earth. The youngest and arguably most spectacular of all the continent-continent collisional belts on Earth is the Himalayan-Tibetan orogen, occupying the east-west trending, high-altitude Himalaya and Karakorum ranges in the south and the vast Tibetan plateau to the north (Figure 1; Figure 2, color insert). This orogenic system was largely created by the Indo-Asian collision over the past 70–50 Ma, and is part of the greater Himalayan-Alpine system that extends from the Mediterranean Sea in the west to the Sumatra arc of Indonesia in the east over a distance of more than 7000 km. This extraordinarily long and complexly amalgamated belt was developed by the closure of the Tethys oceans between two great land masses since the Paleozoic: Laurasia in the north and Gondwana in the south (Hsu et al 1995, Sengor & Natal'in 1996).

The Himalayan-Tibetan orogen and its neighboring regions in east Asia are ideal places for the study of continent-continent collision for several reasons. First, the orogen is active so that many geologic relationships can be demonstrated directly using the methods of neotectonic studies (Armijo et al 1989, Holt et al 1995, Lacassin et al 1998, Van der Woerd et al 1998, Bilham et al 1997, Larson et al 1999, Shen et al 1999). Second, the plate-boundary history is well known, so the cause of intracontinental deformation can be quantitatively defined as a time-dependent, boundary-value problem (Peltzer & Tapponnier 1988, Houseman & England 1996, Royden 1996, Royden et al 1997, Kong & Bird 1996, Peltzer & Saucier 1996, Kong et al 1997). Third, collision processes have produced a variety of geologic features such as large-scale thrust, strike-slip and normal fault systems (Tapponnier et al 1986, Burg & Chen 1984, Burchfiel et al 1992, Yin et al 1994), leucogranite magmatism (Harrison et al 1998b), widespread volcanism (Deng 1989, Arnaud et al 1992, Turner et al 1993, Chung et al 1998, Deng 1998), regional metamorphism (Le Fort 1996, Searle 1996), and formation of intracontinental and continental-margin oceanic basins (Song & Wang 1993, Brias et al 1993, Li et al 1996). All of the preceding geologic features and processes may be useful as proxy indicators in establishing the deep earth conditions involved in the dynamics of continent-continent collision.

Because of its immense size and high elevation, the geologic evolution of the Himalayan-Tibetan orogen is also thought to have played a critical role in controlling global climate change (Ruddiman & Kutzbach 1989, Molnar et al 1993, Quade et al 1995, Harrison et al 1998a, cf. Ramstein et al 1997). The climate change, in turn, may have affected erosion rate, and thus altered the dynamics of the Himalayan-Tibetan orogenic system (Beaumont et al 1992) and its growth pattern (Avouac & Burov 1996). It is this large-scale interaction between lithospheric deformation and atmospheric circulation that potentially makes studies of the Himalayan-Tibetan orogen of greater significance than simply matters of intracontinental deformation induced by continental collision.

In the last three decades, many geologic and geophysical investigations have been conducted in the Himalayan-Tibetan orogen, and have resulted in numerous syntheses dealing with both active tectonics and the overall geologic evolution of the system (Chang & Zheng 1973; Dewey & Burke 1973; Allègre et al 1984;

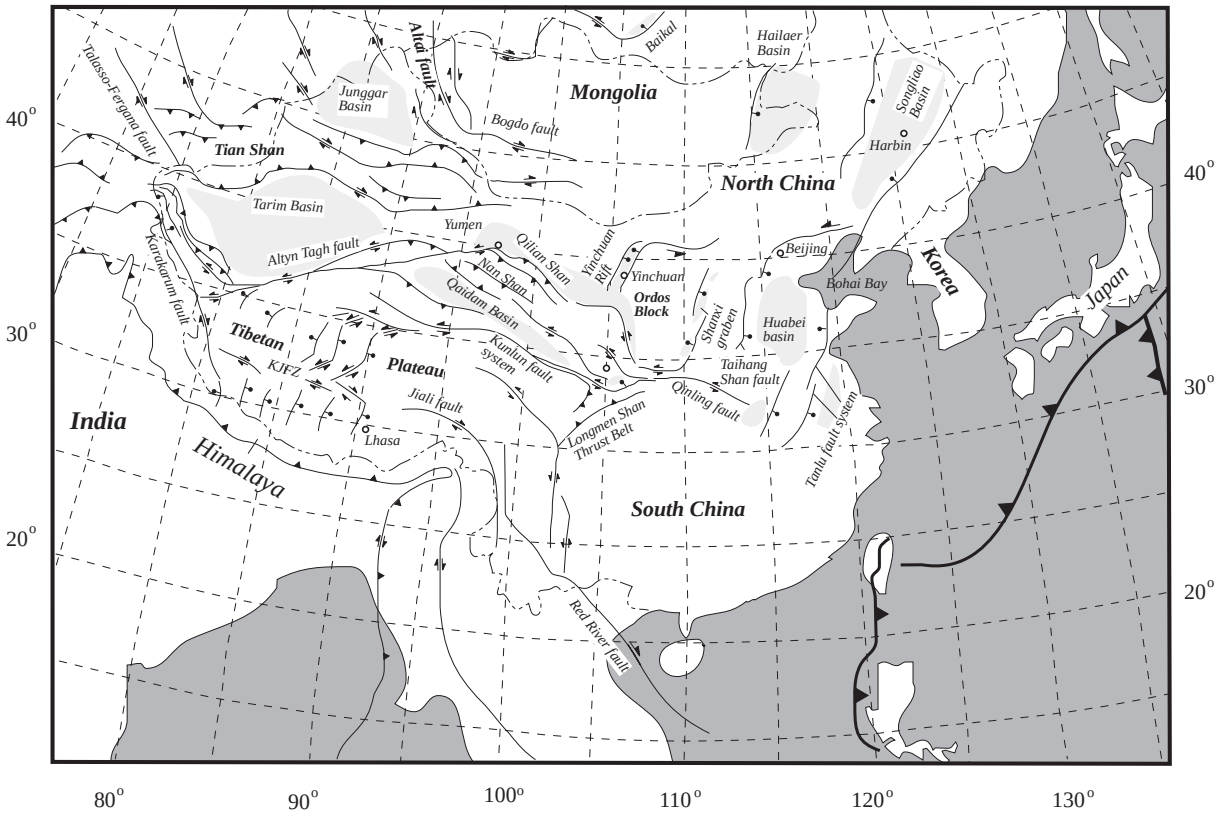

Figure 1 Cenozoic tectonic map of the Indo-Asian collision zone and major active fault systems in Asia.

Molnar 1984; Tapponnier et al 1986; Dewey et al 1988, 1989; Burchfiel & Royden 1991; Harrison et al 1992, 1998a; Molnar et al 1993; Zhao et al 1993; Avouac & Tapponnier 1993; Hsu et al 1995; Nelson et al 1996; Owens & Zandt 1997; England & Molnar 1998; Larson et al 1999; Xu et al 1998). The goal of this article is to provide a coherent picture of how the Cenozoic Himalayan-Tibetan orogen has evolved. To achieve this, we must have a general understanding of the configuration of the amalgamated Eurasian continent immediately prior to the Indo-Asian collision; this information can be used as both a strain marker and an initial condition to determine where, when, and how the intracontinental deformation proceeded in Asia during the Cenozoic. Therefore, this review focuses first on the pre-Cenozoic geologic framework of the Himalayan-Tibetan orogen, and then provides a systematic synthesis of the history of major Cenozoic structures and the occurrence of associated metamorphic, igneous, and sedimentary rock units. The latter forms the observational basis for the interpreted spatial and temporal evolution of the orogen.

PALEOZOIC AND MESOZOIC TECTONICS

The Himalayan-Tibetan orogen was built upon a complex tectonic collage that was created by sequential accretion, from north to south, of several microcontinents, flysch complexes, and island arcs onto the southern margin of Eurasia since the early Paleozoic (Chang & Zheng 1973, Allègre et al 1984, Sengor & Natal'in 1996, Yin & Nie 1996). Because of this complex early history, it is effectively impossible to decipher the Cenozoic tectonic history of the Himalayan-Tibetan orogen without first knowing the crustal composition, pre-Cenozoic structural configuration, and sequence of geologic events associated with the formation of each of these individual tectonic units. In the following section, we comment briefly on the pre-Cenozoic geology of major terranes in the orogen (Figures 2 and 3, color insert) and summarize the overall tectonic evolution of the Himalayan-Tibetan region prior to the Indo-Asian collision (Figure 4).

Himalaya

The Himalaya lie between the Indian shield to the south and the Indus-Yalu suture to the north (Figure 2). They consist of three tectonic slices bounded by three north-dipping Late Cenozoic fault systems: the Main Boundary Thrust, the Main Central Thrust, and the South Tibetan Detachment System (Figures 2 and 3).

The Lesser Himalaya is structurally the lowest slice. It is bounded at the base by the Main Boundary Thrust and at the top by the Main Central Thrust, and consists mainly of Precambrian clastic sediments and metasedimentary rocks (Brookfield 1993). The Greater (or High) Himalaya is bounded by the Main Central Thrust below and the South Tibetan Detachment fault above (Burg &

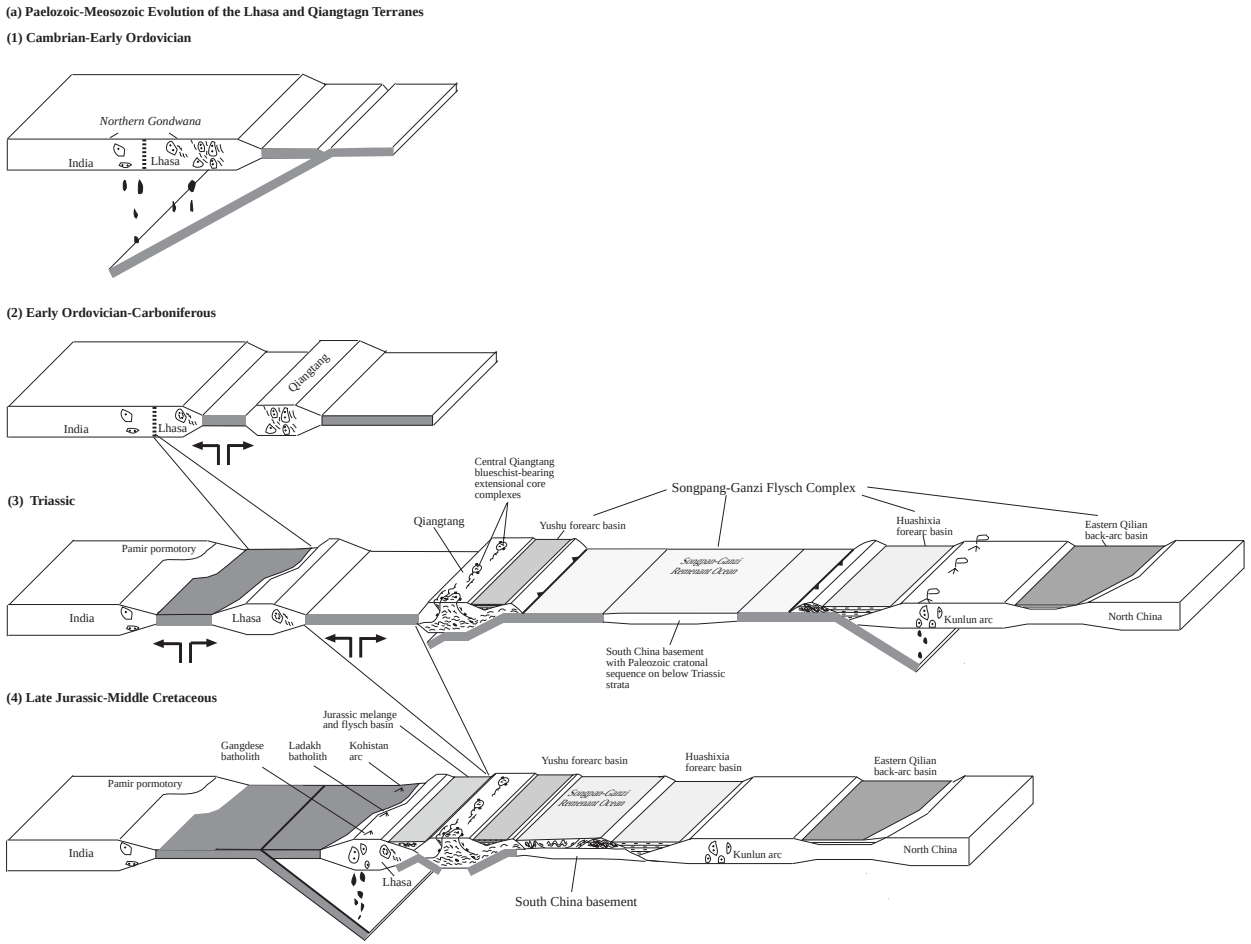

Figure 4 Paleozoic-Mesozoic tectonic evolution of the Himalayan-Tibetan orogen.

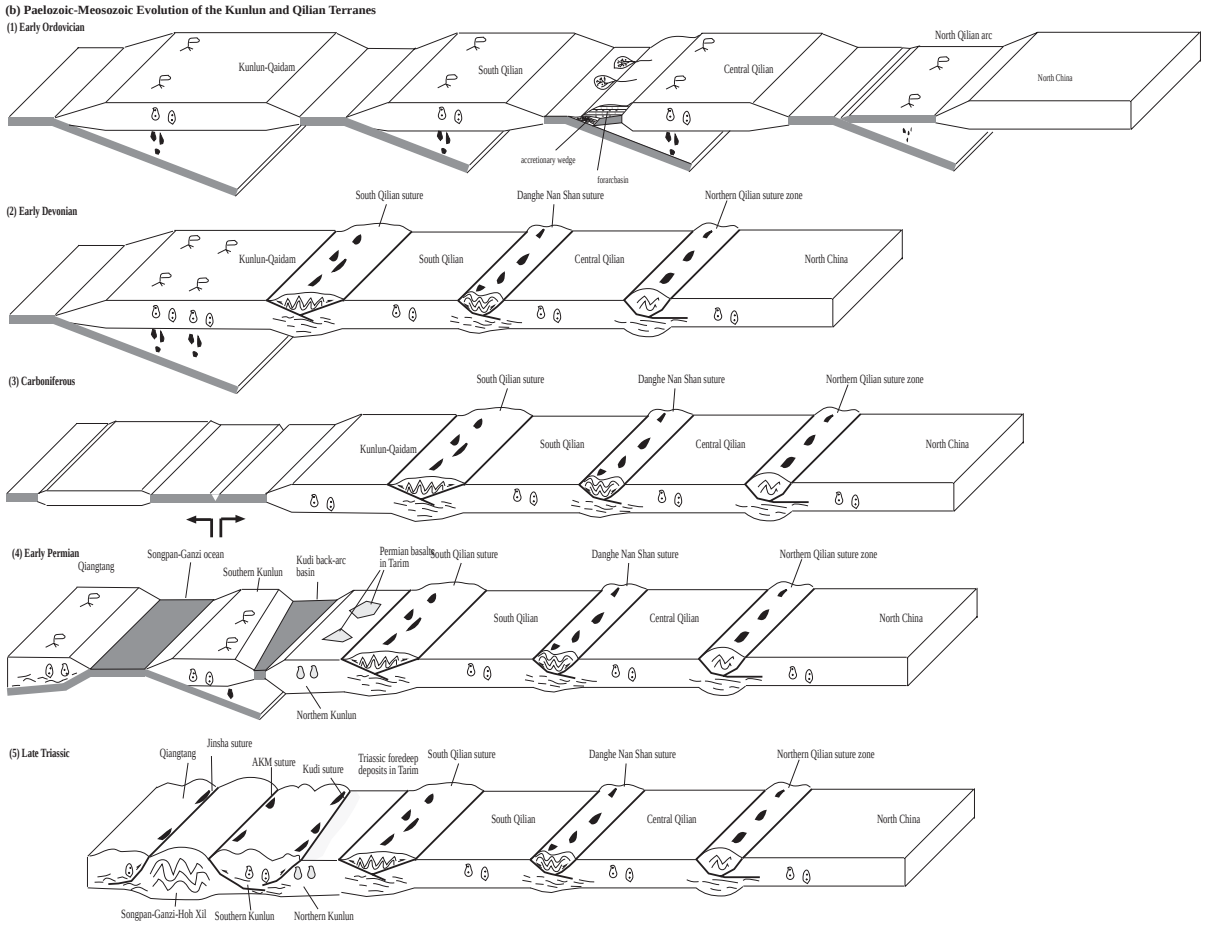

Figure 4 Paleozoic-Mesozoic tectonic evolution of the Himalayan-Tibetan orogen.

Chen 1984, Burchfiel et al 1992, Le Fort 1996) and comprises late Proterozoic to early Cambrian metasedimentary rocks (Parrish & Hodges 1996). The North Himalaya lies between the South Tibetan Detachment fault (Burchfiel et al 1992) and the Great Counter Thrust (Yin et al 1999a). It consists of late Precambrian to early Paleozoic sedimentary and metasedimentary rocks (Yin et al 1988, Burchfiel et al 1992) and thick Permian to Cretaceous continental margin sequences (Brookfield 1993). All three tectonic slices are considered to be parts of the north-facing Himalayan passive continental margin, commonly known as the Tethyan Himalaya, which developed from middle Proterozoic to Cretaceous times (Colchen et al 1982, Brookfield 1993). It appears that Late Cenozoic thrusting in the Himalaya did not involve the Archean/Early Proterozoic gneissic basement that is equivalent to the Indian Shield (Parrish & Hodges 1996).

The Himalayan passive continental margin was intruded by Cambrian to early Ordovician granites (Le Fort et al 1983), which may have been associated with either supercontinent breakup (Murphy & Nance 1991, Hughes & Jell 1999) or final assemblage of Gondwana (Gaetani & Garzanti 1991, Meert & Van der Voo 1997). Between the Ordovician and Permian, all three tectonic slices in the Himalaya formed part of a stable continental platform (Brookfield 1993). In the Permian, rifting accompanied by the eruption of Panjal basalts began to develop in the northern Himalaya. This phase lasted until the end of the Jurassic and was associated with separation of a microcontinent from the northern margin of India (Gaetani & Garzanti 1991). This rifted block has been interpreted as the future Lhasa terrane of southern Tibet (Dewey et al 1988, Le Fort 1996), an inference consistent with widespread occurrence of Gondwanan fauna in the Carboniferous and Permian strata of the Lhasa terrane (Yu & Zheng 1979, Yin 1997). The Mesozoic passive continental margin sequence of the Himalaya was developed continuously until the latest Cretaceous when the collision between India and Asia began affecting its sedimentary facies patterns and its rate of subsidence (Shi et al 1996, Willems et al 1996).

Lhasa Terrane

The Lhasa terrane is bounded by the Indus-Yalu and the Bangong-Nujiang sutures (Chang & Zheng 1973, Allègre et al 1984, Dewey et al 1988, Pierce & Deng 1988; Figure 2). It collided with Qiangtang to the north in the late Jurassic (Dewey et al 1988) near Amdo (Long. 91°E); in the middle Cretaceous near Shiquanhe (Long. 80°E) (Matte et al 1996); and in the northern Karakorum region along the Karakorum Highway (Long. 75°E) (Gaetani et al 1993). Continuing north-south contraction related to the collision lasted until the early Late Cretaceous within the Lhasa terrane, resulting in at least 180 km of internal north-south shortening (Murphy et al 1997).

In Tibet, the Lhasa terrane is about 300-km wide at the longitude of 91°E near Lhasa, and narrows westward to less than 100 km at the longitude of 80°E near Shiquanhe (Figure 2). The Lhasa terrane extends westward across the active right-

slip Karakorum fault and becomes the Ladakh-Kohistan arc terrane in northwestern India and northern Pakistan (Pan 1990, Searle 1996; Figure 2). The Kohistan arc, different from Ladakh and Gangdese batholiths, was built upon oceanic crust (Khan et al 1993, Sullivan et al 1993). Corresponding to the change of name, the Bangong-Nujiang suture becomes the Shyok suture, or the Main Karakorum Thrust (MKT), in the Karakorum region (Figure 2). To the east, the Lhasa terrane makes a 90° turn around the eastern Himalayan syntaxis and becomes a north-south trending belt (Li et al 1982, Zhong 1998).

Ultramafic rocks are distributed widely in the western and eastern Lhasa terrane south of the Bangong-Nujiang suture zone (Liu 1988). They have been interpreted either as representing tectonic slices carried by low-angle thrusts some 100 km or more from their root zone to the north (Girardeau et al 1984, Coward et al 1988), or as indicating more suture zones within the traditionally defined Lhasa terrane (Hsu et al 1995, Matte et al 1996).

Sedimentary strata in the Lhasa terrane consist of a sequence of Ordovician and Carboniferous to Triassic shallow marine clastic sediments (Yu & Zheng 1979, Wang et al 1983, Yin et al 1988). Basement is believed to be mid-Proterozoic to early Cambrian in age, as represented by the Amdo gneiss along the Golmud-Lhasa road in the northern Lhasa terrane (Figure 2; Xu et al 1985, Harris et al 1988, Dewey et al 1988).

The Upper Carboniferous to Lower Permian strata are characterized by volcaniclastic sediments, which are interpreted to have resulted from back-arc extension (Pierce & Mei 1988, Leeder et al 1988). The Upper Permian sequence is characterized by shallow marine strata of dominantly carbonate rocks (Wang et al 1983). These rocks are mostly restricted to the northern part of the Lhasa terrane and were deposited after rifting related to the inferred back-arc extension. Upper Triassic strata, which are mostly restricted in the southeastern Lhasa terrane, consist of volcaniclastic sediments with abundant basalts. This volcanic sequence is interpreted as being a consequence of rifting (Pierce & Mei 1988), possibly related to its separation from India.

The Jurassic strata, which are mainly exposed in the northern part of the Lhasa terrane, consists mostly of turbidites interlayered with volcanic flows and tuffs (Yu & Zhang 1979). They are generally folded with locally well-developed slaty cleavage. Early to Middle Cretaceous limestone and marine deposits are widespread in the Lhasa terrane (Yin et al 1988). But by the end of the Cretaceous, marine sediments are mostly localized immediately south of the Bangong-Nujiang suture at the end of the Cretaceous (Liu 1988). This localization has been attributed to the development of a foreland basin during continuing convergence along the suture between the Qiangtang and Lhasa terranes in the Late Cretaceous, after they had collided in the Late Jurassic and Early Cretaceous (Yin et al 1994; Murphy et al 1997, 1999). Along its southern margin, the Paleozoic and Mesozoic sequences of the Lhasa terrane are intruded by the dominantly Cretaceous to Tertiary Gangdese batholith belt. In the northeastern Lhasa terrane, Late Jurassic plutons are also common (Xu et al 1985). The Cretaceous-Tertiary Gangdese

batholith has been related to north-dipping subduction of a plate carrying India (Chang & Zheng 1973, Allègre et al 1984), while the Jurassic granitoids in northern Lhasa may have been related to southward subduction of the oceanic material between the Lhasa and Qiangtang terranes (Coulon et al 1986) (Figure 4). South of the Gangdese batholith is the Cretaceous to early Tertiary Xigaze forearc basin, one of the best-exposed forearc sequences in the world (Durr 1996). This basin was underthrust along the north-dipping Oligo-Miocene Gangdese thrust at the southwestern and southeastern margins of the Lhasa terrane (Yin et al 1994, 1999a). The southern boundary of the Xigaze forearc basin is the Indus-Yalu suture, which is strongly modified by the development of a major south-dipping late Tertiary thrust system, the Great Counter Thrust (Heim & Gansser 1939, Yin et al 1999a).

One of the most striking geologic relationships in the Lhasa terrane, particularly well-exposed in its southern part, is that the Late Paleocene-Early Eocene (~65–40 Ma) volcanic sequence (Allègre et al 1984, Coulon et al 1986, Leeder et al 1988) is essentially flat-lying (Yu & Cheng 1979, Wang et al 1983, Liu 1988), implying that the Lhasa terrane has experienced no significant Cenozoic north-south shortening in the upper crust. This relationship has been independently documented by Coulon et al (1986), Xizang BGMR (1992), Pan (1993), and Murphy et al (1997).

Based on lithologic characteristics and their distribution, the following interpretation is made for the evolution of the Lhasa terrane (Figure 4). During the latest Proterozoic and the earliest Paleozoic, subduction dipping beneath both India and Lhasa generated Cambrian–early Ordovician granites in the Himalaya and in the northern Lhasa terrane. The granites and their country rocks experienced intense north-south shortening expressed in isoclinal folding and development of widespread foliation in the Amdo gneiss complex (Coward et al 1988, Dewey et al 1988) (Figure 4). This deformational event could have been a result of an amalgamation between India and Lhasa in the early Paleozoic. In the Late Carboniferous and Early Permian (Figure 4), rifting occurred along the northern margin of the Lhasa terrane, which may have caused separation of a northern portion and the opening of an ocean basin (Figure 4). It is possible that the rifted northern part of the early Paleozoic Lhasa terrane is the present Qiangtang terrane (Yin 1997). The southern margin of the Lhasa terrane experienced a rifting event in the Late Triassic, which may mark the initial separation of Lhasa from India and the opening of the Neotethys separating those two continental masses (Gaetani & Garzanti 1991). Subduction of the Indian oceanic lithosphere began during the Middle Cretaceous, leading to creation of the Xigaze forearc basin (Durr 1996) and Gangdese batholith (Allègre et al 1984, Harrison et al 1992) (Figure 4).

Qiangtang Terrane

Qiangtang lies between the Jinsha suture to the north and the Bangong-Nujiang suture to the south (Chang & Zheng 1973, Allègre et al 1984, Pierce & Deng 1988, Dewey et al 1988). It is about 500–600 km wide in central Tibet, but

narrows to <150 km both to the west and the east in the western Kunlun and eastern Tibet (Figure 2). The Qiangtang terrane may extend to the Karakorum region, where it correlates with the Karakorum terrane (Pan 1990, Searle 1991) and which is bounded by a latest Triassic–Early Jurassic melange to the north (Gaetani et al 1993) and the Shyok suture/Main Karakorum Thrust to the south. To the east, the Qiangtang terrane is characterized by the north-facing Triassic Jiangda arc, which is the eastern extension of the Hoh Xil Shan arc along the northern margin of the Qiangtang terrane in central Tibet (Burchfiel et al 1995). The western continuation of this arc may be the Karakorum batholith belt along the northern edge of the Karakorum terrane (Searle 1991). Instead of being Triassic and early Jurassic in age, the age of the Karakorum batholith ranges from the Middle Jurassic to Middle Cretaceous (Searle 1991), which implies that the closure of the Jinsha suture along the northern edge of the Qiangtang-Karakorum terrane may have been diachronous, younging westward.

Investigations conducted during Sino-French and Sino-British expeditions in the 1980s focused mostly on the geology along the Golmud-Lhasa road. Results of these studies did not provide a comprehensive understanding of overall Qiangtang geology because the segment of the Qiangtang terrane along the Golmud-Lhasa road exposes almost exclusively Jurassic strata. It was not clear what the age and nature of basement rocks beneath the Qiangtang are, and how this tectonic unit evolved during the Paleozoic and early Mesozoic. This gap of knowledge has been greatly reduced in the past decade, largely due to a systematic field mapping project conducted by Chinese geologists (Xizang BGMR 1992) and several geologic expeditions in recent years (Kapp et al 1997, 1998; Yin et al 1998a, 1999b; Manning et al 1998; Blisniuk et al 1998).

The first-order geologic framework of Qiangtang is characterized by dominantly metamorphic rocks and Late Paleozoic (Carboniferous and Permian) shallow marine strata in the west, and Triassic-Jurassic shallow marine carbonate rocks interbedded with terrestrial clastic and volcaniclastic strata in the east (Figure 2; Liu 1988). This map pattern results from the presence of the east-plunging Qiangtang anticlinorium, which is at least 600-km long and about 300-km wide (Yin et al 1998a). The anticlinorium is defined by metamorphic rocks and Upper Paleozoic strata in its core and Jurassic to Upper Cretaceous strata on its northern and southern limbs (Kapp et al 1997, 1999a; Yin et al 1998a; Manning et al 1998). The Carboniferous strata consist of shallow marine sequences of quartzite and carbonate rocks, which are interlayered with basalts and mafic sills. The Permian strata are dominated by carbonate deposits, while Triassic and Jurassic strata consist of fluvial sedimentary sequences, volcanic flows, and shallow marine carbonate rocks (Cheng & Xu 1986, Li & Zheng 1993, Li et al 1995, Kapp et al 1999a).

Qiangtang Metamorphic Rocks After the initial discovery of blueschist-bearing metamorphic rocks in the central Qiangtang reported by Hennig (1915), subsequent geologic mapping and petrologic studies by Chinese geologists con-

firmed their existence and extended the occurrence of high-pressure metamorphic rocks for more than 100 km both to the east and west from Hennig's original site (Cheng & Xu 1986, Li et al 1995). Cheng & Xu (1986) interpreted the Qiangtang metamorphic rocks to represent the basement below the Carboniferous strata. Li (1987), Li & Zheng (1993), and Li et al (1995) suggested that the Qiangtang metamorphic rocks represented a suture zone, because the metamorphic rocks consist of highly deformed flysch deposits, mafic and ultramafic igneous bodies, and blueschist-bearing metamorphic rocks. Li et al (1995) further suggested that the suturing of the north and the south Qiangtang occurred during the Triassic, which marks the boundary between Gondwanaland to the south and Laurasia to the north. Hsu et al (1995) interpret the Qiangtang metamorphic rocks as part of an accretionary complex that developed along the southern edge of the Paleozoic Kunlun magmatic arc and was later rifted away to become the independent Qiangtang terrane.

In contrast to the preceding suggestions, abundant mafic volcanic rocks within the metamorphic belt have also been regarded as products of rifting, as indicated by their geochemical characteristics (Zhang et al 1985, Wang et al 1987, Deng et al 1996a). Yin (1997) and Deng (1998) suggested that the inferred rift may have been linked with a paleo-Tethyan ocean to the east, which separated the Kunlun to the north from the Qiangtang to the south either in the Permian or between the Triassic and the Early Jurassic.

Questions regarding the tectonic significance of the Qiangtang metamorphic belt and its potential for exposing the deeper crust of northern Tibet have motivated several detailed geologic investigations in recent years (Kapp et al 1997, 1999a,b; Yin et al 1998a; Manning et al 1998). The most important conclusions of these studies are (*a*) The Qiangtang metamorphic rocks are low- to high-grade metamorphosed melange complexes. This inference is consistent with earlier observations made by Li et al (1995). (*b*) The contacts between the melange complexes below, and the Upper Paleozoic to Upper Triassic sedimentary and volcanic strata above, are not depositional (cf. Cheng & Xu 1986, Li et al 1995), but are low-angle normal faults (i.e. detachment faults), the hanging walls of which moved to the east. (*c*) The melange complexes must have occupied most of the Qiangtang lower crust, because they experienced peak metamorphic conditions at temperatures of 350–550°C and pressures of 8–17 kbars before they were brought up by the low-angle detachment faults. The last conclusion (i.e. that the lower crust of the Qiangtang consists of extensively distributed melange complexes) is consistent with the recent discovery of dominantly lower crustal metasedimentary rocks in the xenoliths of Cenozoic volcanic rocks from the Qiangtang (Deng et al 1996b, Deng 1998).

The contacts between the Qiangtang metamorphic rocks and the overlying Paleozoic-Mesozoic rocks are best documented in the Shuang Hu and Gangma Co areas (Figure 2), where the faults are east-directed and the age of their movement is constrained as being between the Late Triassic and earliest Jurassic (Yin et al 1998a, Kapp et al 1999b). Late Triassic-Early Jurassic cooling ages in the

footwalls of the Falong and Gangma Co detachment faults in the central Qiangtang are related to east-west extension during or immediately after the subduction from the north of the Songpan-Ganzi flysch complex along the Jinsha suture zone (Figure 4; Kapp et al 1999a). This inferred tectonic process for the emplacement of the metamorphic melange complexes in the central Qiangtang is similar to that inferred for the Orocopia-Rand schists in California during the late Cretaceous to early Tertiary eastward subduction of the Farallon plate beneath western North America (Jacobson et al 1996).

The Qiangtang melange is constrained to be at least as young as Late Triassic, because it contains blocks of Carboniferous-Permian strata and Upper Triassic radiolarian fossils (Deng 1996). The absence of Jurassic rocks in the melange strongly suggests that the Late Triassic marks the end of development of the Qiangtang melange. This age coincides with southward subduction of the Songpan-Ganzi flysch complex beneath the Qiangtang along the Jinsha suture zone (Dewey et al 1988, Yin & Nie 1996).

Panafrican age zircons from footwall gneisses of the Gangma Co detachment fault (Kapp et al 1999b) are similar to those in footwall granitoids of the Nyainqentanghlha detachment (D'Andrea et al 1999) and Amdo gneiss (Xu et al 1985) in the Lhasa terrane. Thus the Qiangtang terrane may have been part of eastern Gondwana, which was once connected with the Lhasa terrane and India (Kapp et al 1999b). It could have rifted away from the Lhasa terrane between the Late Carboniferous and the Permian, during which time rift-related basalts and shallow marine strata were deposited in the Qiangtang (Yin et al 1988, Pierce & Mei 1988; Figure 4). The widespread Late Triassic to Early Jurassic volcanic deposits of the Qiangtang may have resulted from southward subduction of the Songpan-Ganzi ocean basin (Kapp et al 1999b; Figure 4).

Relationship Between Thrusting And Early Mesozoic Detachment Faulting The Falong detachment fault in the Shuang Hu region truncates an imbricate thrust system in its hanging wall that repeats a Late Triassic dolostone unit (Figure 4). As detachment faulting occurred in the Early Jurassic (Kapp et al 1999b), there must have been a significant crustal thickening event between the Late Triassic and the Early Jurassic in the central Qiangtang, coeval with the southward subduction of a huge flysch complex in the Songpan-Ganzi-Hoh Xil terrane. Because no Cenozoic thrusts cut the Early Jurassic detachment fault in the Shuang Hu area, it appears that Late Triassic contraction is the only crustal thickening event in the central and eastern Qiangtang regions.

Geologic mapping in the Gangma Co area shows a different cross-cutting relationship. There, the detachment fault is cut by thrusts that involve lower Tertiary strata (Figure 4; Yin et al 1999b). It is the difference in the cross-cutting relationships between thrusting and detachment faulting that has resulted in the current regional map pattern for the exposure of the Qiangtang melange. In the Shuang Hu region of Qiangtang, the metamorphic melange is exposed in a semicircular outcrop beneath the detachment fault. The Shuang Hu core complex and

other adjacent exposures of metamorphic melanges do not define the regional anticlinorium (Figure 2). In contrast, the metamorphic melange in the Gangma Co area to the west is exposed in relatively long strips, a map pattern controlled by the presence of several Cenozoic thrusts. In the Gangma Co area and its adjacent regions to the north and south, the distribution of the Qiangtang melange also defines the structurally deepest part of the Qiangtang anticlinorium. The involvement of Cenozoic thrusts suggests that the Qiangtang anticlinorium developed during the Cenozoic. The involvement of Cretaceous and Tertiary strata at a regional scale defining the anticlinorium supports this interpretation (Liu 1988). Therefore, it is possible that the current distribution of blueschist-bearing metamorphic melange in Qiangtang resulted from the superposition of the following two structural developments: (*a*) Scattered exposures of core complexes were developed in the Late Triassic-Early Jurassic, during or immediately after the underplating of the Songpan-Ganzi flysch complex beneath the Qiangtang terrane (Figure 4), and (*b*) the isolated exposures of the Mesozoic metamorphic core complexes were modified by the development of Cenozoic thrusting and regional folding in the western Qiangtang, which resulted in the formation of the western Qiangtang anticlinorium (Figures 2 and 3). As discussed later, the Qiangtang anticlinorium may be a hanging wall anticline above a large north-dipping Tertiary thrust system along the reactivated Bangong-Nujiang suture zone (Yin et al 1998b).

Songpan-Ganzi-Hoh Xil Terrane

Tectonic Setting The Songpan-Ganzi-Hoh Xil terrane is a triangular tectonic element between the East Kunlun-Qaidam terrane in the north and the Qiangtang terrane in the south. It occupies a large part of the central Tibetan plateau (Figure 2), and its western extension is a long but narrow belt, offset by the left-slip Altyn Tagh fault (Pan 1990, 1996). In Tibet, east of the Altyn Tagh fault, the terrane is bounded by the Jinsha suture to the south and the Anyimaqen-Kunlun-Muztagh suture to the north (Li et al 1982, Molnar et al 1987, Burchfiel et al 1989a, Dewey et al 1988, Deng 1996). In the western Kunlun, it is bounded by the Marza suture to the north and the Karakorum fault to the south (Pan 1996, Deng 1996, cf. Matte et al 1996). In the Pamir, southwest of the northwest-striking Karakorum fault, the northern part of the Southern Pamir terrane between the melange complex in the northern Karakorum in the south (Gaetani et al 1993) and the Rushan-Pshart suture in the north (Burtman & Molnar 1993) may be equivalent to the Tianshuihai terrane of the western Kunlun and the Songpan-Ganzi-Hoh Xil terrane of Tibet (Figure 2).

The closure age of the Rushan-Pshar suture in the Pamir and the western Kunlun Shan and its eastern extension, the Anyimaqen-Kunlun-Muztagh suture, in Tibet, appears too young from east to west. In the Pamir, the closure time of the Rushan-Pshar suture is probably in the mid-Cretaceous (Burtman & Molnar 1993), whereas in the western Kunlun, the closure of the Marza suture occurred in the latest Jurassic (Pan 1990). Farther to the east, in the eastern Kunlun, the

closure of the Anyimaqen-Kunlun-Muztagh suture was completed in the early Jurassic (Dewey et al 1988).

The eastern boundary of the Songpan-Ganzi-Hoh Xil terrane lies along the eastern edge of a southeast-directed, latest Triassic-Early Jurassic thrust belt along the western edge of South China (Figure 2; Burchfiel et al 1995). Triassic strata conformably overlie Paleozoic shallow marine sequences of South China (Burchfiel et al 1995) in that area, suggesting that basement is continental, at least in the very eastern part of the terrane.

The Triassic Yidu arc is bounded by the Litang suture to the north and the Jinsha suture to the south. The Litang suture merges with the Jinsha suture to the west, but appears to terminate within the South China block (Figure 2). This arc forms the southeastern boundary of the Songpan-Ganzi-Hoh Xil terrane and could have been built either on the continental basement of South China (Burchfiel et al 1995) or on an oceanic crust above a west-dipping subduction zone, which later collided with South China (Sengor 1984).

Songpan-Ganzi-Flysch Complex The Songpan-Ganzi-Hoh Xil terrane and its western extension in the western Kunlun Shan are characterized by a thick sequence of Triassic strata of deep marine deposits (Rao et al 1987, Qinghai BGMR 1991, Hou et al 1991, Gu 1994, Nie et al 1994). These Triassic strata, which are mostly of late Triassic age and at least several kilometers thick, are commonly referred to as the Songpan-Ganzi flysch complex. Internally, the Songpan-Ganzi flysch complex was intensely deformed by folding and thrusting during the Late Triassic and Early Jurassic (Chen et al 1994, Burchfiel et al 1995, Worley & Wilson 1996, Worley et al 1997). This deformational event was contemporaneous with collision and subsequent continuing convergence between North and South China (Burchfiel et al 1995, Yin & Nie 1996). The Triassic flysch complex is in fact distributed in a much wider area than the narrowly defined Songpan-Ganzi-Hoh Xil terrane. The former extends north of the Anyimaqen-Kunlun-Muztagh suture on both sides of the Kunlun arc (e.g. Sengor & Natal'in 1996), where the Triassic flysch rests depositionally on top of Paleozoic shallow marine sequences belonging to the passive continental margin of North China (Zhou & Graham 1996). South of the melange zone along the Jinsha suture, the Triassic marine strata are interbedded with volcaniclastic rocks as deposits of a forearc basin. The map relationships between the Triassic flysch deposits and elements in the Triassic convergent boundaries (i.e. Anyimaqen-Kunlun-Muztagh and Jinsha sutures and the Kunlun arc) in central Tibet indicate that the Songpan-Ganzi flysch sediments may have been deposited in several separate tectonic basins (Figure 4). From north to south, they are (*a*) a back arc basin north of the Kunlun arc, which has the North China block as the basement, upon which Triassic flysch was deposited; (*b*) a forearc basin between the Kunlun arc in the north and the Anyimaqen-Kunlun-Muztagh suture (represented by the Huashixia melange zone; see Figures 2 and 4) in the south; (*c*) a remnant basin between the Jinsha and Anyimaqen-Kunlun-Muztagh sutures that consists of the

majority of the Triassic flysch deposits and has depositional contact with the basement of South China; and (*d*) a forearc basin south of the Anyimaqen-Kunlun-Muztagh suture. The preceding tectonic division explains why the Triassic Songpan-Ganzi flysch complex was deposited on top of the basement of both North China (Zhou & Graham 1996) and South China (Burchfiel et al 1995).

The source of the apparently thick Songpan-Ganzi flysch complex in the eastern part of the Songpan-Ganzi-Hoh Xil terrane has been attributed either to the formation of a large accretionary complex as a result of offscraping of deep marine sediments (Sengor 1990) or to a large flux of sediments from the Qinling-Dabie orogenic belt, which was created by the Triassic collision of North China with South China (Yin & Nie 1993, Zhou & Graham 1993). The latter experienced significant denudation in the Late Triassic, which led to the widespread exposure of ultra–high pressure metamorphic rocks (Liou et al 1996, Hacker et al 1996).

Several lines of evidence support the connection between the deposition of the Songpan-Ganzi flysch complex and erosion of the Qinling-Dabie orogenic belt. First, consideration of mass balance shows that the amount of rock eroded from the Qinling-Dabie orogenic system is compatible with the total volume of the Songpan-Ganzi flysch sediments (Nie et al 1994). Second, analyses of sedimentary facies and composition of sandstones in the northeastern part of the complex, in the western Qinling, indicate that Triassic deep-marine sediments were derived from North China (Zhou & Graham 1996). Finally, correlation of provenance using U-Pb dating of single detrital zircon grains in the easternmost part of the flysch complex suggests that the source of its clastic materials is mainly from the southern margin of North China (Bruguier et al 1997).

In contrast to the remnant ocean model for the origin of the Songpan-Ganzi oceanic basin (Yin & Nie 1993, Zhou & Graham 1993), Gu (1994), Hsu et al (1995), and Burchfiel et al (1995) proposed that the Songpan-Ganzi flysch was deposited in a back arc basin behind a north-dipping subduction zone along the Jinsha suture zone. However, the presence of widespread Triassic igneous rocks south of the Jinsha suture zone (Liu 1988) and the lack of Triassic volcanic deposits in the Triassic flysch north of the suture (Qinghai BGMR 1991) have been cited as evidence against this hypothesis (Zhou & Graham 1996). The sporadic plutons intruded into the Triassic flysch complex (Figure 2; Liu 1988) postdate the deposition of the flysch complex.

Eastern Kunlun-Qaidam Terrane

The Eastern Kunlun-Qaidam Terrane is bounded by the Anyimaqen-Kunlun-Muztagh suture to the south (Molnar et al 1987, Pan 1996, Deng 1996) and the southern Qilian suture (Li et al 1978, 1982) to the north (Figure 2). In the south, its geology is dominated by a broad Early Paleozoic arc, on which a younger and narrower Late Permian to Triassic arc was superposed. Together, they are referred to as the Kunlun batholith (Harris et al 1988, Jiang et al 1992).

The western part of the composite Kunlun batholith consists of Middle to Late Proterozoic gneiss, schist, and marble, which were unconformably overlain by stromatolite-bearing Sinian (latest Proterozoic) strata and Cambrian (?) to Middle Ordovician shallow marine carbonate sequences (Qinghai BGMR 1991, Jiang et al 1992, Huang et al 1996). To the east, near the Golmud-Lhasa highway, the gneissic basement rocks north of the active left-slip Kunlun fault were dated by the Rb-Sr method to have formed at 1846 $\pm$ 109 Ma (Zhang & Zheng 1994), and south of the Kunlun fault, in the southeastern part of the East Kunlun-Qaidam terrane, a Sm-Nd age of 1927 $\pm$ 34 Ma was obtained for a deformed diorite (Zhang & Zheng 1994). The Proterozoic gneisses were overlain by Ordovician carbonate sequences (Yin et al 1988). Between the Late Ordovician and Early Carboniferous, volcanic deposits interbedded with marine deposits became widespread in the eastern Kunlun region (Huang et al 1996, Yin et al 1988). Associated with the Paleozoic volcanic rocks are extensive granitic intrusions with ages ranging from dominantly 470–360 Ma in the western Kunlun batholith near Qimen Tagh (Xu et al 1996) to 260–190 Ma in the eastern Kunlun batholith (Harris et al 1988) along the Golmud-Lhasa road.

The Early Paleozoic volcanic activity and associated magmatism were interrupted in the central and northern parts of the East Kunlun-Qaidam block by widespread deposition of Middle-Upper Carboniferous shallow marine carbonate rocks, which have no volcanic clasts (Qinghai BGMR 1991). However, along the southernmost margin of the Kunlun-Qaidam block, the Late Carboniferous-Early Permian marine sediments are interbedded with large amounts of basalts, andesites, and rhylites. Together, their total thickness exceeds 3,500 m (Qinghai BGMR 1991, Pierce & Mei 1988). This localized development of volcanism and the great thickness of submarine sedimentary and volcanic strata suggest to us that the southern Kunlun-Qaidam terrane may have experienced a rifting event that removed part of the southern Kunlun-Qaidam block in the Early Permian (Figure 4). This interpretation is consistent with the geochemistry of the Early Permian volcanics (Pierce & Mei 1988). Subsequent to the rifting event, the northward subduction of the Songpan-Ganzi-Hoh Xil ocean floor beneath the Kunlun batholith began in the latest Permian and lasted until the latest Triassic, which led to both volcanic eruptions and intrusion of granites in the southern Kunlun-Qaidam terrane (Zhang & Zheng 1994). This younger arc is superposed on the older Early Paleozoic arc (Figure 4; Jiang et al 1992). The latest Permian-Triassic arc in the Eastern Kunlun-Qaidam terrane could also be related to south-dipping subduction of the South Qilian terrane (Figures 2 and 4), since Triassic volcanic rocks are widespread in the northeastern margin of the East Kunlun-Qaidam terrane. Intense folding of the Triassic flysch complex (e.g. Burchfiel et al 1995) led to the elimination of the Songpan-Ganzi-Hoh Xil ocean in the Middle Jurassic (Nie et al 1994, Zhou & Graham 1996).

The northern part of the Eastern Kunlun-Qaidam terrane is mostly occupied by the Qaidam basin. Bedrock exposures are scattered along its northernmost edge, immediately south of the South Qilian suture. In this region, Ordovician

shallow marine strata are interbedded with andesites and volcanic tuffs, possibly representing a back arc setting behind the south-facing Ordovician Kunlun arc, along the southern edge of the Eastern Kunlun-Qaidam terrane (Hsu et al 1995) (Figure 4). The closure of the south Qilian suture between the Qilian terranes and the Eastern Kunlun-Qaidam terrane was inferred by Li et al (1978) to be in the latest Triassic, because of the presence of Late Triassic plutons and marine strata in the easternmost part of the southern Qilian. However, the Triassic plutons in the southern Qilian terrane could be part of the Late Permian-Triassic Kunlun batholith, which extends across the eastern end of the Qaidam basin and strikes into the southwestern part of the Qilian Shan (Liu 1988; Figure 2). An alternative interpretation to that of Li et al (1978) is that the collision between the Eastern Kunlun-Qaidam terrane and the southern Qilian belt occurred in the Late Devonian, as indicated by widespread deposition of terrestrial clastic sediments that rest unconformably on top of the folded and metamorphosed Ordovician strata (Figure 4; Cheng 1994, Hsu et al 1995).

Qilian Shan Terranes

Although generally excluded from discussions of Tibet (e.g. Allègre et al 1984, Dewey et al 1989), the Qilian terranes and the Nan Shan are integral parts of the Tibetan plateau. This area consists of complexly deformed early Paleozoic arcs, which were developed at the southern margin of the North China craton before it was offset by the Altyn Tagh fault in the Cenozoic. The Qilian Shan terrane has been traditionally divided into three east-west trending structural units (Li et al 1978, Xiao et al 1978): the northern, central, and southern Qilian belts. The central Qilian belt is thought to have rifted away from the southern margin of North China in the late Proterozoic to the Cambrian, as a result of back-arc spreading behind a north-dipping subduction zone (Figure 4; Xia et al 1996). The northern Qilian belt is an island arc system that was constructed along the southern margin of North China in the Ordovician, as the back arc basin was closing along a north-dipping subduction zone. This tectonic event led to the collision of the northern Qilian arc with the central Qilian belt, which consists mainly of Precambrian gneisses (Xia et al 1996, J Zhang et al 1998). The continuing convergence between the northern and central Qilian belts lasted until the Early Devonian, although the ocean between the two could have been eliminated much earlier, in the Early Silurian or the latest Ordovician (Xia et al 1996).

Collision between the central and the southern Qilian terranes was expressed by the development of a melange zone, involving highly deformed Ordovician and possibly Silurian sequences of marine sediments and volcanics (Cheng 1994, Hsu et al 1995). Cheng (1994) inferred that the closure of the ocean between the central and southern Qilian belts was completed in the Late Devonian, when terrestrial clastic sediments were widely deposited in the region. Late Devonian is also considered to have been the time when the united Qilian terrane was welded with the Eastern Kunlun-Qaidam terrane (Cheng 1994). The development of a series of Early Paleozoic arcs and their synchronous closures in the Devonian

suggest that these arcs all could have been developed as parts of a complex back-arc system behind the south-facing Kunlun arc (Figure 4). This interpretation is similar to that of Hsu et al (1995), but differs significantly from that of Sengor & Natal'in (1996), who regard the Qilian and Eastern Kunlun-Qaidam terranes as parts of a long-evolved accretionary complex in the Paleozoic, and thought that the arcs in the Qilian terrane were originally one single belt that was repeated in map view by a series of strike-slip faults. The strike-slip faults required by the model of Sengor & Natal'in (1996) have not been described in any report of Qilian geology (e.g. Qinghai BGMR 1991, Cheng 1994).

Western Kunlun Shan and the Karakorum Range

The Himalayan-Tibetan orogen becomes a narrow belt at its western end in the western Kunlun Shan and the Karakorum range (Figure 2). Its width measured between India and Tarim is only about 400–500 km, which is a third of the width of the central part of the Himalayan-Tibetan orogen. Tectonically, the region may be divided into five terranes (Pan 1990, 1996; Yin & Bian 1992; Deng 1996; Matte et al 1996; Ding et al 1996; Searle 1996; Zhang & Li 1998). From north to south, they are North Kunlun and South Kunlun terranes (= Eastern Kunlun-Qaidam terrane in Tibet), the Tianshuihai terrane (= Songpan-Ganzi-Hoh Xil terrane to the east), the Karakorum terrane (= Qiangtang terrane), and the Kohistan-Ladakh terrane (= Lhasa terrane). The recognizable suture zones that divide some of these terranes are the Kudi suture, which separates the North and South Kunlun terranes, the Shyok suture, which divides the Karakorum terrane from the Kohistan-Ladakh arc terrane, and the Indus suture, which separates the Kohistan-Ladakh terrane from India. The boundary between the Tianshuihai and South Kunlun terrane is complicated by the active left-slip Karakash (= Karakax) fault (Figure 2), although it has been inferred to be a suture (the Marza suture) separating the two in the latest Paleozoic, and was closed in the Triassic based on the presence of melange complexes and fragments of serpentinites (Deng 1996; Pan 1990, 1996; Hsu et al 1995). The boundary between the Karakorum terrane and the Tianshuihai terrane follows the active right-slip Karakorum fault and is defined by the northern Karakorum melange complex of Gaetani & Garzanti (1991).

There are two contrasting views about the development of the western Kunlun orogenic belt in the Paleozoic and Mesozoic. The first was proposed by Sengor & Okurogullari (1991), who viewed the western Kunlun as a collage of continuously accreted flysch complexes with an arc system that sequentially emplaced plutons southward as the accretionary complex grew larger to the south. In this context, there are no distinctive rigid building blocks for the formation of the orogen. In contrast, the tectonic division of Li et al (1982), Pan (1990), and Deng (1996) implies that the orogen was formed by the development and collision of magmatic arcs with the Tarim block in the north. This view is best summarized in the synthesis by Pan (1990, 1996), which was largely followed by Matte et al (1996).

An important sedimentary sequence in the North Kunlun is a thick pile of marine sedimentary strata of Late Devonian to early Permian in age. In the Sengor & Okurogullari (1991) model, this pile was interpreted to be the capping sequence of an accretionary complex, whereas in the arc-collision model of Pan (1990) and Matte et al (1996), it was viewed as a foredeep deposit developed at the time of ocean closure. Neither model explains the fact that the Carboniferous and Early Permian strata contain no volcanic clasts (Wang 1996). This leads to a third possible explanation for the Late Paleozoic development of the western Kunlun: That is, the Late Devonian to Early Permian sequence could have been produced by rifting along the southern margin of the Tarim block after the development of south-facing arc in the Ordovician (Figure 4; Xu et al 1996, Jia 1997). This may explain the absence of magmatism in the western Kunlun between the Late Ordovician and Early Permian. It also explains the presence of Triassic fossils in the Kudi suture zone, which separates the North and South Kunlun in the western Kunlun Shan (Fang et al 1998). It is possible that the Kudi suture represents the closure of a back arc basin in the Triassic. This basin terminates eastward before it reaches the present eastern Kunlun arc region.

The two-stage development of magmatic arcs, first in the early Paleozoic and then in the Late Permian and the Triassic, in the western Kunlun Shan is similar to the history of the Kunlun batholith along the southern margin of the Eastern Kunlun-Qaidam terrane. The only difference is that the Kudi back arc basin did not extend to the eastern Kunlun. The correlation between composite arcs in the western Kunlun and a composite batholith in the eastern Kunlun supports the early inference that the Kunlun arc may have been offset by the Cenozoic left-slip Altyn Tagh fault for about 550 km in the Cenozoic (Peltzer & Tapponnier 1988).

TIMING OF THE INDO-ASIAN COLLISION

The Cenozoic history of the Himalayan-Tibetan orogeny must be viewed in the broad context of the Indo-Asian collision, which in turn requires an understanding of the convergent history between India and Asia. Remarkable progress has been made in the last two decades in refining the plate kinematics of the two continents during the past ~85 Ma (Patriat & Achache 1984, Dewey et al 1989, Molnar et al 1993). Such quantitative knowledge of plate motion has in turn been used for (*a*) calculating mass balance, (*b*) estimating the total amount of finite strain (i.e. the magnitude of indentation of India into Asia) created by Indo-Asian collision, and (*c*) determining possible modes of strain accommodation mechanisms in the overall collisional system (England & Houseman 1986, Richter et al 1991, Le Pichon et al 1992). However, these deductive approaches are based on two critical assumptions: (*a*) that the elevation distribution of Asia prior to the Indo-Asian collision is known, and (*b*) that the timing for the onset of the Indo-Asian collision is well constrained. As shown previously, significant elevation (~3 km) may have

been already created in Tibet by the early Late Cretaceous, at least in the southern portion of the Tibetan plateau (Murphy et al 1997), and maintained until the onset of the Indo-Asian collision. We here review various lines of evidence that have been used to constrain the timing of the initial collision between India and Asia.

Plate Kinematics and Paleomagnetism

Analysis of Cenozoic magnetic anomalies in the Indian ocean shows that the relative velocity between the Indian and Eurasian plates decreased rapidly from ~15–25 cm/yr to ~13–18 cm/yr at ~50 Ma. This sudden decrease in plate convergent rate has been interpreted as indicating the time for the onset of the Indo-Asian collision (Patriat & Achache 1984). Paleomagnetic results from sedimentary rocks of the Nintyeast Ridge in the Indian ocean similarly show that the northward movement of the Indian plate exhibits a distinct reduction in speed from 18–19 cm/yr to 4.5 cm/yr; this occurred at about 55 Ma (Klootwijk et al 1992), but this change in the rate of motion was interpreted by Klootwijk et al (1992) to indicate the completion of suturing between India and Asia; thus, the initial contact between India and Asia could have been earlier than 55 Ma (Klootwijk et al 1992, 1994). It is difficult to determine whether the slowdown of convergence between India and Asia resulted from an increase in tectonic resistance due to contact of the buoyant Indian continental margin with Asia, or whether it simply reflects a sudden decrease in the spreading rate along the Indian mid-oceanic ridge at ca. 50–55 Ma.

Besse et al (1984) suggested that the collision between India and Asia occurred at about 50 Ma, based on a joint analysis of primary and secondary components of magnetization in late Paleocene sediments from the northernmost margin of India. As pointed out by Jaeger et al (1989), the strata used in that analysis are in fact older, between 60 and 56 Ma, so that the time of collision between India and Asia should be older than 60 Ma.

Stratigraphic and Paleontologic Evidence

Alternatively, the age of the initial Indo-Asian collision has been constrained by the stratigraphic and sedimentologic evolution of the Himalayan passive continental margin. Gaetani & Garzanti (1991) show that an abrupt change from marine to terrestrial deposition occurred at the end of the early Eocene in the Zanskar region of northeastern India (~52 Ma). Although this age has been widely quoted as representing the initial age of the Indo-Asian collision (e.g. Le Fort 1996, Rowley 1996), in fact it only constrains a lower limit (i.e. the youngest age) on the onset of the collision. This is because a large portion (as much as 500–1000 km) of the Indian passive continental margin could have been subducted beneath Asia (Patriat & Achache 1984, Matte et al 1997), potentially eliminating the early record of collision.

Beck et al (1995) showed that accretionary-prism and trench strata along the southern edge of Asia in northwestern Pakistan were thrust over the passive continental margin of India after 66 Ma but before 55 Ma. This relationship suggests

that the elimination of the oceanic lithosphere between India and Asia must have occurred before 55 Ma, because a significant portion of the Indian passive continental margin, which records earlier thrusting events related to initial collision, could have been underthrust beneath Asia before 55 Ma. This implies that 55 Ma is a minimum age for the initial Indo-Asian collision in northwestern Pakistan.

Near Tingri in south-central Tibet (Figure 2), continuous Upper Cretaceous to Lower Tertiary Indian passive continental margin marine strata exposed in Zhepure Mountain were investigated by Willems et al (1996). They found that a drastic change in sedimentary facies and depositional patterns occurred in the Middle Maastrichtian (~70 Ma). Above an unconformity, the Middle Maastrichtian strata are characterized by a sudden transition from marly sandstone to siliciclastic turbidite sediments. In the Lower Paleocene strata, directly above the Maastrichtian strata (66–64 Ma), redeposition of shallow-water clastic rocks are found. This change in depositional patterns along the Indian continental passive margin between 70 and 64 Ma was interpreted by Willems et al (1996) as indicating the initial contact between India and Asia. Similar conclusions were reached by Shi et al (1996), who also noted the widespread breakup of carbonate platforms between the latest Cretaceous (~80 Ma) and the earliest Tertiary (~59 Ma) and interpreted the breakup to represent the time of initial collision between India and Asia. The age, lithologic, and water-depth data of Willems et al (1996) were used by Rowley (1998) for constructing a backstripped subsidence history between 100 and 46 Ma in the Zhepure Mountains area. The subsidence curve of Rowley (1998) shows that a sharp increase in the rate of tectonic subsidence occurred at ~70 Ma, which could reflect the loading of the accretionary margin of Asia over the Indian passive continental margin. However, Rowley (1998) rejected this possible interpretation and suggested instead that the increase in the tectonic subsidence rate owing to initial Indo-Asian collision cannot be detected from the stratigraphic record; this implies that the Indo-Asian collision along the central segment of the Indus-Yalu suture zone must have occurred after ~46 Ma, indicating the youngest age of marine strata in the Zhepure Mountain sequence. A latest Cretaceous time for initial collision between India and Asia was also proposed by Jaeger et al (1989) on the basis of terrestrial faunal exchange between the two continents in the Maastrichtian.

Emplacement of the Spontang ophiolite over the Indian continental shelf sequence in the Zanskar region occurred in the latest Cretaceous (Searle et al 1988; cf. Le Fort 1989). This event was related to the initial collision between India and Asia; it may have provided substantial loading that affected foreland deposition along the northern edge of the Indian craton between the Late Cretaceous and the Early Paleocene (Najman et al 1993, 1994).

Youngest Age of the Gangdese Batholith

Although it has been cited as a way of dating the time of initial collision between India and Asia (Dewey et al 1988, Le Fort 1996), the age of emplacement of the Gangdese batholith varies from ~120 Ma (Xu et al 1985) to 30 Ma (Harrison et

al 1999b). The youngest ages, between 45 and 30 Ma (Honegger et al 1982, Schärer et al 1984, Xu 1990, Harrison et al 1999b), clearly postdate the initial contact between India and Asia, because collision-related Sm-Nd metamorphic ages in the Himalaya are as old as 49 ± 5 Ma (Tonarini et al 1993). The discrepancy among these ages suggests that the youngest age of the Gangdese batholith may be a poor indicator for the termination of subduction of the Indian oceanic lithosphere.

In summary, the existing data suggest that the initial collision between India and Asia could have started as early as latest Cretaceous time (~70 Ma). It is also important to note that most of the stratigraphic evidence cited above constrains only a lower bound for the time of initial collision.

CENOZOIC DEFORMATION IN THE HIMALAYAN-TIBETAN OROGEN

Himalayan Region

It has long been thought that thrusting within the Himalaya is a relatively late stage response in the overall accommodation of India's collision with Asia (e.g. Gansser 1964), and it remains unclear why crustal-scale thrusting within the collision zone was delayed for perhaps 20–40 Ma following the onset of collision. South-directed thrusts within the Himalaya (Figure 3), including the Main Central Thrust and Main Boundary Thrust (Gansser 1964, Bouchez & Pêcher 1981, Arita 1983, Le Fort 1986, Mattauer 1986, Burbank et al 1996), all appear to sole into a common decollement, the Main Himalayan Thrust (Zhao et al 1993, Nelson et al 1996, Brown et al 1996) (Figure 3). In general, the Main Central Thrust places high-grade gneisses (Greater Himalaya) on top of lower-grade schists (Lesser Himalaya). The Main Boundary Thrust juxtaposes those schists against the unmetamorphosed Miocene-Pleistocene molasse (the Siwalik Group). Thrusting is presently active within Quaternary sediments.

Main Central Thrust The Main Central Thrust is defined by a thick shear zone of a few kilometers to >10 km thick (e.g. Grasemann & Vannay 1999). Balanced cross-sections and flexural modeling of gravity data suggest that the north-dipping Main Central Thrust accommodated a minimum of 140 km of displacement and perhaps as much as 500 km (Gansser 1964, Arita 1983, Lyon-Caen & Molnar 1985, Pêcher 1989, Schelling & Arita 1991, Schelling 1992, Srivastava & Mitra 1994). Geochronology from the Main Central Thrust hanging wall indicates that anatexis and simple shear deformation occurred synchronously at 22 ± 1 Ma (Parrish & Hodges 1993, Coleman & Parrish 1995, Hodges et al 1996). Cooling ages in the upper portion of the Main Central Thrust hanging wall suggest that deformation had terminated there by the Middle Miocene (Hubbard & Harrison 1989, Copeland et al 1991). In situ Th-Pb dating of monazite included in garnet has revealed that the peak metamorphic recrystallization in the Main Central

Thrust zone of the central Himalaya occurred at 8–4 Ma (e.g. Harrison et al 1997a). The apparent inverted metamorphism appears to have resulted from activation of a broad shear zone beneath the Main Central Thrust, which juxtaposed two right-way-up metamorphic sequences (e.g. Hubbard 1996). Thermokinematic modeling suggests that the Main Central Thrust was reactivated at ca. 8 Ma (following ~10 m.y. of inactivity?) with a slip rate of ~20 mm/yr. At ~6 Ma, activity shifted progressively from north to south across a broad shear zone, and slip is thought to have terminated at ~3–4 Ma. Recognition of this remarkably youthful phase of metamorphism resolves a number of outstanding problems in Himalayan tectonics. First, this very young phase of metamorphism explains why the Main Central Thrust (and not the thrusts farther to the south) marks the break in slope of the present-day mountain range. Second, the young age of fault activity no longer requires exceptional physical conditions (e.g. very high flow stress, mantle delamination, rapid decompression) to explain the generation of the Himalayan leucogranites. However, it remains unclear when the Main Himalayan Thrust—the decollement to all the major thrusts in the Himalaya—was initiated, because no metamorphic or igneous products specifically ascribable to the Main Central Thrust older than ~25 Ma have yet been documented.

Main Boundary Thrust The surface expression of the Main Boundary Thrust is a generally steep, north-dipping fault that marks the contact between the Lesser Himalayan Formations and the underlying Miocene-Pleistocene Siwalik Formations (Johnson et al 1982, 1985). Significant changes in sedimentation patterns recorded in the magnetostratigraphy of the Himalayan foreland led Burbank et al (1996) to conclude that slip on the MBT began at ~11 Ma and was active during the Pleistocene. Whether or not the Main Boundary Thrust was active during the Late Miocene/Pliocene reactivation of the Main Central Thrust is not presently clear. The geomorphology of the Himalayan front suggests that the Main Boundary Thrust could have been active until recently (Nakata 1989).

South Tibetan Detachment System The South Tibetan Detachment System is a down-to-the-north, low-angle normal fault system that is traceable along the length of the Himalaya (Burg et al 1984, Burchfiel et al 1992) (Figures 2 and 3). This feature places generally low-grade Tethyan metasediments against the Greater Himalayan gneisses (Burg et al 1984, Herren 1987, Burchfiel et al 1992, Edwards et al 1996, Hodges et al 1996). Variably deformed leucogranites, belonging to the High Himalayan granite series, are commonly exposed in both the footwall and hanging wall of the detachment system. By determining crystallization ages of these leucogranites, usually through U-Th-Pb dating of monazite, it has been possible to constrain the timing of this feature at several locations. At various sites where the South Tibetan Detachment System has been mapped, no leucogranite bodies have been observed to cut the trace of the detachment (Burchfiel et al 1992, Edwards et al 1996, Searle et al 1997, Wu et al 1998). Leuco-

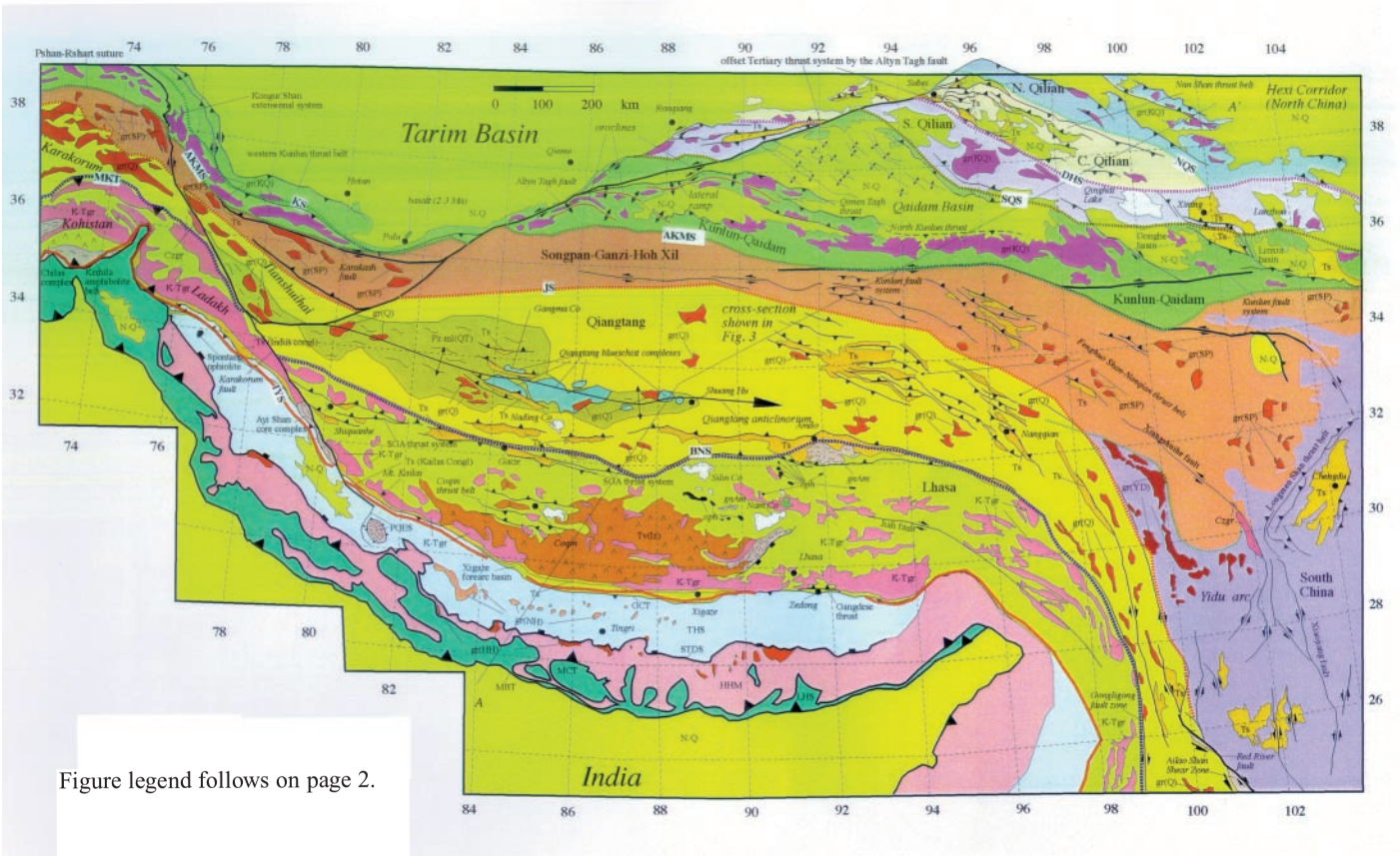

Figure legend follows on page 2.

Figure 2 Simplified tectonic map of the Himalayan-Tibetan orogen. Major lithologic and tectonic units: N-Q, Neogene-Quaternary sediments; Ts, Tertiary sedimentary rocks; Tv(lz), early Tertiary (60--40 Ma) Linzizong volcanic rocks in the Lhasa terrane; gnAm, Amdo gneiss; THS, Tethyan Himalayan sequences (Proterozoic to late Cretaceous passive continental margin strata); HHM, High Himalayan metamorphic rocks; LHS, Lesser Himalayan metasedimentary series. Major plutonic rocks: Czgr, Cenozoic granites in eastern Tibet and northern Karakorum Mountains; gr(NH), North Himalayan granites; gr(HH), High Himalayan leucogranites; K-Tgr, plutonic rocks belonging to the Gangdese batholith, Ladakh batholith, and Kohistan arc; gr(Q), Mesozoic plutonic rocks in the Qiangtang terrane; gr(SGH), Mesozoic plutonic rocks in the Songpan-Ganzi-Hoh Xil terrane; gr(KQ) Paleozoic and Mesozoic plutonic rocks in the Kunlun and Qilian terranes. Major sutures: IYS, Indus-Yalu suture; BNS, Bangong-Nujiang suture; JS, Jinsha suture; AKMS, Ayimaqin-Kunlun-Mutztagh suture; SQS, south Qilian suture; DHS, Danghe Nan Shan suture; NQS, north Qilian suture; KS, Kudi suture. Major Cenozoic structures: PGES, Purang-Gurla Mandhata extensional system; STDS, South Tibet Detachment System; MCT, Main Central Thrust; MBT, Main Boundary Thrust, SGA thrust system, Shiquanhe-Gaize-Amdo thrust system.

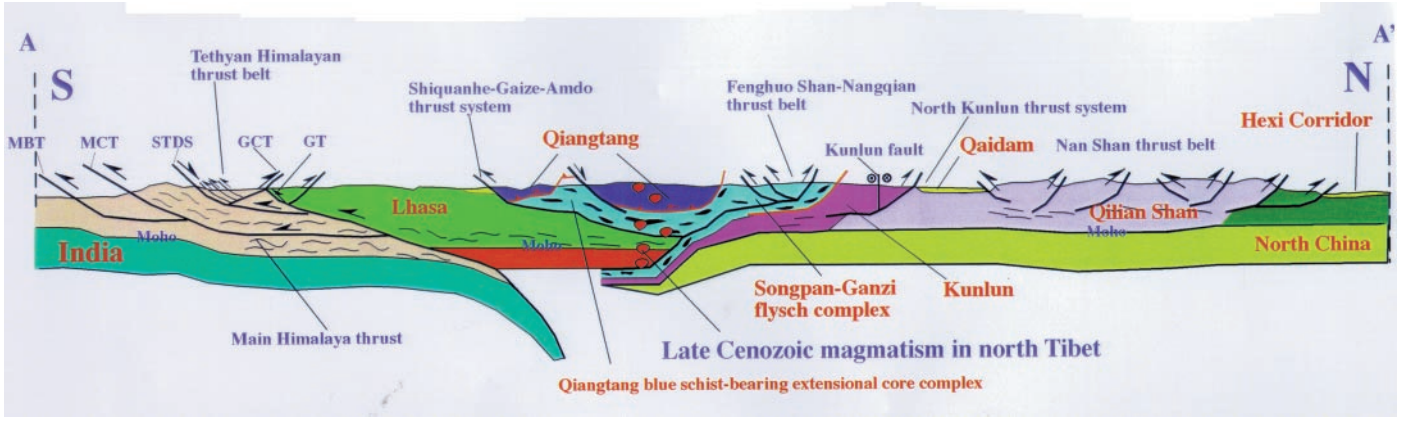

Figure 3 Schematic geologic cross-section across the Himalayan-Tibetan orogen. See Figure 2 for the location of the cross-section.

granites within the footwall at these localities generally contain shear fabrics that appear to be related to slip on the fault. U-Th-Pb dating of accessory minerals yield crystallization ages of 21–19.5 Ma (Zanskar) (Noble & Searle 1995), 17.3 ± 0.2 Ma (Shisha Pangma) (Searle et al 1997), 17–16 Ma (Rongbuk) (Hodges et al 1998, Murphy & Harrison 1999), 16.8 ± 0.6 Ma (Nyalam) (Schärer et al 1986, Xu 1990), ~15 Ma (Dinggye) (Xu 1990), ~11.9 Ma (Wagye La) (Wu et al 1998), and 12.5 ± 0.3 Ma (Gonta La) (Edwards & Harrison 1997). Although the timing of initiation of the South Tibetan Detachment System is not well constrained, these ages and the geologic relationships, including Rongbuk, imply that this fault system was active at 17 Ma or shortly thereafter; for Wagye La and Gonta La, however, it is demonstrated that the fault system was active after 12 Ma. A lower age limit for slip on the detachment system is constrained by the initiation at 8–9 Ma of north-south trending normal faults in southern Tibet (Harrison et al 1995a) that locally cut the South Tibetan Detachment System (Burchfiel et al 1992, Xizang BGMR 1992).

Tethyan Himalayan Thrust Belt This thrust belt is located between the South Tibetan Detachment System and the Indus-Yalu suture (Figure 2). It consists of folds and imbricate thrusts involving the entire passive continental margin sequence of the Tethyan Himalaya, with an estimated amount of shortening of ~130–140 km (Ratschbacher et al 1994). K-Ar dating of syn-kinematic white micas in the thrust belt indicates that shortening started at least by 50 Ma and lasted to about 17 Ma (Ratschbacher et al 1994). One of the K-Ar mica ages of Ratschbacher et al (1994) is 82.8 ± 4.1 Ma, which may imply that the age of thrusting in the Tethyan Himalaya was as old as the late Cretaceous. This is consistent with the initial contact between India and Asia having happened in the latest Cretaceous. The estimated shortening given here should be regarded as a minimum value, because part of northern India carrying Cenozoic folded shelf strata may have been subducted beneath Asia along the Indus-Yalu suture zone.

Gneiss domes of the Tethyan Himalaya (Figure 2) have been interpreted as representing the footwall ramp of the Main Central Thrust (Wu et al 1998). Hauck et al (1998) estimated ~326 km shortening across the Himalaya since the initiation of the Main Central Thrust.

Southern Tibet

Great Counter Thrust and Gangdese Thrust Systems The Indus-Yalu suture zone, where preserved, is bounded by two Cenozoic thrusts (Figure 2). The younger south-dipping thrust marks the southern boundary, juxtaposing the passive continental margin sediments of northern India over the melange complex along the Indus-Yalu suture zone. This fault was first termed the Great Counter Thrust in the Kailas area of western Tibet (Heim & Gansser 1939), but it has been variably named along its long extent (>1200 km) as the Yalu Tsangpo Fault south of Lhasa (Yu & Zheng 1979), the Great Yalu Tsangpo Deep Fault Zone

(Wang et al 1983) or the Backthrust System (Ratschbacher et al 1994) south of Xigaze, the South Kailas Thrust near Mount Kailas (Cheng & Xu 1987a), and the Renbu-Zedong thrust system in the Zedong area (Yin et al 1994). The Counter Thrust System was active at least between 19 and 10 Ma in southeastern Tibet (Quidelleur et al 1997) and during 13–10 Ma in the Mount Kailas region in southwestern Tibet (Yin et al 1999a), but its initiation age is not well constrained.

The older northern boundary of the Indus-Yalu suture is the north-dipping Gangdese thrust (Harrison et al 1992, Yin et al 1994). This fault is underthrust beneath the younger Counter thrust system in southeastern and southwestern Tibet (Yin et al 1999a), eliminating the exposure of the melange complex along the Indus-Yalu suture zone (Figure 2). The age of movement along the north-dipping Gangdese thrust is constrained to have occurred between ~30 Ma and 24 Ma (Yin et al 1994, 1999a, Harrison et al 1999b). The development of this thrust caused extensive denudation of the Gangdese batholith in its hanging wall and underthrusting of the Xigaze forearc strata in its footwall (Figure 2, Yin et al 1994).

Karakorum Fault The western part of Tibet is dominated by the active right-slip Karakorum fault system. Recent studies by Yin et al (1999a) and Murphy et al (1999) suggest that the Karakorum fault system in southwestern Tibet near the Kailas area offsets a unique piercing point for about 66 $\pm$ 10 km. This piercing point is defined by the south-dipping South Kailas Thrust (Cheng & Xu 1987a) and an unconformity in its footwall that is cut by the thrust. The Kailas thrust was active between 13 and 10 Ma (Yin et al 1999a); therefore, the Karakorum fault in the Kailas region must be younger than 10 Ma.

Slip along the Karakorum fault may be transferred to the Karakorum-Jiali fault zone, which extends across Tibet along the Bangong-Nujiang suture zone (Armijo et al 1986, 1989). Field mapping by Kapp et al (1999b) documents south-directed thrusting along the folded Shiquanhe fault, which generally follows the southern edge of the suture zone. Alternatively, the Karakorum fault may be a transfer fault linking the Kongur Shan extensional system to the north, in the Pamir region, with the Gurla Mandhata-Burang extensional system to the south, in western Tibet (Ratschbacher et al 1994).

The age of the Karakorum fault in the Kailas area is significantly younger than that determined in the Bangong Co area, about 200 km northwest of Mount Kailas, along the strike of the Karakorum fault. Searle et al (1998) documented two periods of rapid cooling along the central portions of the Karakorum fault system at 18 Ma to 11.3 Ma, and 11.3 Ma to a recent time. These earlier and later rapid cooling events are attributed to transpressional and transtensional fault motion, respectively. The timing and style of faulting near the Mount Kailas area in southwest Tibet can only be attributed to the second transtensional phase (Murphy et al 1999). An explanation for the lack of 18–11 Ma transpressional deformation along the Karakorum fault in southwestern Tibet is that the southeastern tip of the fault had not then reached its present position. Its slip at this time was

transferred to several thrusts in the Bangong Co and Shiquanhe areas northwest of its present termination near the Gurla Mandhata Mountains. Geologic maps by Cheng & Xu (1987), Matte et al (1996), and Kapp et al (1999b) show several south-directed thrust faults extending eastward, away from the Karakorum fault system. The largest of these are the south-directed Wujiang-Domar thrust (Matte et al 1996) and the Mandong-Cuobei thrust (Cheng & Xu 1987a), which place gneisses belonging to the Karakorum metamorphic complex over mid-Jurassic limestones. Along the eastern arm of Bangong Co, near Wujiang, the Wuijiang-Domar thrust carries gently folded Tertiary red beds in its hanging wall, indicating that deformation along the thrust is Cenozoic in age (Matte et al 1996).

Timing and slip constraints for the Karakorum fault and its relationship with the adjacent Tertiary thrust systems led to the suggestion that it may have initiated as a transfer fault (Murphy et al 1999). Between about 18 and 11 Ma, it was linked with thrust systems at its northwestern end in the central Pamir, along the Rushan-Pshart suture zone (Burtman & Molnar 1993, Strecker et al 1995), and with the Wujiang-Domar and Mandong-Cuobei thrust systems at its southeastern end, in western Tibet (De Terra et al 1932, Cheng & Xu 1987a, Kapp et al 1999b, Matte et al 1996). As the Pamir promontory continued to indent northward, the length of the Karakorum fault increased and propagated southeastward from 11 Ma until the present. During this period, the Karakorum fault system has been a transtensional structure that lengthens southward into southwestern Tibet and rotates clockwise as the Pamir orocline develops (Rumelhart et al 1999) (Figure 5).

The southern end of the Karakorum fault most likely terminates at the evolving Gurla Mandhata detachment fault system, which includes the currently active Purang rift system. The Gurla Mandhata fault separates the east-dipping (10–15°) Neogene-Quaternary Purang Conglomerate in its hanging wall from a thick zone (>500 m) of mylonitic marbles, gneisses, and leucogranites in its footwall (Yin et al 1996, 1999a; Murphy et al 1999). The marble unit forms the uppermost part of the footwall and is isoclinally folded into large west-verging nappes. Abundant kinematic indicators including ductile normal faults, asymmetric folds, and S-C mylonitic fabrics indicate that the west-dipping mylonitic shear zone slipped normally. Farther into the interior of Mt. Gurla Mandhata, young (ca. 8 Ma) non-mylonitic leucogranitic sills and dikes intrude into ductile mylonite with a ca. 19 Ma Th-Pb monazite age (Figure 2).

Central Tibet

Central Tibet is bounded in the south by the Bangong-Nujiang suture zone and to the north by the southern edge of the Qaidam basin. There are three major Cenozoic contractional systems in this region, from south to north: (*a*) the south-directed Shiquanhe-Gaize-Amdo thrust system, (*b*) the Fenghuo Shan-Nangqian fold and thrust belt, and (*c*) the north-directed Qimen Tagh-North Kunlun thrust system. All three thrust belts are spatially associated with Tertiary foreland basin

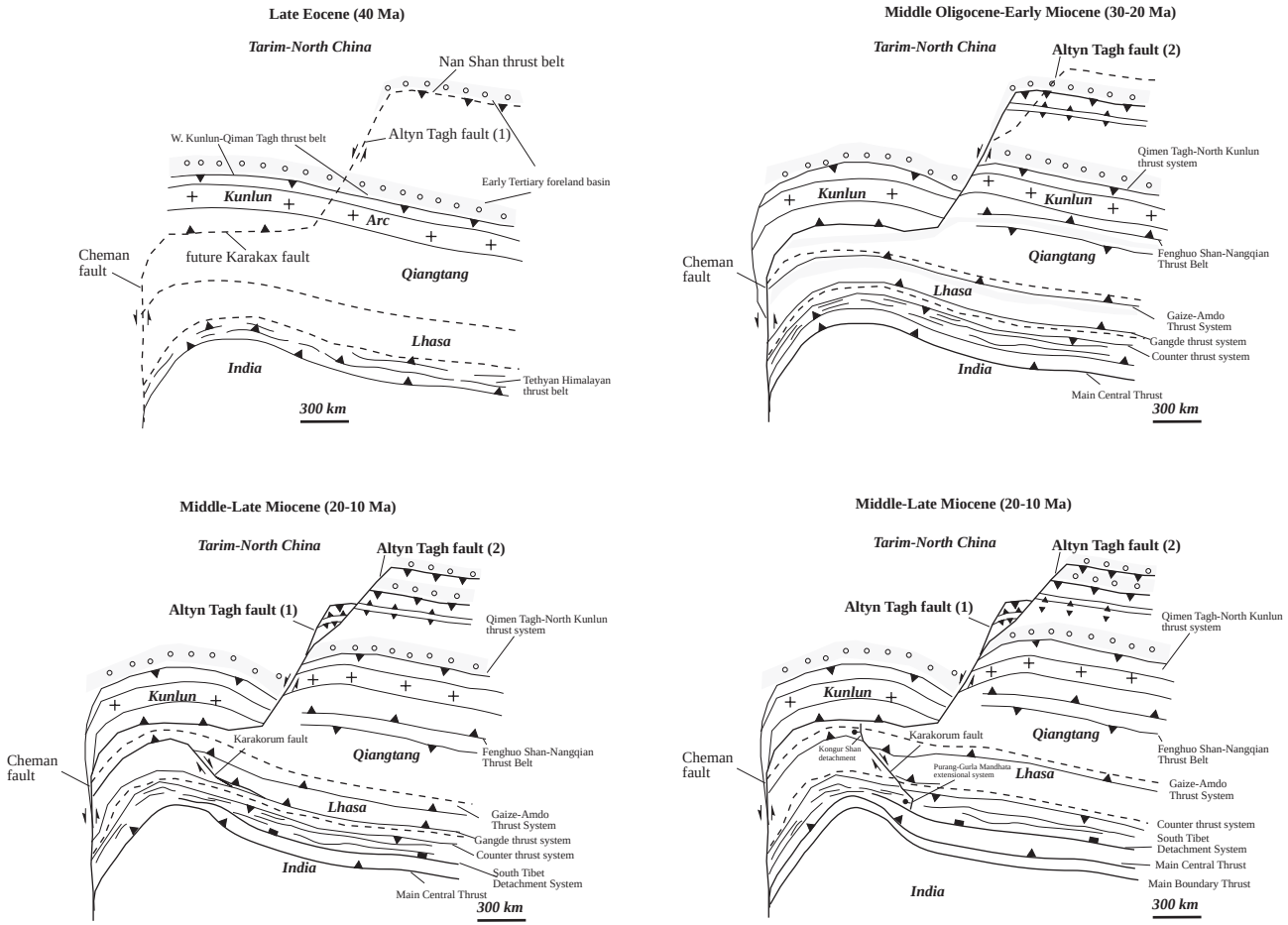

Figure 5 Schematic diagrams showing the evolution of major Cenozoic structures in the central and northwestern Himalaya and the Tibetan plateau regions. Karakax fault = Karakash fault.

development (Figure 2). In addition, a major left-slip fault, the Kunlun fault, lies in the central Kunlun Shan (Kidd & Molnar 1988, Van der Woerd et al 1998).

Shiquanhe-Gaize-Amdo Thrust System In general, this thrust system follows the trace of the Bangong-Nujiang suture zone (SGA thrust system in Figure 2). Although it is a Mesozoic suture separating the Lhasa and Qiangtang terranes, many have recognized that it was reactivated by a series of north-dipping thrusts that characteristically cut Tertiary strata (Figure 2; Cheng & Xu 1987a, 1987b; Wang et al 1983; Yu & Zheng 1979; Cheng & Xu 1986; Coward et al 1988; Dewey et al 1988). The thrust relationship along the suture zone can be clearly observed in at least four places: (*a*) near Amdo, where Triassic-Jurassic strata are thrust over Tertiary red beds (Coward et al 1988, Dewey et al 1988); (*b*) south of Shuang Hu, along Zajia Tsangpo, where Jurassic rocks were thrust over Tertiary red beds (Yin et al 1998b, Kapp et al 1999b); (*c*) near Gaize, where Jurassic rocks were thrust over a thick (1–2 km) sequence of Tertiary conglomerate (Yin et al 1998b, Kapp et al 1999b); and (*d*) near Shiquanhe, where Permian and Cretaceous strata are thrust over Tertiary conglomerates (Cheng & Xu 1986, Kapp et al 1999b).

The Shiquanhe-Gaize-Amdo thrust system was active in the mid-Tertiary, but its initiation and termination ages are not well constrained. Near Nading Co (Figure 2), the Tertiary strata are divided into the Paleogene Nading Co and the Oligo-Miocene Kangtuo formations (Cheng & Xu 1986). The older unit consists mainly of volcanic flows, and was dated at 31 Ma by the K-Ar method in one location (Cheng & Xu 1986). The younger unit consists of conglomerate, sandstone, and locally basaltic flows of unknown age. The older unit is cut by Cenozoic thrusts near Nading Co (Cheng & Xu 1986), and the lithologically correlative Kangtuo Formation is cut by thrusts near Gangma Co (Yin et al 1999c).

Near Amdo, a coarsening upward sequence, grading from mudstone to conglomerate, is overthrust by the Amdo gneiss (Figure 2). Ostracods (*Cypois*, sp., *Eucypris*, sp.), gastropods (*Amnicola* sp., *Gyraulus* sp., *Pseudamnicola* sp., *Physa* sp.), and arthropods (*Erotylidae* incertae Sedis) indicate that the sequence is Oligocene in age (Yu & Zheng 1979).

Near Gaize, 1–2 km of interbedded conglomerates, sandstones, and locally andesitic flows are present in the footwall of a north-dipping thrust system (Cheng & Xu 1986, Kapp et al 1999b; Figure 3). Cobbles in the section are dominantly limestone, sandstone, and volcanic breccias. These terrestrial deposits rest on top of the late Cretaceous marine limestone, and have been designated as Tertiary in age (Cheng & Xu 1986), although Liu (1988) assigned a late Cretaceous age for these rocks. The lower age bound for the Shiquanhe-Gaize-Amdo thrust in the Gaize area is taken to be post-latest Cretaceous (Kapp et al 1999b).

The age of the folded conglomerate sequence cut by the Shiquanhe thrust, an element of the overall Shiquanhe-Gaize-Amdo thrust system, can generally be constrained as postdating the late Cretaceous but predating the mid-Miocene. Cheng & Xu (1987a) assigned a Tertiary age to the Shiquanhe conglomerate based

on the unconformable relationship between the conglomerate unit and underlying late Cretaceous marine strata. A flat-lying volcanic flow, dated as 20–18 Ma, rests on top of the tilted conglomerate unit (Arnaud & Vidal 1990). This relationship may constrain the upper age limit for Tertiary folding and thrusting in the region.

The exact magnitude of thrusting along the Shiquanhe-Gaize-Amdo thrust system is not well constrained, because the rocks in the hanging wall and footwall of these major thrusts cannot be matched. However, regional structural relationships and lithostratigraphic distribution indicate that the thrust system may have accommodated some 200-km or a greater amount of crustal thrusting. As speculated by Yin et al (1998b) and Kapp et al (1999b), the thrust system may consist of a crustal-scale ramp at mid-crustal level beneath the central Qiangtang. Movement of the Qiangtang terrane along the ramp could have created the 600-km-long Qiangtang anticlinorium (Figure 3). The crustal-scale ramp model is similar to that for the relationship between the Purcell anticlinorium and the Lewis thrust in the Southern Canadian Rockies (Price 1981). The model implies that the north limb of the anticlinorium lies above the footwall thrust ramp. In that case, the Lhasa terrane has been underthrust beneath Qiangtang for at least ~200 km (Figure 3).

Fenghuo Shan–Nangqian Fold and Thrust Belt This belt lies along the northern edge of the Qiangtang terrane and continues across the Jinsha suture zone into the Songpan-Ganzi-Hoh Xil terrane (Figure 2). In the Fenghuo Shan region, this belt is characterized by thrusts that dip both to the north and to the south, juxtaposing variously Permian to Jurassic aged strata over Tertiary strata (Figure 2). The most noticeable stratigraphic unit in the region is the Fenghuo Shan Group, which is at least 4 km thick (Qinghai BGMR 1991). The age of the Fenghuo Shan Group is controversial. According to Qinghai BGMR (1991), it belongs to the Upper Cretaceous, although the fossils collected from the strata are not unique to the Late Cretaceous. Other researchers have argued that the Fenghuo Shan Group belongs to the Lower Tertiary and is most likely Eocene in age, based on the presence of charophytes, fresh water gastropods, ostracods, and plant fragments (Smith & Xu 1988). Leeder et al (1988) related the deposition of the Fenghuo Shan Group to the development of Early Tertiary thrusting.

The Fenghuo Shan strata are tightly folded and are intruded by 42–5 Ma Tertiary intrusions (Zhang & Zheng 1994). They are also overlain by gently folded Miocene and younger strata (Zhang & Zheng 1994). Both Tertiary sequences are cut by thrusts that juxtapose variously Permian-Triassic strata with the Tertiary units. Because the Permian and Triassic strata are both a few kilometers thick, the vertical throw along each thrust fault in the fold and thrust belt is from a few kilometers up to ~10 km. The style of deformation and the distribution of thrusts in the region (Zhang & Zheng 1994) suggest that the total shortening across the thrust belt is at least 60–80 km.

Qimen Tagh–North Kunlun Thrust System This thrust system consists of two major thrusts: the Qimen Tagh thrust to the northwest and the North Kunlun thrust

to the southeast (Figure 2). Both faults juxtapose the Proterozoic metamorphic rocks and Paleozoic sedimentary and igneous rocks over Tertiary strata of the Qaidam basin (Figure 2; Bally et al 1986, Song & Wang 1993). This fault system is currently active, as is evident from numerous fault scarps along its trace. At the western end, the fault system turns sharply from a northwestern trend to a southwestern trend and is subparallel to the Altyn Tagh fault directly to its north. To the east, the Qimen Tagh thrust dies out into the Qaidam basin. Its slip is transferred to the North Kunlun thrust (Figure 2; Bally et al 1986). The Qimen Tagh fault appears to have been active in two separate episodes, as indicated by the stratigraphic records in its footwall: (*a*) during the Paleocene when a sequence of conglomerates accumulated along the southwestern part of the Qaidam basin, and (*b*) during the past 5–6 Ma since the Early Pliocene, when a thick sequence of coarse clastic sediments accumulated along the southern margin of the Qaidam basin (Song & Wang 1993).

The magnitude of thrusting along the Qimen Tagh–North Kunlun fault is not constrained, but slip variation along the left-slip Altyn Tagh fault indicates that this thrust system could have accommodated a total of ~270 km north-south shortening.

Kunlun Fault The Kunlun fault is east-west trending and is ~1000 km long in central Tibet. It generally follows the trace of the Anyimaqen-Kunlun-Muztagh suture (Figure 1). The total slip along the Kunlun fault is about 75 km, based on the offset of a meta-sedimentary unit interpreted from Landsat images (Kidd & Molnar 1988) (Figure 1). The late Quaternary slip rate on this feature is 12 ± 3 mm/yr, derived from cosmogenic dating of offset stream risers (van der Woerd et al 1998). If the fault has moved at a uniform rate of 12 mm/yr since its initiation, the magnitude of slip along the Kunlun fault implies that the Kunlun fault has been active over the past 7 Ma.

The Kunlun fault splits into several branches at its western end, which appear to be linked with several north-south trending rifts. In the east, the Kunlun fault bounds several north-south trending basins to its north (e.g. the Lingxia basin). The Kunlun fault may serve as a transfer fault linking east-west extensional structures to its north and south. Farther to the east, the Kunlun fault has been considered to be linked with the active north-south trending Longmen Shan thrust system (Chen et al 1994) and the left-slip Qinling fault (Y Zhang et al 1998; Figures 1 and 2).

Northern Tibet

Cenozoic structures in northern Tibet, north of the Kunlun Shan, are dominated by the Altyn Tagh fault system (Figure 2). This system consists of the Nan Shan thrust belt, the Western Kunlun thrust belt, the left-slip portion of the main Altyn Tagh fault, the left-slip Karakash Valley fault, and minor compressional and

strike-slip structures along the southern margin of the Tarim basin and in the western part of the Qaidam basin (Figure 2).

The Altyn Tagh fault system is in many respects comparable to the San Andreas system. It extends for more than 1,200 km and bounds the rather rigid Tarim basin to the northwest (comparable to the Pacific plate) and the more deformable Tibetan plateau to the southeast (comparable to the North American continent) (Figure 1). The Altyn Tagh system consists of many strands of subparallel faults, though they are not all presently active (Cowgill et al 1997). Past geologic investigations of the main Altyn Tagh strand were largely conducted by Landsat-image interpretation (e.g. Molnar & Tapponnier 1975, Tapponnier & Molnar 1979, Peltzer et al 1989, Avouac & Peltzer 1993) or by reconnaissance field studies (Molnar et al 1987). The only systematic geologic survey along the entire length of the fault system has been made by geologists from the China State Bureau of Seismology between 1985 and 1988 (CSBS 1992). However, that work only emphasized the neotectonic aspects of the fault system.

Characteristics of the Altyn Tagh Fault Between the Tarim and Qaidam basins (Figure 2), the fault is confined to a relatively narrow zone ($<$30 km). South of this fault segment, in the Qaidam basin, are numerous folds involving strata as young as Quaternary with their axes trending perpendicular to the Altyn Tagh fault. No obvious bending of the fold axes are apparent from the map relations (Liu 1988; Figure 2), implying that the Qaidam basement is rigid and that the Altyn Tagh fault is relatively weak. South of Qaidam, several apparently oroclinal folds are present on the south side of the Altyn Tagh fault. The change in the map pattern of the fold axes occurs across the Qimen Tagh thrust, south of which there is a drastic increase in average elevation, from $\sim$3 km in Qaidam to $\sim$5 km south of the fault. Two questions may be raised in relation to these observations: (*a*) Is the oroclinal pattern controlled by the presence of a thrust ramp or induced by rotation about the vertical axes (Figure 6)? (*b*) Is the change in fold axis orientation between Qaidam and the central Tibetan plateau a result of the contrast in crustal thickness and relative mechanical strength? The upper mantle in central Tibet between the Kunlun Shan and the Bangong-Nujiang suture zone is interpreted as abnormally hot (McNamara et al 1995), and it is thought that Neogene to Quaternary volcanism is widespread (Deng 1989; Xie et al 1992; Arnaud et al 1992; Turner et al 1993, 1996). For that reason, the difference in fold-axis patterns could reflect the contrast in mechanical strength between the two regions.

Portions of the Altyn Tagh fault are seismically active. The two largest historical earthquakes (both with a magnitude of M = 7.2) occurred near Qiemo of the central Altyn Tagh fault in 1924 (CSBS 1992) (Figure 2), and contemporary instrumental recordings reveal minor to medium levels of seismicity along the entire fault system (CSBS 1992). The CSBS seismicity map for the period 1970–1989 shows intense activity within a $\sim$150–200 km diameter area centered on the western segment of the Altyn Tagh fault west of Qiemo—although many of these events are probably not on the main fault. Focal mechanisms of several

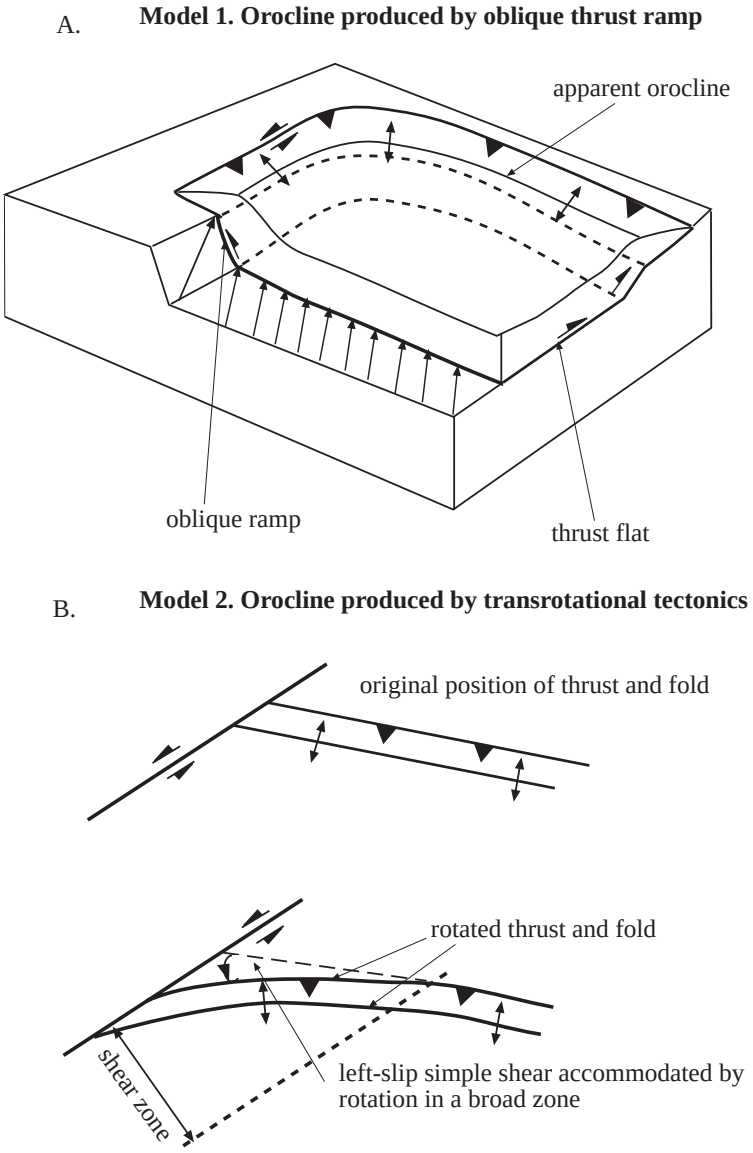

Figure 6 Contrasting models for the curvilinear belts of structures along the Altyn Tagh fault system. (*a*) The curved belt reflects its original geometry controlled by the presence of an oblique thrust ramp. (*b*) Thrusts and folds were originally straight on map view and were bent later by simple shear deformation along the broad zone of the Altyn Tagh fault system.

events in this cluster show dominantly extensional faulting with E-W to ESE-WNW tension axes (Molnar & Lyon-Caen 1989).

GPS surveys suggest that the eastern segment of the Altyn Tagh fault east of Qiemo has moved at a rate no greater than 20 mm/yr within a time span of a few years, and probably closer to ~10 mm/yr. GPS measurements were performed in 1998 along the entire length of the fault system, during which the sites observed in 1997 were reoccupied (Yin et al 1999b). Preliminary analysis indicates that the eastern end of the Altyn Tagh fault against the Nan Shan has a slip rate of 8 ± 4 mm/yr. At its western end, in the western Kunlun, the north-south convergent rate is 2 ± 4 mm/yr. The GPS stations along the southwestern rim of the Tarim basin show a systematic decrease from west to east in convergent rate relative to the stable interior of the Eurasia, suggesting that the Tarim block is currently rotating clockwise. An independent GPS survey was conducted by Bendick et al (1998) across the central segment of the Altyn Tagh fault system between Rouqiang and Huatugou. They had installed a 500-km-long GPS array across the fault zone in 1994; these GPS stations were remeasured in 1998, and yielded a slip rate of 18 ± 5 mm/yr across the Altyn Tagh fault.

Within a time span of a few thousand to a few tens of thousands of years, the minimum Quaternary slip rate along the fault is ~5 mm/yr based on mapping and ^{14}C dating of offset geomorphic features (CSBS 1992). Assuming that deposition of large alluvial fans in the Altyn Tagh region was related to the end of the last Ice Age, Peltzer et al (1989) suggested that the Holocene slip rate on the fault was ~20–30 mm/yr. A branch of the easternmost segment of the Altyn Tagh fault system was investigated by Meyer et al (1996, 1998), who suggest a minimum slip rate of ~4 mm/year in the Holocene. A branch of the western Altyn Tagh fault system makes a sharp turn from its east-northeast strike to a west-northwest strike along the Karakash valley in the western Kunlun Shan. This segment of the Altyn Tagh fault, commonly referred to as the Karakash fault (Matte et al 1996), offsets a sequence of Quaternary alluvial fans. Age determination of these offset fans using the cosmogenic dating method yields a slip rate along the Karakash fault of ~30 mm/yr (Ryerson et al 1999). This rate is significantly greater than those estimated across the central and eastern portions of the Altyn Tagh fault from the GPS studies.

Translation and Rotation along the Altyn Tagh System The Altyn Tagh fault system is an association of kinematically related faults and folds that are distributed in a broad zone and have together accommodated overall left-slip simple shear deformation (Figure 2). This broad definition allows us to address the question of how translation (fault slip) and rotation (non-coaxial deformation) may have contributed to the overall left-slip deformation across this fault zone during the Indo-Asian collision.

(1) Fault Slip. Estimating the magnitude of fault slip along a major strike-slip fault requires determination of piercing points (Crowell 1962; Sylvester 1988)

and establishment of paleogeographic reconstruction domains (Powell 1993) across the fault. Speculations on the total left slip along the Altyn Tagh fault vary significantly from (*a*) ~1200 km on the basis of matching Paleozoic suture zones in the Qilian Shan with that in the western Kunlun Shan (Figure 2) (CSBS 1992); (*b*) ~550 km by matching late Paleozoic magmatic belts in the western and eastern Kunlun Shan across the fault (Peltzer & Tapponnier 1988); and (*c*) ~200 km based on inferences from the measured Pliocene-Quaternary slip rate and duration of fault movement along the Altyn Tagh fault (Burchfiel & Royden 1991). It is important to note that the offset markers used in some of these inferences are broad tectonic features (plutonic belts, suture zones) that have poor spatial definition for their margins, rendering high uncertainties. In addition, because the offset markers formed in the Paleozoic, it is difficult to determine whether the offset of the geologic features occurred in the Paleozoic and Mesozoic, or in the Cenozoic during the Indo-Asian collision. In contrast to the correlation of broad geologic features, detailed geologic mapping along the eastern segment of the Altyn Tagh fault conducted recently revealed a piercing point that constrains a fraction of the total slip along the eastern Altyn Tagh fault (east of Rouqiang). This piercing point is defined by a pair of oppositely dipping Cenozoic thrusts that have moved toward one another (Yin et al 1999b). They are present in the Jinyang-Suekuli Shan north of the fault and the Donghe/Yema Nan Shan south of the fault ~280 km to the east (Figure 2). In both areas, overturned ductile nappes involving late Proterozoic strata in their hanging walls are juxtaposed by Tertiary thrusts with a Tertiary foreland basin in their common footwall. The Tertiary strata consist of gypsum-bearing red beds, and are of Late Eocene-Oligocene in age based on the presence of freshwater ostracods (Xinjiang BGMR 1989). We infer that the Cenozoic thrusting in both areas occurred in the late Eocene-Oligocene (~40–32 Ma), synchronous with deposition of the footwall foreland basin. This correlation yields an estimated left slip of ~280 ± 30 km along the eastern segment of the Altyn Tagh fault since the early Oligocene, and an average slip rate of ~7–9 mm/yr assuming that the offset of the Tertiary basin and the two thrusts occurred immediately after the development of the basin.

The fact that Cenozoic thrusts are offset by the Altyn Tagh fault indicates that an older Altyn Tagh fault must have existed before the development of the currently active fault strand. This older fault must lie north of the currently active fault, and bound the inactive thrust system in the Jinyan-Suekuli Shan to the south and the undeformed Tarim basin to the north. As suggested by Cowgill et al (1997, 1999), this inferred older Altyn Tagh fault may be the Checheng fault that is imaged by subsurface seismic data (Jia et al 1991, Jia 1997). The amount of shortening in the Jinyan-Suekuli Shan, ~60–100 km (A Yin & G Gehrels, unpublished mapping) requires that the older and inactive Altyn Tagh fault has an accumulative left slip of equivalent amount.

The estimated ~280 ± 30 km left slip along the eastern Altyn Tagh fault yields a value for the the minimum amount of north-south shortening absorbed by the Nan Shan thrust belt in the Cenozoic of ~280 km. When adding the

80 ± 20 km shortening recorded in the Jinyan-Suekuli Shan before the development of the currently active Altyn Tagh fault, the total minimum estimate of north-south shortening accommodated by the Nan Shan thrust belt in the Cenozoic is on the order of 360 ± 50 km.

Geology in the western and eastern Kunlun Shan are remarkably similar. Both areas experienced two episodes of arc magmatism in the Ordovician and Late Permian-Triassic, with an interruption between the Late Carboniferous and the Early Permian, possibly caused by a rifting event along their southern margins (Figure 2). This similarity in geologic history supports the speculation that the western segment of the Altyn Tagh fault has a total slip of ~550 km (Peltzer & Tapponnier 1988). This estimate is significantly different from that of ~280 km along the eastern segment of the Altyn Tagh fault north of the Qimen Tagh thrust, and implies that about 270 km of north-south shortening has been accommodated by structures between the Danghe Nan Shan (the southernmost range of the Nan Shan) and the Qimen Tagh. The obvious structural candidate to have absorbed this amount of shortening is the Qimen Tagh thrust (Figure 2).

(2) Rotation. Rotational tectonics along a strike-slip fault system is a familiar expression of simple-shear deformation in a zone of continental deformation. In the San Andreas fault system, this process has been accommodated by rotation of crustal blocks about vertical axes (Luyendyk et al 1985, Luyendyk 1989). Consideration of transrotational tectonics by Dickinson (1996), in conjunction with transtensional tectonics in the Basin and Range (Dickinson & Wernicke 1997), helped reconcile the long-noted disparate estimates of San Andreas transform motion made by summing fault offsets on land and the global analysis of sea-floor magnetic anomalies.

The possible role of transrotation in the left-slip Altyn Tagh fault zone is indicated on the existing Chinese geologic maps along the fault (e.g. Liu 1988) (Figure 2). Several possible oroclinal folds, which bend for nearly 90°, appear to exist south of the Altyn Tagh fault. Because rock units as young as Eocene are involved in this oroclinal bending, it is likely that the folds were developed during movement along the Altyn Tagh fault in the Cenozoic. Straightening these oroclines along their regional NW-strike would require an additional ~110–130 km left-slip simple shear across a ~100-km-wide zone (Figure 2). An alternative to the oroclinal interpretation is that the apparent pattern of oroclinal bending was produced by an oblique thrust-ramp geometry, which requires no rotation about vertical axes (Figure 6).

(3) Rotation of the Altyn Tagh fault. Despite repeated suggestions about the rotation of major tectonic blocks and their bounding faults in Asia (e.g. Davy & Cobbold 1988), it has remained unclear whether the Altyn Tagh fault itself had been rotated during the Indian-Asian collision. Paleomagnetic analysis of samples from Eocene–Early Oligocene strata along the Altyn Tagh fault (Rumelhart 1998, Rumelhart et al 1999) shows that the fault has not been rotated more than 8° since

the Early Oligocene (~35 Ma, see Rumelhart 1998). Given the range of uncertainty of this study (±7°), it is most likely that the fault has not rotated at all, an inference consistent with the results from Chen et al (1993) who showed that Tarim, which is the northern bounding block of the Altyn Tagh fault, has rotated no more than 7° since the late Cretaceous.

Lithospheric Structure of the Altyn Tagh Fault The Altyn Tagh fault may be either a crustal-scale transfer fault (Burchfiel et al 1989b) or a lithospheric-scale thrust (Deng 1989, Arnaud et al 1992). The mode of deformation has also been proposed to be decoupled vertically with strike-slip faulting in the upper crustal level (Burchfiel et al 1989b) and shortening in the mantle lithosphere (Willett & Beaumont 1994). Teleseismic experiments across the central Altyn Tagh fault between Ruoqiang and Mangya reveal a low P-wave velocity anomaly directly below the Altyn Tagh fault down to ~140 km (Wittlinger et al 1998). Quaternary basaltic eruption along the trace of the western Altyn Tagh fault in the Ashiko basin, a small pull-apart structure (CSBS 1992), and near Pulu (Liu 1988, Deng 1998) (Figure 2) shows that the western Altyn Tagh fault cuts the lithosphere and has served as a conduit to tap basaltic magma from the upper mantle to the surface. The lack of Quaternary basaltic eruption along the eastern segment of the Altyn Tagh fault east of Qiemo may indicate that in that region the fault is a crustal scale structure, as suggested by Burchfiel et al (1989b).

Western Kunlun Thrust Belt The Tarim block is thought to have been subducted southward beneath the western Kunlun for at least 80 km in the Cenozoic (Lyon-Caen & Molnar 1984), creating the north-directed western Kunlun thrust belt (Figure 2). Together with the active left-slip Karakash fault, the western Kunlun thrust belt defines the western termination of the Altyn Tagh fault system (Burchfiel et al 1989b; Figure 2). Geologic mapping in the eastern part of the western Kunlun thrust belt (Cowgill et al 1998) and subsurface data from the southwest Tarim basin (Jia 1997) indicate north-south shortening across the eastern part of the thrust belt of between 50 and 100 km. This magnitude appears to increase westward based on paleomagnetic studies. The western Kunlun Shan has experienced more than 20° of clockwise rotation about a vertical axis since the early Oligocene (Rumelhart et al 1999). The pivotal point for the western Kunlun Shan rotation may have been located at its eastern end near Pulu (Figure 2). If this is the case, a simple geometric relationship may be used to estimate the minimum amount of crustal shortening predicted in the western Kunlun thrust belt, assuming that Tarim has not rotated (Chen et al 1992); this yields a minimum north-south shortening since the early Oligocene—about 85 ± 43 km in the eastern part and about 187 ± 84 in the central part of the western Kunlun thrust belt (Rumelhart et al 1999).

The clockwise vertical-axis rotation of the western Kunlun Shan may have been caused by northward indentation of the Pamir (Figure 5). This rotation is in mirror image to the counterclockwise vertical-axis rotation in the western Pamir

(Bazhenov et al 1994). The detected rotation in the western Kunlun Shan may also explain the occurrence of left-slip motion along the Karakorum fault, which is south of and subparallel to the western Kunlun thrust belt (Figures 1 and 5). The Karakorum fault, bounding the western Kunlun Shan to the north and the combined Tianshuihai-Karakorum block to the south, may have been an accommodation zone for the clockwise rotation of the two blocks.

The age of initiation of the western Kunlun thrust belt is best constrained by a recent study on the biostratigraphy, magnetostratigraphy, and sedimentology of its Tertiary foreland basin (Rumelhart 1998). This study shows that the thrust belt began developing before the early Oligocene, a time that is marked by a drastic increase in sedimentation rate and input of coarse clastic sediments into the basin.

If the 550-km offset of the eastern and western Kunlun arcs by the Altyn Tagh fault occurred in the Cenozoic (Peltzer & Tapponnier 1988), then the western Kunlun thrust belt at the western termination of the Altyn Tagh fault system cannot be the structure that absorbed this offset, because the two arcs are both on the same side of the Altyn Tagh fault (Figure 2). A termination structure must lie south of the offset arc in the western Kunlun Shan. There are three possible ways to explain the offset. First, the arc is offset by the left-slip Karakash fault, which is the southwestern extension of the Altyn Tagh fault. If this is the case, then a structure that terminates the Karakash fault farther to the west is required. Judging from the existing geologic map of the region (Liu 1988), the Karakash fault links in the west with a thrust that bounds a Tertiary basin. The magnitude of shortening along that thrust appears to be small, because the extent of the Tertiary basin along the strike of the fault is rather short, less than 70 km long (Figure 2). Such a short length of thrust would not have been able to have accommodated the hundreds of kilometers of shortening required by the offset of the Kunlun arcs. A comparison may be made with the Lewis thrust, in the southern Canadian Rockies and northwestern Montana of the United States, which has a length of $\sim$500 km and a maximum displacement of about 200 km (Price 1981).

Alternatively, the offset of the Kunlun arcs by the Altyn Tagh fault was absorbed by a major north-dipping thrust system in the southern part of the western Kunlun Shan, south of the western Kunlun arc (Figure 5). Recent deep seismic reflection studies across the foreland of the western Kunlun thrust belt (Figure 2) suggest that a major sequence of north-dipping reflectors are present immediately north of the northern edge of the western Kunlun Shan (Gao et al 1999a). These reflectors can extend to a depth of $\sim$100 km, and appear to truncate south-dipping reflectors representing the south-dipping subduction of the Tarim block. Because the south-dipping reflectors should reflect the Cenozoic movement of Tarim beneath the western Kunlun, the cross-cutting relationship suggests that the north-dipping reflectors, younger than the south-dipping reflectors, should also be Cenozoic in age. When the north-dipping reflectors are extended upward, the top of the sequence is projected to lie approximately along the active trace of the Karakash fault. This geometrical relationship may be interpreted in two ways: (*a*) the Karakash fault changes its attitude from nearly vertical at the surface to a shallow

angle dipping to the north, or (*b*) the north-dipping reflectors represent the expected north-dipping Tertiary thrust system that has absorbed some 500 km of offset along the Altyn Tagh fault (Figure 5). A surface expression of the inferred north-dipping thrust system in the southern part of the western Kunlun Shan is the thrust near Tianshuihai, in which Silurian metamorphic rocks are thrust over late Cretaceous strata (Figures 2 and 3).

The last possibility is that the Kunlun arc is not offset significantly by the Altyn Tagh fault and has a slip of 200–300 km rather than ~550 km. Instead, it has been oroclinally bent into its current configuration (Figure 6). This large scale bending of the Kunlun arc is consistent with the presence of several apparently large oroclines south of the Qaidam basin (Figure 2).

Nan Shan Thrust Belt The Cenozoic Nan Shan thrust belt marks the eastern termination of the Altyn Tagh fault system (Figure 2). Although some 340 km of north-south shortening can be inferred to have occurred in the Cenozoic across the thrust belt, based on the amount of left slip along the eastern Altyn Tagh fault (Figure 2), an independent estimate of the total amount of crustal shortening has not been obtained. This is partially because the thrust belt is superposed on several early suture systems, which had resulted in complex structural and lithostratigraphic relationships prior to the Cenozoic deformation (Figure 4).

The age of initiation of the Nan Shan thrust belt dates the onset of Altyn Tagh fault movement in the region, because the two are kinematically linked. Magnetostratigraphic analysis, apatite fission-track cooling ages of clasts, and the biostratigraphy of Tertiary foreland sediments in the Subei area suggest that these Tertiary sediments are at least as old as the Middle Oligocene (Wang 1997, Rumelhart 1998). Sedimentologic studies of the Subei Tertiary strata indicate that they were deposited in a foreland basin, with clasts coming from the emerging topographic high of a thrust hanging wall to the south (Rumelhart 1998). This result suggests not only that the Nan Shan thrust belt has been in existence since the Oligocene, but that the Altyn Tagh fault also reached the Nan Shan region at that time. This is consistent with the Late Eocene-Early Oligocene piercing point being offset by the presently active strand of the Altyn Tagh fault (Figures 2 and 5). The Nan Shan thrust belt could have started to deform in the early Paleocene, because Paleocene-Eocene red beds are widely distributed in the northeastern Qilian Shan north and south of Xining (Qinghai BGMR 1991). This would imply that the Altyn Tagh fault, the transfer fault system for the thrust belt, had developed in the northernmost part of the Tibetan plateau at the very beginning of the Indo-Asian collision. Thus, the Nan Shan thrust belt cannot be the result of northward propagation of the plateau development in the past few million years, as some researchers have speculated (e.g. Meyer et al 1998).

Eastern Tibet

Eastern Tibet is traditionally interpreted as being part of the broad accommodation zone (~700 km wide), which has absorbed deformation induced by the indentation of India into Asia (Dewey et al 1989). It lies between the main part of the

Tibetan plateau, east of longitude 95°E, north of the Himalaya, and west of South China, and is dominated by complex systems of Cenozoic strike-slip and dip-slip faults (Figure 2). From east to west and from north to south, these faults are the Longmen Shan thrust belt, the Xiangshuihe-Xiaojiang fault system, the Jiali-Gaoligong fault system, and the Ailao Shan–Red River fault system (Wang et al 1998). The deformation in the region has been accommodated by three mechanisms: (*a*) southeastward extrusion of the Indochina block (Peltzer & Tapponnier 1988, Leloup et al 1995), (*b*) block rotation (Davy & Cobbold 1988, Royden et al 1997), and (*c*) internal deformation (Wang & Burchfiel 1997, Wang et al 1998). How the three components of deformation are quantitatively partitioned remains uncertain, however.

Extrusion Extrusion of the Indochina block during the Indo-Asian collision has long been speculated about on the basis of analogue modeling (Tapponnier et al 1982). The model requires a conjugate set of strike-slip faults that are operating simultaneously to assist the movement of large continental blocks. It is clear now that the currently active right-slip Red River fault was a left-slip fault earlier in the history of the Indo-Asian collision. The Red River fault can be traced from southeastern Tibet through Yunnan to the South China Sea (Tapponnier & Molnar 1977, Allen et al 1984, Leloup et al 1995, Wang & Burchfiel 1997, Wang et al 1998). The active fault follows the northeastern edges of narrow gneissic belts that extend from the Dan Nuy Con Voi range in Vietnam through the Ailao Shan and Diancang Shan massifs in Yunnan, and can be traced to the Xuelong Shan near the border of Tibet (Tapponnier et al 1990). Although the Red River fault was interpreted as a pure right-slip fault that occurred throughout the Cenozoic (e.g. Dewey et al 1989), field investigations show that the semi-continuous metamorphic belt directly south of the active Red River fault represents the ductile portion of a major mid-Tertiary left-slip fault zone, known as the Ailao Shan shear zone (Leloup et al 1995).

In the gneissic cores along the Ailao Shan shear zone, most rock types are mylonitic; the foliation is generally steep and parallel to the strike of the shear zone, and stretching lineations are subhorizontal (Leloup et al 1995). There is abundant evidence of non-coaxial deformation and kinematic indicators demonstrating a left-lateral sense of shear (Leloup et al 1995, Wang et al 1998). U-Pb ages of accessory minerals from late syntectonic leucogranites parallel to the foliation and affected by left-lateral shears—inferred to date the late increments of left-lateral shear—cluster between 23 and 24 Ma (Leloup et al 1995).

Apparent left-lateral offset of geologic features on each side of the Red River shear zone varies between 300 and 740 km (Leloup et al 1995). The opening kinematics of the South China Sea, deduced from magnetic anomalies (Briais et al 1993), are compatible with a left-slip movement (with a slightly oblique component) of 540 km between 32 and 17 Ma (i.e. a slip rate of ~4 cm/yr); this suggests that the South China sea is a pull-apart basin at the southeast termination of the fault zone. $^{40}Ar/^{39}Ar$ thermochronometry within the Ailao Shan yields a pattern of cooling ages consistent with the diachronous initiation of transtensional

faulting, which propagated along the Ailao Shan shear zone at a rate of ~4 cm/yr between 25 and 17 Ma (Harrison et al 1996). These results are consistent with predictions of fault kinematics based on the South China Sea magnetic anomalies (Briais et al 1993). The sense of motion on the Red River fault reversed at about 5 Ma (Leloup et al 1993, Harrison et al 1996), and became right-slip with normal throw in places.

The conjugate shear system to the left-slip Ailao shear zone consists of the right-slip Gaoligong shear zone in the east and the right-slip Sagaing fault to the west (Figure 2). The Gaoligong shear zone is marked by a 2–5 km thick zone of mylonitic gneisses. K-Ar and $^{40}Ar/^{39}Ar$ dates of muscovite and biotites from the mylonitic shear zone yield cooling ages between 11 and 24 Ma, which are interpreted as representing the duration of fault movement along the Gaoligong shear zone. The age range overlaps the duration of motion along the Ailao Shan shear zone (Leloup et al 1995). However, the magnitude of right slip along the shear zone is unknown.

Internal Deformation The observations just described are consistent with the hypothesis that extrusion of Indochina from southern Asia during the middle Cenozoic accommodated a significant portion of the Indo-Asian convergence during the mid-Tertiary (Tapponnier et al 1982). However, debate has been centered on whether (*a*) the extrusion tectonics have been largely accomplished by rigid block motion (Leloup et al 1995), so that simple rigid block kinematic models (Avouac & Tapponnier 1993) can be applied to describe the fault motions, or (*b*) extrusion has been associated with distributed deformation (Burchfiel et al 1995, Arne et al 1997, Wang & Burchfiel 1997), in which case strike-slip faults are transfer structures with variable slip along their strikes. It is clear that Tertiary deformation has occurred within the Indochina block south of the Ailao Shan shear zone. For example, the Wuling thrust belt in the middle Cenozoic Simo fold belt, directly south of the Ailao Shan shear zone, has accommodated some 50–60 km of shortening perpendicular to that zone (Wang & Burchfiel 1997) (Figure 2). However, the total magnitude of deformation within Indochina is highly uncertain, which makes the comparison of rigid block motion versus internal deformation difficult.

Rotation Field studies (Ratschbacher et al 1996, Wang & Burchfiel 1997, Wang et al 1998), paleomagnetic analysis (Huang & Opdyke 1993, Huang et al 1992, Chen et al 1995), and GPS surveys (King et al 1997) all show that eastern Tibet rotated clockwise around the eastern Himalayan syntaxis during the Cenozoic. The cumulative rotation in the Cenozoic is greater than 60° (Huang & Opdyke 1993, Huang et al 1992). If these results are regionally significant, they imply that the Ailao Shan shear zone has been rotated more than 14° required by both the extrusion model and the opening of the South China sea (Leloup et al 1995), as pointed out by Wang & Burchfiel (1997). Royden (1996) and Royden et al (1997) interpreted the rotation around the eastern Himalayan syntaxis as a result

of continental convergence where the lower crust is weak, allowing decoupling of upper crustal motions from those of the lower crust and the mantle.

Late Cenozoic North-South Trending Rifts in the Himalayan-Tibetan Orogen

Geologic Setting Since the initial recognition of active north-south trending rifts in Tibet (Tapponnier & Molnar 1977, Molnar & Tapponnier 1978, Ni & York 1978), our knowledge of these structures has greatly improved because of (*a*) several detailed field investigations (Tapponnier et al 1981; Armijo et al 1986, 1989; Mercier et al 1987; Burchfiel et al 1991; Yin et al 1999c), and (*b*) improved quality of Landsat imagery (Rothery & Drury 1984), as well as availability of seismic reflection and refraction data across some parts of the north-south trending rift valleys in southern Tibet (Cogan et al 1998). Because the age of initiation of east-west extension in Tibet has been argued to represent the time when the plateau reached its present elevation (Molnar & Tapponnier 1978, England & Houseman 1989), which in turn may have been related to the intensification of the Asian monsoon (e.g. Harrison et al 1992, Molnar et al 1993), several efforts have been made to constrain the timing of extension in Tibet and the Himalaya. In the Nyainquentanghla region of southeast Tibet, the onset of east-west extension is constrained to be 8 $\pm$ 1 Ma (Harrison et al 1995b). An upper bound on the initiation of the Yadong-Gulu rift—the largest of the north-south trending graben—is constrained by the fact that the rift cuts the South Tibetan Detachment System, which was active until at least 12 Ma (Edwards & Harrison 1997, Wu et al 1998).

The age of minor extension in southernmost Tibet near Xigaze (Figures 1 and 2) was estimated by dating a north-south trending dike swarm, which was emplaced at 18 $\pm$ 1 Ma (Yin et al 1994). These dikes predate a major thrust system, the south-dipping Renbu-Zedong thrust that was active between 18 and 10 Ma (Quidelleur et al 1997). This cross-cutting relationship suggests that the stress condition for dike emplacement may be significantly different from that required for the formation of north-south trending Tibetan rifts, because the rifts postdate the Renbu-Zedong thrust and have not been cut by any contractional structures since their initiation. It is argued that farther to the south in the Himalaya, east-west extension started at or before $\sim$14 Ma (Coleman & Hodges 1995). Again, such an event would predate crustal thickening produced by the Great Counter Thrust in southernmost Tibet and northern Himalaya (Yin et al 1994, 1999c). Therefore, dike emplacement in the Himalaya and Tibet should be distinguished from the initiation of the regionally extensive north-south Tibetan rifts.

In contrast to our knowledge about east-west extension in southern Tibet, studies of north Tibetan rifts have been mostly based on fault-plane solutions of earthquakes and interpretations of Landsat images (Molnar & Lyon-Caen 1989, Rothery & Drury 1984, Armijo et al 1986). Because of the lack of surface geo-

logical investigations, the geometry, timing, and magnitude of Cenozoic rifting in northern Tibet are poorly constrained. One exception comes from recent geologic mapping conducted in north-central Tibet, in the Gangma Co and Shuang Hu regions (Figure 7); this mapping documented the presence of major north-south striking active normal fault systems with 4–8 km displacements (Yin et al 1999c). In addition, kinematic analysis conducted by Blisniuk et al (1998) on active faults south of Shuang Hu suggest that northeast-striking faults in the region are left-slip faults, and are linked to north-south trending normal faults (Figure 7).

Modeling degradation of a normal fault scarp (e.g. Avouac 1993) in the Shuang Hu region yields a minimum estimate of slip rate of ~2 mm/yr (Yin et al 1999c). With the assumption of a constant slip rate, the total displacement across the Shuang Hu fault of ~6–8 km implies that the onset of the normal fault system began at about 3–4 Ma. This age estimate is significantly younger than the initiation age of 8 ± 1 Ma for the Nyainqentanghla fault. It is also much younger than the beginning of Cenozoic igneous activity in central Tibet at ~35 Ma (Chung et al 1998, Deng 1998). An asynchronous relationship between the initiation of rifts and igneous activity is also observed in southern Tibet, where the emplacement of the 18 Ma dikes (Yin et al 1994) occurred about 10 m.y. earlier than rift initiation (Harrison et al 1995b). In both southern and central Tibet, igneous activity and rifting do not overlap spatially (Figure 1). The preceding relationships indicate that igneous activity in Tibet is unrelated to the initiation of rifting, and bears no implications for the timing of the Tibetan plateau reaching its present elevation.

Mechanisms for the Formation of Tibetan Rifts An analysis of high-resolution, digital topography across north-south trending rifts in Tibet yielded an average effective elastic thickness for the Tibetan upper crust of ~6–7 km (Masek et al 1994), which implies that Tibetan east-west extension is an upper crustal process. This idea was recently advocated by Nelson et al (1996) and Cogan et al (1998), based on seismic reflection studies across southern Tibet.

The mantle lithosphere is clearly involved with east-west extension beneath Tibet and the Himalaya (Chen & Kao 1996), however, implying that deformation between the upper crust and the upper mantle may have been coupled. This mode of deformation is similar to that of the formation and development of the Baikal rift and Shanxi graben in central Asia: Both have involved the mantle lithosphere and exhibit localized extension (Deverchere et al 1991, Rupple et al 1993, Gao et al 1994, van der Beek 1997, Delvaux et al 1997, Wang et al 1996). Rifts in Tibet and in north-central Asia not only share the same mode of extension, they were also initiated broadly at about the same time during the Late Miocene and earliest Pliocene (i.e. 8–5 Ma; Delvaux et al 1997, Wang et al 1996). The similarities in the mode of extension, the direction of extension, and timing of initial extension strongly suggest that rifts in Tibet and those in North China and southeast Siberia have shared the same origin. In particular, the overall Late Miocene–

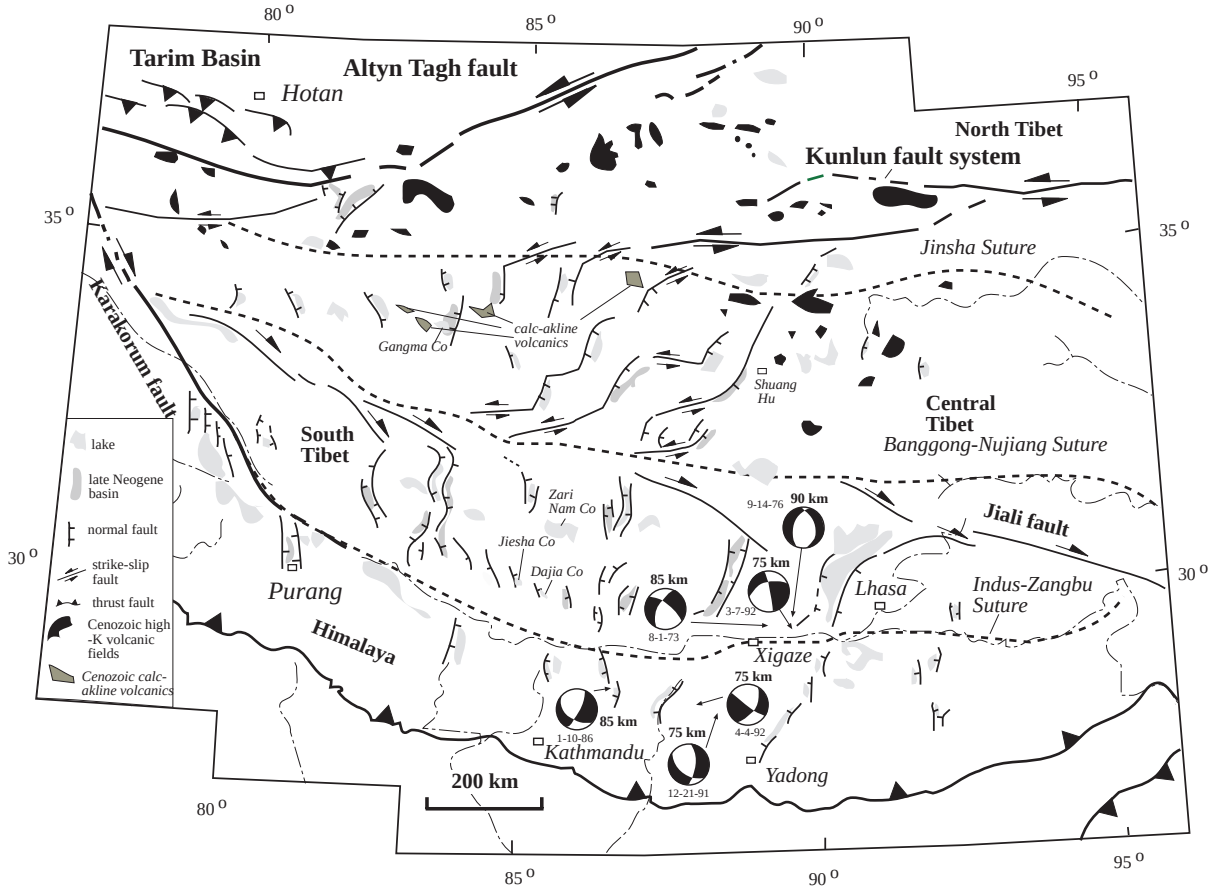

Figure 7 Major late Cenozoic rifts in the Himalayan-Tibetan orogen and distribution of Cenozoic volcanic rocks excluding the early Tertiary Linzizong volcanic rocks (shown in Figure 2). Modified after Armijo et al (1986), Yin et al (1999c), and Yin (1999).

Early Pliocene east-west extension in eastern Asia may have been triggered and possibly sustained by a protracted back arc extensional process related to large-scale mantle flow beneath Asia (Yin & Kong 1997, Yin 1999).

Relationship to Strike-Slip Faults The Karakorum-Jiali fault zone (Figure 7) is variably inferred as being the result of eastward extrusion of northern Tibet (Armijo et al 1986, 1989) or oblique convergence between India and Tibet (McCaffrey & Nabelek 1998). Alternatively, the Karakorum-Jiali fault zone may be explained as an accommodation zone that transfers east-west extension from more widely spaced rifts in the south to the more closely spaced rifts in the north (Yin 1999). This mechanism may also apply to the relationship between the left-slip Kunlun fault and north-south trending rifts in central Tibet. The latter interpretation implies that the major east-west trending strike-slip faults in central Tibet are transfer zones, linking north-south trending extensional systems. The presence of these transfer structures does not require eastward extrusion of discrete individual blocks such as north Tibet between the Kunlun and the Karakorum faults (Armijo et al 1986). Instead, the strike-slip faults may have facilitated more distributed eastward expansion of the Tibetan plateau (Yin et al 1999c).

SYN-COLLISIONAL IGNEOUS ACTIVITIES

Himalayan Leucogranites and Their Significance in Collisional Tectonics

An apparently unique feature of the Himalayan range is the presence of two roughly parallel granite belts—the High Himalayan leucogranites (HHL) and the North Himalayan granites (NHG) (Figure 2). The High Himalayan leucogranites form a discontinuous chain of sills and granite pods exposed on either side of the South Tibetan Detachment System (Figure 2). Magmatic temperatures have been estimated at ca. 700–750°C (Montel 1993). The North Himalayan granite belt runs parallel to, and ~80 km to the north of, the High Himalaya, and is composed of about one and a half dozen generally elliptical plutons (Figure 2). Exposed plutons of the northern belt appear mainly to have been intruded at relatively shallow depths into the Tethyan cover rocks and well above the South Tibetan Detachment System (Le Fort 1986).

Plutons from the High Himalayan leucogranite belt vary in crystallization age from 24.0 to 17.2 Ma, but most of the large granite bodies composing the majority of the leucogranite were emplaced during two pulses at 23 ± 1 Ma and 19 ± 1 Ma (Harrison et al 1998b). Crystallization ages for granites assigned to the North Himalayan belt range from 17.6 to 9.5 Ma (Harrison et al 1998b). Note, however, that classifying Himalayan granites into two discrete belts may be misleading in that temporally contiguous, northward-propagating melting (Harrison et al 1997b) could produce spatially discontinuous patterns as a result of variable exposure.

The juxtaposition of the Greater Himalaya and Lesser Himalaya across the Main Central Thrust is associated, at most locations in the Himalaya, with an increase in metamorphic grade at higher structural levels (i.e. shallower depths). Thermobarometric studies of the Greater Himalaya indicate a general decrease in pressure and temperature with increasing distance above the Main Central Thrust. Typically, pressures of 7–8 kbar were achieved adjacent to the thrust (kyanite grade), whereas peak pressures at the structurally highest levels were only about 3–4 kbar (sillimanite grade) (Harrison et al 1999b). Metamorphism within the Lesser Himalaya typically increases from chlorite to kyanite grade over a north-south distance of ~20 km. The region approximately bounded by the garnet isograd in the Lesser Himalaya and the hanging wall gneisses of the Greater Himalaya is typically characterized by a highly sheared, typically 4–8 km thick zone of distributed deformation with a top-to-the-south shear sense, referred to as the MCT (Main Central Thrust) zone.

The juxtaposition of inverted metamorphic sequences and anatexis with large-scale faults within the Himalaya has led to the development of numerous models that assume partial melting and inverted metamorphism are spatially and temporally related. Models have included melting induced by thermal relaxation following nappe emplacement accompanied by fluid influx from the subducting footwall (e.g. Le Fort 1975); frictional heating during thrusting (e.g. Arita 1983, England et al 1992, England & Molnar 1993); radioactive heating alone or combined with other sources under prolonged deep crustal residence (e.g. Molnar et al 1983); and accretion of highly radioactive crust to the Main Central Thrust hanging wall coupled with high denudation rates (e.g. Royden 1993, Huerta et al 1996). The origin of the North Himalayan granites has not been as closely tied to the development of Himalayan faulting, but their relative youth has been ascribed to a low rate of fluid infiltration across the Main Central Thrust (Le Fort 1986) and to heat focusing by thermal refraction off Tethyan metasediments with low thermal conductivity (Pinet & Jaupart 1987). Other models (e.g. Bird 1978, Nelson et al 1996) have proposed (*a*) that thrusting within the Himalaya is caused by melting, rather than vice versa (i.e. regions of the crust thermally weakened by melting are the loci of deformation that leads to large-scale faulting), or (*b*) that anatexis is due to decompression resulting from slip on the STDS rather than to thrusting (e.g. Harris & Massey 1994).

The anatexis of the Greater Himalaya need not be restricted to regions immediately below the Main Central Thrust ramp, as proposed by England et al (1992), because recrystallization of the Main Central Thrust footwall is in fact a Late Miocene-Pliocene phenomenon and thus was not temporally related to production of the Early and Middle Miocene Himalayan leucogranites (Harrison et al 1998b). An alternative explanation (Harrison et al 1998b) is that the spatial and temporal variations of granite emplacement were the result of continuous slip on a shallow dipping decollement that cuts through crust that had been previously metamorphosed crust during the Eocene-Oligocene Eohimalayan phase (Le Fort 1996) of the Indo-Asian collision. During this stage, the protolith of the Greater Himalaya

underwent high-grade metamorphism and anatexis (see Pecher 1989; Hodges et al 1994, 1996; Parrish & Hodges 1996; Edwards & Harrison 1997; Coleman 1998; Vance & Harris 1999). As a consequence, a stratified paragenetic sequence was produced, in which dehydration and partial melting reactions caused the metamorphic grade to increase regularly with depth.

The question of whether Himalayan anatexis could largely reflect decompression melting resulting from slip on the South Tibetan Detachment System (e.g. Harris & Massey 1994) was addressed quantitatively by Harrison et al (1999a). They found that tectonic decompression was problematic for the following reasons: (*a*) the extremely rapid and large-magnitude denudation required to produce relatively minor melting in likely source rock compositions, (*b*) the implausibility of decompression producing multiple anatectic pulses separated by several million years from a common source region, and (*c*) the lack of definitive timing constraints linking slip on the normal faults with anatexis.

Syn-Collision Igneous Activities in Tibet North of the Indus-Yalu Suture

If collision between India and Asia was initiated in the latest Cretaceous and earliest Tertiary around 70–65 Ma, then igneous activity in the Himalaya and Tibet after this time should be regarded as post-collisional. This means that the distribution of post-collisional igneous rocks covers nearly the entire Himalayan-Tibetan orogen (Figure 1).

In southern Tibet, between the Indus-Yalu and the Bangong-Nujiang suture zone, the Paleogene Linzizong volcanic sequence and its associated youngest phases of the Gangdese plutons form an east-west linear belt along the southern margin of the Lhasa terrane (Liu 1988, Yin et al 1988, Pierce & Mei 1988, Coulon et al 1986) (Figure 1). The Linzizong rocks are dominantly andesites and ignimbrites that have been dated between 60 and 40 Ma (Coulon et al 1986, Pan 1993). Their geochemistry is calc-alkaline, characteristic of an Andean continental margin (Coulon et al 1986, Pierce & Mei 1988). However, distinctively young ages of potassic calc-alkaline lavas between 15 and 10 Ma have also been reported in the southern part of the Lhasa terrane, about 100 km west of Lhasa (Coulon et al 1986). Their occurrence suggests that Andean-type arc magmatism was produced well after the initial collision and the cessation of the subduction of the oceanic lithosphere. This observation highlights again the idea that the age of arc magmatism is not a reliable indicator for when the onset of collision between India and Asia occurred.

The occurrence of the Linzizong volcanic eruptions may have been related to the breakoff of the oceanic lithosphere from the Indian continental lithosphere. Alternatively, the voluminous eruption of the volcanics and associated plutonic emplacement were triggered by the initial subduction of the Indian continental shelf, which brought a large quantity of sediments in the mantle. The younger episodes of calc-alkaline volcanism (Coulon et al 1986) and plutonism (Harrison

et al 1999b) could have been related to thrusting along the Gangdese thrust and the younger Main Himalayan Thrust, which carried the sedimentary strata of the Indian continental shelf farther down into the mantle.

In central Tibet, between the southern margin of the Qaidam basin and the Bangong-Nujiang suture zone, post-collisional igneous rocks, dominantly volcanics and small intrusions, are widely scattered (Deng 1989, 1998; Xie et al 1992; Arnaud et al 1992; Turner et al 1993; Chung et al 1998; Zhang & Zheng 1994) (Figure 7). The igneous rocks can be divided into a highly potassic group and a calc-alkaline group (Deng 1998). The former generally occupies the northern part of central Tibet, whereas the latter is distributed farther to the south (Deng 1998). The age of the high-potassic volcanic rocks ranges from $\sim$60 Ma to $<$1 Ma (Turner et al 1993, Chung et al 1998, Deng 1998). The age of the calc-alkaline volcanics, determined by the K-Ar method, ranges from 29 to 20 Ma (Deng 1989).

Highly potassic volcanism in central Tibet started between 40 Ma and 60 Ma, and lasted until the late Quaternary (Chung et al 1998, Deng 1998). For such a wide range of ages, it is difficult to relate the genesis of volcanism to a sudden tectonic process such as convective removal of the mantle lithosphere (Turner et al 1993). Instead, it is possible that the northern Tibetan lower crust, which is largely made up of Triassic melange, was subducted to mantle depths during thrusting along the Fenghuo Shan-Nangqian fold and thrust belt, and along the Qimen Tagh-North Kunlun thrust system (Figure 3). The 20–40 Ma calc-alkaline igneous rocks in the central Qiangtang may be related to subduction of the Lhasa terrane beneath Qiangtang (Figures 3 and 7).

The young highly potassic volcanic rocks erupted in the past 20 Ma are distributed along the Altyn Tagh and Kunlun faults (Figure 1). The emplacement of these rocks could have been related to local pull-apart basins (Yin & Nie 1996), although the inferred small fractional melting of mantle lithosphere (Arnaud et al 1992) could also have been related to the addition of water-rich minerals into the upper mantle by Tertiary underthrusting of the Songpan-Ganzi-Hoh Xil flysch complex and the melange basement of Qiangtang (Figure 3). The model shown in Figure 3 is different from that of Arnaud et al (1992), Willett & Beaumont (1994), and Jin et al (1996), who suggest that Tarim—not the tectonic blocks within the Tibetan plateau—was subducted beneath Tibet in the Cenozoic. There are several arguments against that suggestion. First, no substantial foreland basin deposits were developed along the entire length of the Altyn Tagh fault at the southern edge of Tarim, which is in contact with Tibet (Li et al 1996). Second, if the highly potassic volcanism in northern Tibet was induced by the subduction of Tarim, then the Pulu basalts (Figure 2) lie directly along the trace of subduction. This geometry is incompatible with the subduction of Tarim as a cause for the volcanism. The mixed old ($\sim$35 Ma) and young (20–0 Ma) ages of volcanism in northern areas of central Tibet preclude a proposed northward younging of volcanism related to a northward propagation of the Tibetan plateau uplift (Matte et al 1996, Meyer et al 1998). However, the wide age distribution of syn-collisional volcanism in Tibet does not preclude the possibility of viscous heating in the

upper mantle during the development of the Cenozoic Himalayan-Tibetan orogen (Kincaid & Silver 1996).

DEFORMATION OF THE DEEP CRUST AND THE UPPER MANTLE IN THE HIMALAYAN-TIBETAN OROGEN

Establishing the three-dimensional geometry of crustal and lithospheric structures is a key to understanding the evolution of the Himalayan-Tibetan orogen. Although the broad characteristics of crustal and upper mantle seismic velocity distribution for the Himalaya and Tibet have been constrained by many regional studies, using seismic stations mostly outside the Tibetan plateau (Liu et al 1990, Bourjot & Romanowics 1992, Curtis & Woodhouse 1997, Curtis et al 1998, Griot et al 1998), the poor spatial resolution of these studies prevents them from being linked to specific structures within the region. Since the early 1990s, several experiments have been conducted using seismological arrays across central and southern Tibet; these experiments provided new constraints on regional phase propagation in the crust and the mantle (McNamara et al 1994), shear wave anisotropy of the upper mantle (McNamara et al 1994, 1995; Herquell et al 1995; Hirn et al 1995; Guilbert et al 1996; Lave et al 1996; Sandvol et al 1997), and deep crustal and lithospheric structures across the Himalaya and southern Tibet (Nelson et al 1996, Owens and Zandt 1997, Yuan et al 1997, Makovsky et al 1996, Alsdorf et al 1998, Hauck et al 1998). In addition to the tomographic study across the central Altyn Tagh fault (Wittlinger et al 1998), seismic refraction and reflection investigations have also been carried out in northern Tibet and the western Kunlun Shan (Gao et al 1999a,b). In the following section, we address some of the major issues raised by these recent seismologic studies.

Subduction of the Indian Continental Lithosphere Beneath Tibet

It has long been speculated that the Indian shield may have been underthrust beneath Asia (Argand 1924, Powell & Conaghan 1973, Ni & Barazangi 1984, Beghoul et al 1993, Jin et al 1996). This hypothesis contrasts with the models of wholesale lithospheric thickening (Dewey & Burke 1973, Dewey et al 1988, Kincaid & Silver 1996) and crustal thickening via lower crustal flows (Zhao & Morgan 1987, Royden 1996, Royden et al 1997). Using surface wave phase velocity inversion, Curtis & Woodhouse (1997) suggest that the Indian lithosphere could have been subducted beneath the entire plateau if its average velocity was reduced by alteration or if its thickness was only ~85 km. Studies of shear wave anisotropy in central and southern Tibet (McNamara et al 1994, 1995; Herquell

et al 1995; Hirn et al 1995; Guilbert et al 1996; Sandvol et al 1997) consistently show a broad boundary (<100 km wide) within the Qiangtang terrane that separates a southern region (with undetectable to weak anisotropy) from a northern region (with strong anisotropy) as measured by shear wave birefringence. Chen & Ozalaybey (1998) found that this boundary correlates with a local high Bouguer gravity anomaly, indicating mass excess at depth. They interpreted the boundary to mark the northern edge of the subducted Indian mantle lithosphere beneath Tibet in the central Qiangtang (33°N).

Owens & Zandt (1997) suggest that the Indian continental lithosphere was subducted beneath the Tibetan crust at a low angle, implying that the southern Tibetan mantle lithosphere was pushed northward below central and northern Tibet. Their suggestion is based on observation of a high P-wave velocity (7.2–7.5 km/s) in the lower crust at depths of 60–75 km beneath the Lhasa terrane and the northernmost part of the Himalaya south of the Indus-Yalu suture. They interpret that velocity as reflecting tectonic underplating of the Indian lower crust onto the Tibetan crust. However, this high-velocity layer, most likely of mafic or intermediate composition, is located directly below the Gangdese batholith in southern Tibet, and could have been generated alternatively by magmatic underplating during the emplacement of the late Cretaceous to early Tertiary plutons by a process similar to that observed in the Basin and Range province of the western United States during the Late Cenozoic (Gans et al 1989).

In contrast to the flat subduction model of Owens & Zandt (1997), Kosarev et al (1998) suggested that the Indian mantle lithosphere plunged into the Tibetan mantle with a northward dip. This proposal is based on *P*-to-*S* converted teleseismic waves recorded by temporary broadband networks, and also shows that the mantle lithosphere of the Qaidam basin may have been subducted southward beneath central Tibet. The postulated southward subducted mantle lithosphere beneath the lithosphere in central Tibet exhibits a different form—it is highly imbricated, in contrast to the more coherent conversion boundary in the south that is suggested to represent subduction of the Indian mantle lithosphere.

Reflection seismological studies across the Himalaya and southern Tibet have indicated that major structures in the Himalaya—such as the Main Boundary Thrust and the Main Central Thrust—all sole into a common decollement, the Main Himalayan Thrust, which dips at about 7° to the north between 20 km depth at the crest of the High Himalaya and 40 km depth approximately 70 km south of the Indus-Yalu suture (Zhao et al 1993). Linear projection of the Main Himalayan Thrust northward implies that the Indian crust underthrusts the surface expression of the Indus-Yalu suture within the Tibetan crust. However, the exact geometry of the subducted Indian continental crust north of the Indus-Yalu suture is not well constrained (Nelson et al 1996, Makovsky et al 1996). The minimum amount of crustal shortening of 330 km across the Himalaya implies that the Indian mantle lithosphere underthrusts beneath Tibet to at least 32°N (Hauck et al 1998).

Shear-Wave Anisotropy

Studies of the shear wave anisotropy using different station spacing between 30 and 100 km show remarkably consistent results (McNamara et al 1994, 1995; Herquell et al 1995; Hirn et al 1995; Guilbert et al 1996; Lave et al 1996; Sandvol et al 1997). In general, the direction of fast polarization is approximately east-west to east-northeast–west-southwest between Lhasa and Golmud (Figure 2). Lave et al (1996) suggest that the anisotropy was induced by shearing within the asthenosphere as a result of eastward extrusion of the Tibetan lithospheric block, because the direction of the fast polarization beneath Tibet is similar to the present-day direction of motion of the Tibetan crust relative to stable Eurasia. In contrast, McNamara et al (1994) and Silver (1996) attributed the seismic anisotropy to deformation of the Tibetan mantle lithosphere related to Cenozoic north-south shortening. This implies that the fabric recorded by seismic anisotropy is a result of finite strain accumulated over a long geologic interval (Davis et al 1997). Because the strain path for deformation of the Tibetan lithosphere is unconstrained (for example, we do not know the initial state of finite strain in the Tibetan mantle lithosphere prior to the Indo-Asian collision), relating various contributing factors at different geologic times to the observed total strain always renders non-unique solutions.

Bright Spots

Seismic bright spots have been widely observed in the southern Tibetan crust at a depth of about 15 km during the reflection seismological surveys conducted by Project INDEPTH; these bright spots have been interpreted to indicate the presence of a partially molten lower crust beneath Tibet (Nelson et al 1996, Brown et al 1996, Kind et al 1996). This interpretation is disputed by Makovsky & Klemperer (1999), who performed a systematic modeling of reflection-amplitude variation with offset. The results of their study indicate that the bright spots in the Tibetan crust may instead represent the presence of relatively large quantities of free aqueous fluids. The presence of seismicity at upper mantle depths of 80–110 km in southern Tibet, near the seismic reflection profiles of Project INDEPTH, indicates that the upper mantle is cold enough to experience brittle deformation. An extremely high thermal gradient in the Tibetan crust would be required to create extensive melts in the Tibetan crust—a situation considered unlikely by Makovsky & Klemperer (1999).

Low Velocity Zone in Northern Tibet

The crust of northern Tibet in the Songpan-Ganzi-Hoh Xil terrane and the northern part of the Qiangtang terrane appears to have a low S-wave velocity and a high Poisson's ratio (McNamara et al 1994, Owens & Zandt 1997). These observations have been interpreted as indicating that the lower crust of the central Tibetan region is undergoing partial melting. This interpretation is consistent with

the observation that *Pn* velocity is low and *Sn* waves are absent or inefficiently transmitted in the upper mantle of central Tibet (McNamara et al 1994). The Songpan-Ganzi-Hoh Xil terrane consists of thick sections of flysch complexes, which are mostly pelites deposited in a deep marine setting (Figure 2). These rocks would significantly lower the seismic velocities and exhibit high Poisson's ratio, because they are easily deformable. The high Poisson's ratio in the northern Qiangtang terrane could be related to the subduction of the Songpan-Ganzi-Hoh Xil terrane (Yin et al 1998a, Kapp et al 1999a). Dehydration reactions in the flysch complex—which may have been underthrust to depths of 60–80 km by Mesozoic thrusting (Yin et al 1998a, Kapp et al 1999a) and by thrusting along Cenozoic thrust faults such as the Fenghuo Shan–Nangqian and the Qimen Tagh–North Kunlun thrust systems (Figures 2 and 3)—may have produced large quantities of free water in the central Tibetan crust. These fluids may have assisted partial melting in northern Tibet, as expressed by the widespread volcanism (Figure 7).

SUMMARY

1. Our synthesis shows that at least 1400 km of north-south shortening has been absorbed by the Himalayan-Tibetan orogen since the onset of the Indo-Asian collision at about 70 Ma. This amount of shortening is distributed as follows: $>$360 km across the Himalaya, $>$60 km across the Gangdese thrust system, $\sim$250 km along the Shiquanhe-Gaize-Amdo thrust system, $>$60–80 km across the Fenghuo Shan-Nangqian fold and thrust belt, $\sim$270 km across the Qimen Tagh–North Kunlun thrust system, and $\sim$360 km across the Nan Shan thrust belt. The shortening is expressed in two modes at the surface: (*a*) discrete thrust belts with relatively narrow zones of contraction or regional decollement (e.g. the Main Central Thrust, the Qimen Tagh–North Kunlun thrust system, and the Shiquanhe-Gaize-Amdo thrust system), and (*b*) distributed shortening over a wide region involving basement rocks (the Nan Shan thrust belt and the western Kunlun thrust system).
2. The crustal shortening, which has led to eventual construction of the Tibetan plateau, began at the same time in the early Paleocene ($>$50 Ma) in the Tethyan Himalaya to the south and in the Nan Shan and Qilian Shan some 1400 km to the north. This indicates that the plateau has been constructed between the northern Qilian suture zone and the northern margin of the Indian continent without sequential propagation from south to north.
3. The Paleozoic and Mesozoic tectonic histories in the Himalayan-Tibetan orogen have exerted a strong control over the Cenozoic strain history and strain distribution in the region. First, the Cenozoic thrust belts are commonly developed along or near major suture zones. Second, the presence of extensive Triassic flysch complex as in the Songpan-Ganzi-Hoh Xil and the Qiangtang

can be spatially correlated with Cenozoic volcanism and thrusting in central Tibet. Third, the distribution of basement-involved thrust faults in the Nan Shan and western Kunlun Shan closely follows earlier tectonic belts produced by Paleozoic to early Mesozoic arc-continent collisional tectonics. Finally, the extensive Middle Cretaceous crustal shortening in the Lhasa terrane may explain why this terrane has behaved more or less as a rigid block during the Cenozoic Indo-Asian collision.

4. The Early Cenozoic tectonic history of the Himalayan-Tibetan orogen has guided the Late Cenozoic strain distribution and petrogenesis in the Himalayan region. The onset of thrusting along the Main Himalayan Thrust may have been delayed until the Late Cenozoic by the accommodation of convergence elsewhere in the orogen. Thickening of the Greater Himalaya during the Eocene-Oligocene appears to have produced a stratified metamorphic sequence with depth. Late Cenozoic slip on the shallow dipping Main Himalayan Thrust has produced the unique spatial and temporal variations of Himalayan granite emplacement.
5. The main strike-slip faults in the western part of the Himalaya orogen are transfer faults linking either major thrust belts (the Altyn Tagh system) or extensional systems (the Karakorum fault). The Altyn Tagh fault consists of at least two main strands. The northern strand was mainly developed prior to the early Oligocene, although segments of the fault remain active. It has at least 60–80 km of left slip, and offset could have as much as 120 km. The southern strand is currently active. It has about 550 km left-slip offset in its western segment and about 280 km offset in its eastern segment. The differential slip has been absorbed by the Qimen Tagh-North Kunlun thrust system, along the southern edge of the Qaidam basin. Considering both strands together, the total slip along the Altyn Tagh fault system in the Cenozoic exceeds 600 km.

   The Karakorum fault in western Tibet and the Pamir developed as a result of northward indentation of Pamir into Asia. That indentation created the Pamir arc, which induced clockwise rotation of the western Kunlun Shan on its eastern limb and counterclockwise rotation on its western limb in western Pamir. As the Pamir arc lengthens and expands, the right-slip Karakorum fault extends farther both to the north and to the south. Its currently active strand terminates at the Kongur Shan detachment fault system in the north and the Purang-Gurla Mandhata extensional system in the south. Karakorum fault slip is no more than 200 km, and only a few tens of kilometers at its southern end. The Kunlun fault in central Tibet also serves as a transfer structure, transferring eastward spreading of the Tibetan plateau into both east-west contraction along the Longmen Shan fold and thrust belt and east-west extension in North China to the east.

   In the eastern part of the Himalayan-Tibetan orogen, strike-slip faulting along the Ailao Shan and Gaoligong shear zones accommodated several hundreds of southeastward extrusions of the Indochina block during the mid-Tertiary. The relative importance of this extrusion compared to that of block

rotation at both regional and local scales, and compared to the magnitude of internal deformation within the extruding block, remains uncertain.

6. The initiation of the Indo-Asian collision, defined by the elimination of the oceanic lithosphere, may have started as early as the late Cretaceous. This implies that the magnitude of convergence between India and Asia may be much greater than was previously thought.
7. Although some geophysical studies have inferred, based simply on geometric arguments, that the Indian continental crust did not subduct beneath the Tibetan lithosphere, the occurrence of syn-collisional calc-alkline type volcanism in southern and central Tibet appears to require that some portion of the continental crusts from both north and south must have been subducted into the mantle beneath Tibet.
8. At least five different mechanisms may have been responsible for the generation of syn-collisional igneous activity: (*a*) early crustal thickening followed by slip along a shallow dipping decollement (Himalayan leucogranites), (*b*) slab break-off during the early stage of the Indo-Asian collision (Linzizong volcanic sequence in southern Tibet), (*c*) continental subduction in southern and central Tibet, which generated calc-alkline magmatism, (*d*) formation of releasing bends and pull-apart structures that serve both as a possible mechanism to generate decompressional melting and as conduits to tap melts (Pulu basalts and other late Neogene-Quaternary volcanic flows along the Altyn Tagh and the Kunlun faults), and (*e*) viscous dissipation in the upper mantle and subduction of Tethyan flysch complexes to mantle depths may be the fundamental cause for widespread and protracted partial melting in the Himalayan-Tibetan orogen in the Cenozoic.
9. The marked difference in seismic properties of the crust and the upper mantle between southern and central Tibet is a result of both Mesozoic and Cenozoic tectonics. The former, however, has played the decisive role. The presence of extensive exposed melanges and flysch complexes in central Tibet localized Tertiary contractional deformation, which in turn has led to the release of a large quantity of free water into the upper mantle and the lower crust of central Tibet, causing extensive partial melting.

ACKNOWLEDGMENTS

We thank our students Liz Catlos, Eric Cowgill, Jessica D'Andrea, Mike Murphy, Paul Kapp, Peter Rumelhart, Matt Spurlin, and Mike Taylor, who participated in many field expeditions in the Himalayan and Tibetan regions; these studies provided the fundamental basis for this paper. We also thank our Chinese colleagues Chen Xunhua, Chen Zhengle, Din Ling, Wang Xiaofeng, and Zhang Qing for many years of collaborative research in China. Discussions with Deng Wanming, Pan Yusheng, and numerous other colleagues from both the United States and China honed the ideas presented here. Critical review by Kevin Burke greatly improved the original draft. This work was supported by grants from the National Science Foundation.

LITERATURE CITED

Allègre, CJ and 34 others. 1984. Structure and evolution of the Himalayan-Tibet orogenic belt. *Nature* 307:17–22

Allen CR, Gillespie AR, Han Y, Sieh KE, Zhang B, Zhu C. 1984. Red River and associated faults, Yunnan province, China: Quaternary geology, slip rates, and seismic hazard. *Geol. Soc. Am. Bull.* 95:686–700

Alsdorf D, Brown L, Nelson KD, Makovsky Y, Klemperer S, Zhao WJ. 1998. Crustal deformation of the Lhasa terrane, Tibet plateau from Project INDEPTH deep seismic reflection profiles. *Tectonics* 17:501–19

Argand E. 1924. La tectonique de l' Asie, *Proc. 13th Int. Geol. Congr.* 7:171–372

Arita K. 1983. Origin of the inverted metamorphism of the Lower Himalayas, central Nepal. *Tectonophysics* 95:43–60

Armijo R, Tapponnier P, Han T. 1989. Late Cenozoic right-lateral strike-slip faulting in southern Tibet. *J. Geophys. Res.* 94:2787–838

Armijo R, Tapponnier P, Mercier JL, Han T-L. 1986. Quaternary extension in southern Tibet: field observations and tectonic implications. *J. Geophys. Res.* 91:13803–72

Arnaud N, Vidal Ph. 1990. Geochronology and geochemistry of the magmatic rocks from the Kunlun-Karakorum geotraverse. *Colloque Kunlun-Karakorum*, IGP, Paris. 52 pp.

Arnaud NO, Vidal Ph, Tapponnier P, Matte P, Deng WM. 1992. The high K_2O volcanism of northwestern Tibet: geochemistry and tectonic implications. *Earth Planet. Sci. Lett.* 111:351–67

Arne D, Worley B, Wilson C, Chen SF, Foster D, et al. 1997. Differential exhumation in response to episodic thrusting along the eastern margin of the Tibetan Plateau. *Tectonophys.* 280:239–56

Avouac JP. 1993. Analysis of scarp profiles, evaluation of errors in morphological dating. *J. Geophys. Res.* 98:6745–54

Avouac JP, Burov EB. 1996. Erosion as a driving mechanism of intracontinental mountain growth. *J. Geophys. Res.* 101:17747–69

Avouac JP, Peltzer G. 1993. Active tectonics of southern Xinjiang, China: analysis of terrace risers and normal fault scarp degradation along the Hotan-Qira fault system. *J. Geophys. Res.* 98:21773–807

Avouac JP, Tapponnier P. 1993. Kinematic model of active deformation in central Asia. *Geophys. Res. Lett.* 20:895–98

Bally AW, Chou I-M, Clayton R, Eugster HP, Kidwell S, et al. 1986. Notes on sedimentary basins in China—report of the American Sedimentary Basins delegation to the People's Republic of China. *USGS Open File Report* 86-327. 108 pp.

Bazhenov ML, Perroud H, Chauvin A, Burtman VS, Thomas JC. 1994. Paleomagnetism of Cretaceous red beds from Tadzhikistan and Cenozoic deformation due to India-Eurasia collision. *Earth Planet. Sci. Lett.* 124:1–18

Beaumont C, Fullsack P, Hamilton J. 1992. Erosional control of active compressional orogens. In *Thrust Tectonics*, ed. KR McClay, pp. 1–18. New York: Chapman & Hall

Beck RA, Burbank DW, Sercombe WJ, Riley GW, Barndt JK, et al. 1995. Stratigraphic evidence for an early collision between northwest India and Asia. *Nature* 373:55–58

Beghoul N, Barzangi M, Isack B. 1993. Lithospheric structure of Tibet and western North America: mechanisms of uplift and a comparative study. *J. Geophys. Res.* 98:1997–2016.

Bendick R, Bilham R, Yin G, Larson K, Peltzer G, Freymueller J. 1998. Slip rate of the Altyn Tagh Fault at 90 degrees east. *Eos* 79:F207

Besse J, Courtillou V, Possi JP, Westphal M, Zhou YX. 1984. Paleomagnetic estimates of crustal shortening in the Himalayan thrusts and Zangbo suture. *Nature* 311:621–26

Bilham R, Larson K, Freymueller J, Project Idylhim members. 1997. GPS measurements of present-day convergence across the Nepal Himalaya. *Nature* 386:61–64

Bird P. 1978. Initiation of intracontinental subduction in the Himalaya. *J. Geophys. Res.* 83:4975–87

Blisniuk PM, Siwen S, Kuchel O, Ratschbacher L. 1998. Late Neogene extension in the Shuang Hu graben, central Tibet. *Eos* 79:794

Bouchez JL, Pêcher A. 1981. The Himalayan Main Central Thrust pile and its quartz-rich tectonites in central Nepal. *Tectonophysics* 78:23–50

Bourjot L, Romanowiczs B. 1992. Crust and upper mantle tomography in Tibet using surface waves. *Geophys. Res. Lett.* 19:881–84

Briais A, Patriat P, Tapponnier P. 1993. Updated interpretation of magnetic anomalies and seafloor spreading stages in the South China Sea: implications for the Tertiary tectonics of SE Asia. *J. Geophys. Res.* 98:6299–328

Brookfield ME. 1993. The Himalayan passive margin from Precambrian to Cretaceous. *Sedimentary Geol.* 84:1–35

Brown LD, Zhao W, Nelson KD, Hauck M, Alsdorf D, et al. 1996. Bright spots, structure, and magmatism in Southern Tibet from INDEPTH seismic reflection profiling. *Science* 274:1688–91

Bruguier O, Lancelot JR, Malavieille J. 1997. U-Pb dating on single detrital zircon granites from the Triassic Songpan-Ganzi flysch (Central China); provenance and tectonic correlations. *Earth Planet. Sci. Lett.* 152:217–31

Burbank DW, Beck RA, Mulder T. 1996. The Himalayan foreland basin. In *The Tectonics of Asia*, ed. A Yin, TM Harrison, pp. 149–88. New York: Cambridge University Press

Burchfiel BC, Chen Z, Hodges KV, Liu Y, Royden LH, et al. 1992. The South Tibetan Detachment System, Himalayan orogen: extension contemporaneous with and parallel to shortening in a collisional mountain belt. *Geol. Soc. Am. Spec. Pap.* 269:1–41

Burchfiel BC, Chen Z, Liu Y, Royden LH. 1995. Tectonics of the Longmen Shan and adjacent regions, central China. *Int. Geol. Rev.* 37:661–735

Burchfiel BC, Chen Z, Royden LH, Liu Y, Deng C. 1991. Extensional development of Gabo valley, southern Tibet. *Tectonophysics* 194:187–93

Burchfiel BC, Deng Q, Molnar P, Royden LH, Wang Y, et al. 1989b. Intracrustal detachment with zones of continental deformation. *Geology* 17:748–52

Burchfiel BC, Molnar P, Zhao Z, Linag K, Wang S, et al. 1989a. Geology of the Ulugh Muztagh area, northern Tibet. *Earth Planet. Sci. Lett.* 94:57–70

Burchfiel BC, Royden LH. 1991. Tectonics of Asia 50 years after the death of Emile Argand. *Ecologae Geol. Helv.* 84:599–629

Burg JP, Brunel M, Gapais D, Chen GM, Liu GH. 1984. Deformation of leucogranites of the crystalline Main Central Sheet in southern Tibet (China). *J. Struct. Geol.* 6:535–42

Burg JP, Chen GM. 1984. Tectonics and structural formation of southern Tibet, China. *Nature* 311:219–23

Burtman VS, Molnar P. 1993. Geological and geophysical evidence for deep subduction of continental crust beneath the Pamir. *Geol. Soc. Am. Special Paper* 281:1–76

Chang C-F, Zheng S-L. 1973. Tectonic features of the Mount Jolmo Lungma region in southern Tibet, China. *Scientia Geologica Sinica.* 1:1–12

Chen H, Dobson J, Heller F, Hao J. 1995. Paleomagnetic evidence for clockwise rotation of the Simao region since the Cretaceous: a consequence of India-Asia

collision. *Earth Planet. Sci. Lett.* 134:203–17

Chen SF, Wilson CJL, Deng QD, Zhao XL, Luo ZL. 1994. Active faulting and block movement associated with large earthquakes in the Min Shan and Longmen Mountains, northeastern Tibetan plateau. *J. Geophys. Res.* 99:24025–38

Chen W-P, Kao H. 1996. Seismotectonics of Asia: some recent progress. In *The Tectonic Evolution of Asia*, ed. A Yin, TM Harrison, pp. 37–52. Cambridge, UK: Cambridge Univ. Press

Chen W-P, Ozalaybey S. 1998. Correlation between seismic anisotropy and Bouguer gravity anomalies in Tibet and its implications for lithospheric structures. *Geophys. J. Int.* 135:93–101

Chen Y, Cogne J-P, Courtillot V. 1992. New Cretaceous paleomagnetic results from the Tarim basin, northwestern China. *Earth Planet. Sci. Lett.* 114:17–38

Chen Y, Cogne J-P, Courtillot V, Tapponnier P, Zhou XY. 1993. Cretaceous paleomagnetic results from western Tibet and tectonic implications. *J. Geophys. Res.* 98:17981–18000

Cheng J, Xu G. 1986. Unpublished geologic map of the Gaize region at a scale of 1:1000,000 and the geologic report, Xizang Bureau of Geology and Mineral Resources, p. 369 (in Chinese)

Cheng J, Xu G. 1987a. Unpublished geologic map of the Gedake region at a scale of 1:1000,000 and the geologic report, Xizang Bureau of Geology and Mineral Resources, p. 363 (in Chinese)

Cheng J, Xu G. 1987b. Unpublished geologic map of the Ritu region at a scale of 1:1000,000 and the geologic report, Xizang Bureau of Geology and Mineral Resources, p. 598 (in Chinese)

Cheng YQ. 1994. *Outline of Chinese Regional Geology.* Beijing: Geologic Publishing House. 517 pp. (in Chinese)

Chung, S-L, Lo C-C, Lee T-Y, Zhang Y, Xie Y, et al. 1998. Diachronous uplift of the Tibetan plateau starting 40 Myr ago. *Nature* 394:769–73

Cogan MJ, Nelson KD, Kidd WSF, Wu CD. 1998. Shallow structure of the Yadong-Gulu rift, southern Tibet, from refraction analysis of Project INDEPTH common midpoint data. *Tectonics* 17:46–61

Colchen M, Bassoullet JP, Mascle G. 1982. La paleogeographie des orogenes, l'example de l'Himalaya. *Mem. Geol. l'Univ. Dijon.* 7:453–71

Coleman ME. 1998. U-Pb constraints on Oligocene-Miocene deformation and anatexis within the central Himalaya, Marsyandi valley, Nepal. *Am. J. Sci.* 298:553–71

Coleman ME, Hodges KV. 1995. Evidence for Tibetan Plateau uplift before 14 Myr ago from a new minimum estimate for east-west extension. *Nature* 374:49–52

Coleman ME, Parrish RR. 1995. Constraints on Miocene high-temperature deformation and anatexis within the Greater Himalaya from U-Pb geochronology. *EOS* 76:F708

Copeland P, Harrison TM, Hodges KV, Maréujol P, Le Fort P, Pêcher A. 1991. An Early Pliocene thermal perturbation of the Main Central Thrust, Central Nepal: implications for Himalayan tectonic. *J. Geophys. Res.* 96:8475–500

Coulon C, Maluski H, Bollinger C, Wang S. 1986. Mesozoic and Cenozoic volcanic rocks from central and southern Tibet: $^{39}Ar/^{40}Ar$ dating, petrological characteristics and geodynamical significance. *Earth Planet. Sci. Lett.* 79:281–302

Coward MP and 9 others. 1988. Folding and imbrication of the Indian crust during Himalayan collision. *Phil. Trans. R. Soc. Lond.* A326:89–116

Cowgill E, Yin A, Rumelhart P, Foster D, Chen Z, Wang XF. 1998. Magnitude and timing of Cenozoic Shortening in the W Kunlun Shan. *EOS* 79:F816

Cowgill E, Yin A, Rumelhart P, Wang XF, Zhang Q. 1997. Kinematics of the Central Altyn Tagh Fault System, NW China. *EOS* 78:173

Cowgill E, Yin A, Wang XF, Zhang Q. 1999. Late Cenozoic left-reverse slip movement along the Northern Altyn Tagh Fault and its possible development as the northern

boundary of a transpressional strike-slip duplex. *Geology.* In review

Crowell JC. 1962. Displacement along the San Andreas fault, California. *Geol. Soc. Am. Spec. Pap.* 71:1–61

CSBS (Chinese State Bureau of Seismology). 1992. *The Altyn Tagh Active Fault System.* Beijing: Seismology Publishing House. 319 pp.

Curtis A, Trampert J, Snieder R, Dost B. 1998. Eurasian fundamental mode surface wave phase velocities and their relationship with tectonic structures. *J. Geophys. Res.* 103:26919–47

Curtis A, Woodhouse JH. 1997. Crust and upper mantle shear velocity structure beneath the Tibetan plateau and surrounding regions from interevent surface wave phase velocity inversion. *J. Geophys. Res.* 102:11789–813

D'Andrea J, Harrison TM, Grove M. 1999. The thermal and physical state of the South Tibetan middle crust between 20–8 Ma: U-Th-Pb and Nd isotopic evidence from the Nyainqentanglha Massif. In *14th Himalaya-Karakorum-Tibet Workshop,* Abstract volume, pp. 29–30. Germany: Kloster Ettal

Davis P, England P, Houseman G. 1997. Comparison of shear wave splitting and finite strain from the India-Asia collision zone. *J. Geophys. Res.* 102:27511–22

Davy Ph, Cobbold P. 1988. Indentation tectonics in nature and experiment, 1. Experiments scaled for gravity. *Bull. Geol. Inst., Univ. Uppsala* 14:129–41

Delvaux D, Moeys R, Stapel G, Petit C, Levi K, et al. 1997. Paleostress reconstructions and geodynamics of the Baikal region, Central Asia, Part 2. Cenozoic rifting. *Tectonophysics* 282:1–38

Deng W. 1989. Cenozoic volcanic rocks in the northern Ngari district of the Tibet—Discussion on the concurrent subduction. *Acta Petrol. Sin.* 3:1–11 (in Chinese)

Deng W. 1996. The ophiolites of the geotraversers from Yecheng to Shiquanhe. In *Geological Evolution of the Karakorum and Kunlun Mountains,* ed. P Yusheng, pp. 51–93. Beijing: Seismological Press

Deng W. 1998. *Cenozoic Intraplate Volcanic Rocks in the Northern Qinghai-Xizang Plateau.* Beijing: Geologic Publishing House. 180 pp. (in Chinese with English abstract)

Deng W, Yin J, Guo Z. 1996a. Basic-ultramafic and volcanic rocks in Chagbu-Shuanghu area of northern Xizang (Tibet), China. *Sci. China (Series D)* 39:359–68

Deng W, Zheng X, Matsumoto Y. 1996b. Petrological characteristics and ages of Cenozoic volcanic rocks from the Hoh Xil Mountains, Qinghai. *Acta Petrol. Miner.* 15:289–98 (in Chinese with English abstract)

Deverchere J, Houdry F, Diament M. 1991. Evidence for seismogenic upper mantle and lower crust in the Baikal rift. *Geophys. Res. Lett.* 18:1099–102

Dewey JF, Burke K. 1973. Tibetan, Variscan and Precambrian basement reactivation: products of continental collision. *J. Geol.* 81:683–92

Dewey JF, Cande S, Pitman WC. 1989. Tectonic evolution of the India-Eurasia collision zone. *Ecol. Geol. Helv.* 82:717–34

Dewey JF, Shackelton RM, Chang C, Sun Y. 1988. The tectonic evolution of the Tibetan Plateau. *Phil. Trans. R. Soc. Lond.* A327:379–413

Dickinson WR. 1996. Kinematics of transrotational tectonism in the California Transverse Ranges and its contribution to cumulative slip along the San Andreas transform fault system. *Geol. Soc. Am. Spec. Pap.* 305:1–46

Dickinson WR, Wernicke BP. 1997. Reconciliation of San Andreas slip discrepancy by a combination of interior Basin-Range extension and transrotation near the coast. *Geology* 25:663–65

Ding D, Wang D, Liu W, Sun S. 1996. *The Western Kunlun Orogenic Belt and Basin.* Beijing: Geologic Publishing House. 230 pp.

Durr SB. 1996. Provenance of Xigaze fore-arc basin clastic rocks (Cretaceous, south Tibet). *Geol. Soc. Am. Bull.* 108:669–84

Edwards MA, Harrison TM. 1997. When did the roof collapse? Late Miocene N-S extension in the High Himalaya revealed by Th-Pb monazite dating of the Khula Kangri granite. *Geology* 25:543–46

Edwards MA, Kidd WSF, Li J, Yue Y, Clark M. 1996. Multi stage development of the southern Tibet detachment system near Khula Kangri. New data from Gonto La. *Tectonophys.* 260:1–20

England P, Houseman G. 1986. Finite strain calculations of continental deformation 2. Comparison with the India-Asia collision zone. *J. Geophys. Res.* 91:3664–76

England P, Houseman G. 1989. Extension during continental convergence, with application to the Tibetan Plateau. *J. Geophys. Res.* 94:17561–69

England P, Le Fort P, Molnar P, Pêcher A. 1992. Heat sources for Tertiary metamorphism and anatexis in the Annapurna-Manaslu region, Central Nepal. *J. Geophys. Res.* 97:2107–28

England P, Molnar P. 1993. The interpretation of inverted metamorphic isograds using simple physical calculations. *Tectonics* 12:145–57

England P, Molnar P. 1998. The field of crustal velocity in Asia calculated from Quaternary rates of slip on faults. *Geophys. J. Int.* 130:551–82

Fang A, Li J, Hou Q, Zhou H, Wan S, Li H. 1998. The first discovery of radiolarian fossils in Yixikegou flysch section of Kuda, west Kunlun, China. *Sci. Geol. Sin.* 33:300

Fletcher RC, Hallet B. 1983. Unstable extension of the continental lithosphere: a mechanical model for Basin-and-Range structure. *J. Geophys. Res.* 88:7457–66

Gaetani M, Garzanti E. 1991. Multicyclic history of the northern India continental margin (northwestern Himalaya). *Am. Assoc. Pet. Geol. Bull.* 75:1427–46

Gaetani M, Jadoul F, Erba E, Garzanti E. 1993. Jurassic and Cretaceous orogenic events in the North Karakorum: age constraints from sedimentary rocks. In *Himalayan Tectonics*, ed. PJ Treloar, MP Searle, 74:39–52. *Geol. Soc. Spec. Publ.*

Gans P, Mahood GA, Schermer E. 1989. Synextensional magmatism in the Basin and Range Province; a case study from the eastern Great Basin. *Geol. Soc. Am. Spec. Pap.* 233:1–53

Gansser A. 1964. *The Geology of the Himalayas.* New York: Wiley Interscience. 289 pp.

Gao R, Cheng X, Wu G. 1999b. Lithospheric structure and geodynamic model of the Golmud-Ejin transect in northern Tibet. In *Himalaya and Tibet: Mountain Roots to Mountain Tops*, ed. A Macfarlane, RB Sorkhabi, J Quade. *Geol. Soc. Am. Spec. Pap.* 328:9–17

Gao R, Li D, Lu D, Li Y, Huang D, et al. 1999a. Deep seismic reflection profiles across contact zone of Western Kunlun and Tarim along the Xinjiang geotransect in NW China. In *14th Himalaya-Karakorum-Tibet Workshop*, Abstract volume, pp. 49–50. Germany: Kloster Ettal

Gao S, Davis PM, Liu H, Slack PD, Zorin YA, et al. 1994. Asymmetric upwarp of the asthenosphere beneath the Baikal rift zone, Siberia. *J. Geophys. Res.* 99:15319–30

Girardeau J, Marcous J, Allegre CJ, Bassoullet JP, Tang Y, et al. 1984. Tectonic environment and geodynamic significance of the Neo-Cimmerian Donqiao ophiolite, Bangong-Nujiang suture zone, Tibet. *Nature* 307:27–31

Grasemann B, Vannay J-C. 1999. Flow controlled inverted metamorphism in shear zones. *J. Struct. Geol.* 21:743–50

Griot D-A, Mantagner J-P, Tapponnier P. 1998. Phase velocity structure from Rayleigh and Love waves in Tibet and its neighboring regions. *J. Geophys. Res.* 103:21215–32

Gu XX 1994. Geochemical characteristics of the Triassic Tethys-turbidites in northwestern Sichuan, China: implications for provenance and interpretation of the tectonic setting. *Geochim. Cosmochim. Acta* 58:4615–31

Guilbert J, Poupinet G, Jiang M. 1996. A study

of azimuthal P wave residuals and shear wave splitting across the Kunlun range (Northern Tibetan Plateau). *Phys. Earth Planet. Inter.* 95:167–74

Hacker BR, Wang X, Eide EA, Ratschbacher L. 1996. The Qinling-Dabie ultra-high pressure collisional orogen. In *The Tectonic Evolution of Asia*, ed. A Yin, TM Harrison, pp. 345–70. Cambridge, UK: Cambridge Univ. Press

Harris N, Massey J. 1994. Decompression and anatexis of Himalayan metapelites. *Tectonics* 13:1537–46

Harris NBW, Xu R, Lewis CL, Hawkeworth CJ, Zhang Y. 1988. Isotope geochemistry of the 1985 Tibet Geotraverse, Lhasa to Golmud. *Phil Trans. R. Soc. Lond.* A327:263–85

Harrison TM, Copeland P, Kidd WSF, Lovera OM. 1995b. Activation of the Nyainqentanghla shear zone: implications for uplift of the southern Tibetan Plateau. *Tectonics* 14:658–76

Harrison TM, Copeland P, Kidd WSF, Yin A. 1992. Raising Tibet. *Science* 255:1663–70

Harrison TM, Grove M, Lovera OM, Catlos EJ. 1998b. A model for the origin of Himalayan anatexis and inverted metamorphism. *J. Geophys. Res.* 103:27017–32

Harrison TM, Grove M, McKeegan KD, Coath CD, Lovera OM, Le Fort P. 1999a. Origin and episodic emplacement of the Manaslu instrusive complex, Central Himalaya. *J. Petrol.* 40:3–19

Harrison TM, Leloup PH, Ryerson FJ, Tapponnier P, Lacassin R, Chen W. 1996. Diachronous initiation of transtension along the Ailao Shan-Red River shear zone, Yunnan and Vietnam. In *The Tectonic Evolution of Asia*, ed. A Yin, TM Harrison, pp. 208–26. New York: Cambridge University Press

Harrison TM, Lovera OM, Grove M. 1997b. New insights into the origin of two contrasting Himalayan granite belts. *Geology* 25:899–902

Harrison TM, McKeegan KD, Le Fort P. 1995a. Detection of inherited monazite in the Manaslu leucogranite by $^{208}Pb/^{232}Th$ ion microprobe dating: crystallization age and tectonic significance. *Earth Planet. Sci. Lett.* 133:271–82

Harrison TM, Ryerson FJ, Le Fort P, Yin A, Lovera OM, Catlos EJ. 1997a. A Late Miocene-Pliocene origin for the Central Himalayan inverted metamorphism. *Earth Planet. Sci. Lett.* 146:E1–8

Harrison TM, Yin A, Grove M, Lovera OM, Ryerson FJ. 1999b. Displacement history of the Gangdese Thrust, Southeastern Tibet. *J. Geophys. Res.* In review

Harrison TM, Yin A, Ryerson FJ. 1998a. Orographic evolution of the Himalaya and Tibet. In *Tectonic Boundary Conditions for Climate Reconstructions*, ed. TJ Crowley, K Burke, pp. 39–72. New York: Oxford Univ. Press

Hauck ML, Nelson KD, Brown LD, Zhao WJ, Ross AR. 1998. Crustal structure of the Himalayan orogen at 90 degrees east longitude from Project INDEPTH deep reflection profiles. *Tectonics* 17:481–500

Heim A, Gansser A. 1939. *Central Himalaya Geological Observations of Swiss Expedition*, pp. 1–246. Zurich: Gebruder Fretz

Hennig A. 1915. Zur petrographie und geologie von sudwest Tibet. In *Southern Tibet*, Volume 5, ed. S Hedin. Stockholm: Norstedt. 220 pp.

Herquell G, Wittlinger G, Guilbert J. 1995. Anisotropy and crustal thickness of Northern-Tibet. New constraints for tectonic modeling. *Geophys. Res. Lett.* 22:1925–28

Herren E. 1987. Zanskar shear zone: Northeast-southwest extension within the Higher Himalaya. *Geology* 15:409–13

Hirn A, and 10 others. 1995. Seismic anisotropy as an indicator of mantle flow beneath the Himalayas and Tibet. *Nature* 375:571–74

Hodges KV, Bowring S, Davidek K, Hawkins D, Krol M. 1998. Evidence for rapid displacement on Himalayan normal faults and the importance of tectonic denudation in the evolution of mountain ranges. *Geology* 26:483–86

Hodges KV, Hames WE, Olszewski WJ,

Burchfiel BC, Royden LH, Chen Z. 1994. Thermobarometric and $^{40}Ar/^{39}Ar$ geochronologic constraints on Eohimalayan metamorphism in the Dinggy area, southern Tibet. *Contrib. Miner. Petrol.* 117:151–63

Hodges KV, Parrish RR. Searle MP. 1996. Tectonic evolution of the central Annapurna Range, Nepalese Himalayas. *Tectonics* 15:1264–91

Holt WE, Li M, Haines A. 1995. Earthquake strain rates and instantaneous relative motion within central and east Asia. *Geophys. J. Int.* 122:569–93

Honegger K, Dietrich V, Frank W, Gansser A, Thoeni M, Trommsdorff V. 1982. Magmatism and metamorphism in the Ladakh Himalaya (the Indus-Tsangpo suture zone). *Earth Planet. Sci. Lett.* 60:253–92

Hou L, Luo D, Fu D, Hu S, Li K. 1991. *Triassic Sedimentary-Tectonic Evolution in Western Sichuan and Eastern Xizang Region.* Beijing: Geologic Publishing House. 220 pp. (in Chinese with English summary)

Houseman G, England P. 1996. A lithospheric thickening model for the Indo-Asian collision. In *The Tectonic Evolution of Asia*, ed. A Yin, TM Harrison, pp. 3–17. New York: Cambridge Univ. Press

Hsu K and 15 others. 1995. Tectonic evolution of the Tibetan Plateau: a working hypothesis based on the archipelago model of orogenesis. *Int. Geol. Rev.* 37:473–508

Huang H, Huang Q, Ma Y. 1996. *Geology of Qaidam Basin and its Petroleum Prediction.* Beijing: Geological Publishing House. 257 pp.

Huang K, Opdyke ND. 1993. Paleomagnetic results from Cretaceous and Jurassic rocks of south and southwest Yunnan: evidence for large clockwise rotations in the Indochina and Shan-Thai-Malay terranes. *Earth Planet. Sci. Lett.* 117:507–24

Huang K, Opdyke ND, Li J, Peng X. 1992. Paleomagnetism of Cretaceous rocks from eastern Qiangtang terrane. *J. Geophys. Res.* 97:1789–99

Hubbard MS. 1996. Ductile shear as a cause of inverted metamorphism: example from the Nepal Himalaya. *J. Geol.* 104:493–99

Hubbard MS, Harrison TM. 1989. 40Ar/39Ar age constraints on deformation and metamorphism in the MCT Zone and Tibetan Slab, eastern Nepal Himalaya. *Tectonics* 8:865–80

Huerta AD, Royden LH, Hodges KV. 1996. The interdependence of deformational and thermal processes in mountain belts. *Science* 273:637–39

Hughes NC, Jell PA. 1999. Biostratigraphy and biogeography of Himalayan Cambrian trilobites. In *Himalaya and Tibet: Mountain Roots to Mountain Tops*, ed. A Macfarlane, RB Sorkhabi. *Geol. Soc. Am. Spec. Pap.* 328:109–16

Jacobson CE, Oyarzabal FR, Haxel GB. 1996. Subduction and exhumation of the Pelona-Orocopia-Rand schists, southern California. *Geology* 24:547–50

Jaeger J-J, Courtillot V, Tapponnier P. 1989. Paleontological view of the ages of the Deccan traps, the Cretaceous/Tertiary boundary and the India-Asia collision. *Geology* 17:316–19

Jia C. 1997. *Tectonic characteristics and petroleum: Tarim Basin, China.* Beijing: Petroleum Industry Press. 295 pp.

Jia C, Yao H, Wi G, Li L. 1991. Plate tectonic evolution and characteristics of major tectonic units of the Tarim basin. In *The Tarim Basin*, ed. X Tong, D Liang, pp. 207–25. Urumuqi: Xinjiang Scientific Publishing House (in Chinese)

Jiang C, Yang J, Feng B, Zhu Z, Zhao M, et al. 1992. *Opening-Closing Tectonics of Kunlun Mountains.* Beijing: Geologic Publishing House. 224 pp. (in Chinese with English abstract)

Jin Y, McNutt MK, Zhu YS. 1996. Mapping the descent of Indian and Eurasian plates beneath the Tibetan Plateau from gravity anomalies. *J. Geophys. Res.* 101:11275–90

Johnson NM, Opdyke ND, Johnson GD, Lindsay EH, Tahirkheli RAK. 1982. Magnetic polarity stratigraphy and ages of Siwalik

Group rocks of the Potwar Plateau, Pakistan. *Paleogeog. Paleoclimat. Paleoecol.* 37:17–42

Johnson NM, Stix J, Tauxe L, Cerveny PF, Tahirkheli RAK. 1985. Paleomagnetic chronology, fluvial processes, and tectonic implications of the Siwalik deposits near Chinji Village, Pakistan *J. Geol.* 93:27–40

Kapp P, Murphy MA, Yin A, Ding L. 1999b. Cenozoic shortening along the Banggong-Nujiang suture zone, central Tibet. In *14th Himalaya-Karakorum-Tibet Workshop*, Abstract volume, pp. 81–83. Germany: Kloster Ettal

Kapp P, Yin A, Manning CE, Murphy M, Harrison TM, et al. 1998. Post-mid-Cretaceous shortening along the Banggong-Nujiang suture and in west-central Qiangtang, Tibet. *EOS* 79:794

Kapp P, Yin A, Manning CE, Murphy M, Harrison TM, et al. 1999a. Blueschist-bearing metamorphic core complexes in the Qiangtang block reveal deep crustal structure of northern Tibet. *Geology.* In press

Kapp P, Yin A, Murphy M, Harrison TH, Ryerson FJ. 1997. Discovery of a major blue schist bearing detachment fault system in the Shuang Hu region of the Qiangtang block, northern Tibet. *Geol. Soc. Am. Abstr. Prog.* 29:144

Khan MA, Jan Q, Weaver BL. 1993. Evolution of the lower crust in Kohistan, N. Pakistan: temporal arc magmatism through early, mature and intra-arc rift stages. In *Himalayan Tectonics*, ed. PJ Treloar, MP Searle, 74:123–38. *Geol. Soc. Spec. Publ.*

Kidd WSF, Molnar P. 1988. Quaternary and active faulting observed on the 1985 Academia Sinica-Royal Society Geotraverse of Tibet. *Phil. Trans. R. Soc. Lond. A* 327:337–63

Kincaid C, Silver P. 1996. The role of viscous dissipation in the orogenic process. *Earth Planet. Sci. Lett.* 142:271–88

Kind R, Ni J, Zhao W, Wu J, Yuan X, et al. 1996. Evidence from earthquake data for a partially molten crustal layer in southern Tibet. *Nature* 274:1692–1694

King RW, Shen F, Burchfiel BC, Chen Z, Li Y, et al. 1997. Geodetic measurement of crustal motion in southwest China. *Geology* 25:1279–82

Klootwijk CT, Conaghan PJ, Nazirullah R, de Jong KA. 1994. Further palaeomagnetic data from Chitral (Eastern Hindukush): evidence for an early India-Asia contact. *Tectonophys.* 237:1–25

Klootwijk CT, Gee FS, Peirce JW, Smith GM, McFadden PL. 1992. An early India contact: paleomagnetic constraints from Ninetyeast Ridge, ODP Leg 121. *Geology* 20:395–98

Kong X, Bird P. 1996. Neotectonics of Asia: thin-shell, finite-element models with faults. In *The Tectonics of Asia*, ed. A Yin, TM Harrison, pp. 18–35. New York: Cambridge Univ. Press

Kong X, Yin A, Harrison TM. 1997. Evaluating the role of pre-existing weakness and topographic distributions in the Indo-Asian collision by use of a thin-shell numerical model. *Geology* 25:527–30

Kosarev G, Kind R, Sobolev SV, Yuan X, Hanka W, Oreshin S. 1998. Seismic evidence for a detached Indian lithospheric mantle beneath Tibet. *Science* 283:1306–9

Lacassin R, Replumaz A, Leloup PH. 1998. Hairpin river loops and slip-sense inversion on southeast Asian strike-slip faults. *Geology* 26:703–6

Larson K, Burgmann R, Bilham R, Freymueller JT. 1999. Kinematics of the India-Eurasia collision zone from GPS measurements. *J. Geophys. Res.* 104:1077–93

Lave J, Avouac JP, Laccassin R, Tapponnier P, Montagner JP. 1996. Seismic anisotropy beneath Tibet: evidence for eastward extrusion of the Tibetan lithosphere? *Earth Planet. Sci. Lett.* 140:83–96

Leeder MR, Smith AB, Yin J. 1988. Sedimentology, palaeoecology and palaeoenvironmental evolution of the 1985 Lhasa to Golmud Geotraverse. *Phil. Trans. R. Soc. Lond.* A327:107–43

Le Fort P. 1975. Himalayas, the collided range. Present knowledge of the continental arc. *Am. J. Sci.* 275A:1–44

Le Fort P. 1986. Metamorphism and magmatism during the Himalayan collision. In *Collision Tectonics*, ed. MP Coward, AC Ries. *Geol. Soc. Spec. Publ.* 19:159–72

Le Fort P. 1989. The Himalayan orogenic segment. In *Tectonic Evolution of the Tethyan Region*, ed. AMC Sengor, pp. 289–386. Berlin: Kluwer Acad.

Le Fort P. 1996. Evolution of the Himalaya. In *The Tectonics of Asia*, ed. A Yin, TM Harrison, pp. 95–106. New York: Cambridge Univ. Press

Le Fort P, Debon F, Sonet J. 1983. The lower Palaeozoic ''Lesser Himalaya'' granitic belt: emphasis on the Simchar pluton of Central Nepal. In *Granites of Himalayas, Karakorum and Hindu Kush*, ed. FA Shams, pp. 235–53. Lahore: Punjab Univ.

Leloup PH, Harrison TM, Ryerson FJ, Chen W, Li Q, et al. 1993. Structural, petrological and thermal evolution of a Tertiary ductile strike-slip shear zone, Diancang Shan (Yunnan, PRC). *J. Geophys. Res.* 98:6715–43

Leloup PH, Lacassin R, Tapponnier R, Zhong D, Lui X, et al. 1995. Kinematics of Tertiary left-lateral shearing at the lithospheric-scale in the Ailao Shan-Red River shear zone (Yunnan, China). *Tectonophysics* 251:3–84

Le Pichon X, Fournier M, Jolivet L. 1992. Kinematics, topography, shortening, and extrusion in the India-Eurasia collision. *Tectonics* 11:1085–98

Li C. 1987. The Longmu Co-Shuanghu-Lancangjiang Suture as the northern boundary of the Gandwanaland in the Carboniferous and Permian. *Bull. Changcun Coll. Geol. Sci.* 17:155–66 (in Chinese)

Li C, Liren C, Ke H, Zengrong Y, Yurong H. 1995. *Study on the Paleo-Tethys Suture Zone of Lungmu Co-Shuanghu, Tibet.* Beijing: Geological Publishing House. 131 pp. (in Chinese with English abstract)

Li C, Zheng A. 1993. Paleozoic stratigraphy in the Qiangtang region of Tibet: relations of the Gandwana and Yangtze continents and ocean closure near the end of the Carboniferous. *Int. Geol. Rev.* 35:797–804

Li CY, Liu Y, Zhu BC, Feng YM, Wu HC. 1978. Structural evolution of Qinling and Qilian Shan. In *Scientific Papers in Geology and International Exchange*, pp. 174–97. Beijing: Geologic Publishing House (in Chinese)

Li CY, Wang Q, Liu X, Tang Y. 1982. *Explanatory Notes to the Tectonic Map of Asia.* Beijing: Cartographic Publishing House

Li D, Liang D, Jia C, Wang G, Wu Q, He D. 1996. Hydrocarbon accumulations in the Tarim basin, China. *Am. Assoc. Pet. Geol. Bull.* 80:1587–603

Liou JG, Zhang RY, Wang X, Eide EA, Ernst WG, Maruyama S. 1996. Metamorphism and tectonics of high-pressure and ultrahigh pressure belts in the Dabie-Sulu region, China. In *The Tectonic Evolution of Asia*, ed. A Yin, TM Harrison, pp. 300–44. New York: Cambridge Univ. Press

Liu FT, Wa H, Liu J-H, Hu G, Li Q, Qu K. 1990. 3-D velocity images beneath the Chinese continent and adjacent regions. *Geophys. J. Int.* 101:379–94

Liu ZQ. 1988. *Geologic Map of the Qinghai-Xizang Plateau and its Neighboring Regions (scale at 1:1,500,000).* Chengdu Institute of Geology and Mineral Resources. Beijing: Geologic Publishing House

Luyendyk BP. 1989. Crustal rotation and fault slip in the continental transform zone in southern California. In *Paleomagnetic Rotations and Continental Deformation*, ed. C Kissel, C Laj, pp. 229–46. Dordrecht, Holland: Kluwer Acad.

Luyendyk BP, Kamerling MJ, Terres RR, Hornafius JS. 1985. Simple shear of southern California during Neogene time suggested by paleomagnetic declinations. *J. Geophys. Res.* 90:12454–66

Lyon-Caen H, Molnar P. 1984. Gravity anomalies and the structure of western Tibet and the southern Tarim Basin. *Geophys. Res. Lett.* 11:1251–54

Lyon-Caen H, Molnar P. 1985. Gravity anomalies, flexure of the Indian plate, and the structure, support and evolution of the Himalaya and the Ganga Basin. *Tectonics* 4:513–38

Makovsky Y, Klemperer SL. 1999. Measuring the seismic properties of Tibetan bright spots. Evidence for free aqueous fluids in the Tibetan middle crust. *J. Geophys. Res.* 104:10795–825

Makovsky Y, Klemperer SL, Huang L, Lu D, Project INDEPTH Team. 1996. Structural elements of the southern Tethyan Himalaya crust from wide-angle seismic data. *Tectonics* 15:997–1005

Manning CE, Kapp P, Yin A, Murphy M, Harrison TM, et al. 1998. Metamorphism and exhumation of Mesozoic melange in north-central Tibet. *EOS* 79:815

Masek JG, Isacks BL, Gubbels TL, Fielding EJ. 1994. Erosion and tectonics at the margins of continental plateaus. *J. Geophys. Res.* 99:13941–56

Mattauer M. 1986. Intracontinental subduction, crustal stacking wedge and crust-mantle decollement. In *Collision Tectonics*, ed. MP Coward, AC Ries. *Geol. Soc. Lond. Spec. Publ.* 19:37–50

Matte P, Mattauer M, Olivet JM, Griot DA. 1997. Continental subduction beneath Tibet and the Himalayan orogen: a review. *Terra Nova* 9:264–70

Matte P, Tapponnier P, Arnaud N, Bourjot L, Avouac JP, et al. 1996. Tectonics of Western Tibet, between the Tarim and the Indus. *Earth Planet. Sci. Lett.* 142:311–30

McCaffrey R, Nabelek J. 1998. Role of oblique convergence in the active deformation of the Himalayas and southern Tibet plateau. *Geology* 26:691–94

McNamara DE, Owens TJ, Silver PG, Wu FT. 1994. Shear wave anisotropy beneath the Tibetan Plateau. *J. Geophys. Res.* 99: 13655–65

McNamara DE, Owens TJ, Walter WR. 1995. Observations of the regional phase propagation in the Tibetan plateau. *J. Geophys. Res.* 100:22215–29

Meert JG, Van der Voo R. 1997. The assembly of Gondwana 800–550 Ma. *J. Geodyn.* 23:223–35

Mercier J-L, Armijo R, Tapponnier P, Carey-Gailhardis E, Han TL. 1987. Change from Tertiary compression to Quaternary extension in southern Tibet during the India-Asia collision. *Tectonics* 6:275–304

Meyer B, Tapponnier P, Bourjot L, Metivier F, Gaudemer Y, et al. 1998. Crustal thickening in Gansu-Qinghai, lithospheric mantle subduction, and oblique, strike-slip controlled growth of the Tibet plateau. *Geophys. J. Int.* 135:1–47

Meyer B, Tapponnier P, Gaudemer Y, Peltzer G, Guo S, Chen Z. 1996. Rates of left-lateral movement along the easternmost segment of the Altyn Tagh fault, east of 96ºE (China). *Geophys. J. Int.* 124:29–44

Molnar P. 1984. Structure and tectonics of the Himalaya: constraints and implications of geophysical data. *Annu. Rev. Earth Planet. Sci.* 12:489–518

Molnar P, Burchfiel BC, Zhao Z, Lian K, Wang S, Huang M. 1987. Geologic evolution of northern Tibet: results of an expedition to Ulugh Muztagh. *Science* 23:299–305

Molnar P, Chen W-P, Padovani E. 1983. Calculated temperatures in overthrust terrains and possible combinations of heat sources responsible for the Tertiary granites in the Greater Himalaya. *J. Geophys. Res.* 88:6415–29

Molnar P, England P, Martinod J. 1993. Mantle dynamics, the uplift of the Tibetan Plateau, and the Indian monsoon. *Rev. Geophys.* 31:357–96

Molnar P, Lyon-Caen H. 1989. Fault plane solutions of earthquakes and active tectonics of the northern and eastern parts of the Tibetan Plateau. *Geophys. J. Int.* 99:123–53

Molnar P, Tapponnier P. 1975. Cenozoic tectonics of Asia; effects of a continental collision. *Science* 189:419–26

Molnar P, Tapponnier P. 1978. Active tectonics of Tibet. *J. Geophys. Res.* 85:5361–75

Montel J-M. 1993. A model for monazite/melt

equilibrium and application to the generation of granitic magmas. *Chem. Geol.* 119:127–46

Murphy JB, Nance RD. 1991. Supercontinent model for the contrasting character of Late Proterozoic orogenic belts. *Geology* 19:469–72

Murphy MA, Harrison TM. 1999. The relationship between leucogranites and the South Tibetan detachment system, Rongbuk Valley, southern Tibet. *Geology* 27:831–34

Murphy MA, Yin A, Harrison TM, Durr SB, Chen Z, et al. 1997. Significant crustal shortening in south-central Tibet prior to the Indo-Asian collision. *Geology* 25:719–22

Murphy MA, Yin A, Kapp P, Harrison TM, Din L, Guo J. 1999. Southward propagation of the Karakoram fault system into southwest Tibet: timing and magnitude of slip. *Geology* (in review)

Najman Y, Clift P, Johnson MRW, Roberson AHF. 1993. Early stages of foreland basin evolution in the Lesser Himalaya, N. India. In *Himalayan Tectonics*, ed. PJ Treloar, MP Searle. *Geol. Soc. Spec. Publ.* 74:541–58

Najman YMR, Enkin RJ, Johnson MRW, Robertson AHF, Baker J. 1994. Paleomagnetic dating of the earliest continental Himalayan foredeep sediments: implications for Himalayan evolution. *Earth Planet. Sci. Lett.* 128:713–18

Nakata T. 1989. Active faults of the Himalaya in India and Nepal. In *Tectonics of the Western Himalaya*, ed. LL Malinconico, RJ Lillie. *Geol. Soc. Am. Spec. Pap.* 232:243–64

Nelson KD and 27 others. 1996. Partially molten middle crust beneath Southern Tibet: synthesis of Project INDEPTH results. *Science* 274:1684–96

Ni J, Barazangi M. 1984. Seismotectonics of the Himalayan collision zone: geometry of the underthrusting Indian plate beneath the Himalaya. *J. Geophys. Res.* 89:1147–63

Ni J, York J. 1978. Late Cenozoic tectonics of the Tibetan plateau. *J. Geophys. Res.* 83:5377–84

Nie S, Yin A, Rowley D, Jin Y. 1994. Exhumation of the Dabie shan ultra-high pressure rocks and accumulation of the Songpan-Ganzi flysch sequence, central China. *Geology* 22:999–1002

Noble SR, Searle MP. 1995. Age of crustal melting and leucogranite formation from U-Pb zircon and monazite dating in the western Himalaya, Zanskar, India. *Geology* 23:1135–38

Owens TJ, Zandt G. 1997. Implications of crustal property variations for models of Tibetan plateau evolution. *Nature* 387:37–43

Pan Y. 1990. Tectonic features and evolution of the western Kunlun Mountain region. *Sci. Geol. Sin.* 3:224–32 (in Chinese with English abstract)

Pan Y. 1993. Unroofing history and structural evolution of the southern Lhasa terrane, Tibetan Plateau: implications for the continental collision between India and Asia. Ph.D. dissertation. State Univ. New York, Albany

Pan Y. 1996. Regional geologic evolution and conclusion. In *Geologic Evolution of the Karakorum and Kunlun Mountains*, ed. P Yunsheng, pp. 263–88. Beijing: Seismological Press

Parrish RR, Hodges KV. 1993. Miocene (22 ± 1 Ma) metamorphism and two stage thrusting in the Greater Himalayan sequence, Annapurna Sanctuary, Nepal. *Geol. Soc. Am. Abstr. Progr.* 25:A174

Parrish RR, Hodges KV. 1996. Isotopic constraints on the age and provenance of the Lesser and Greater Himalayan sequences, Nepalese Himalaya. *Bull. Geol. Soc. Am.* 108:904–11

Patriat P, Achache J. 1984. India-Eurasia collision chronology has implications for crustal shortening and driving mechanism of plates. *Nature* 311:615–21

Pêcher A. 1989. Metamorphism in the central Himalaya. *J. Metamorph. Petrol.* 7:31–41

Peltzer G, Saucier F. 1996. Present day kinematics of Asia derived from geologic fault rates. *J. Geophys. Res.* 101:27943–56

Peltzer G, Tapponnier P. 1988. Formation and evolution of strike-slip faults, rifts, and basins during the India-Asia collision: an experimental approach. *J. Geophys. Res.* 93:15085–117

Peltzer G, Tapponnier P, Amijio R. 1989. Magnitude of late Quaternary left-lateral displacement along the north edge of Tibet. *Science* 246:1285–89

Pierce JA, Deng W. 1988. The ophiolites of the Tibetan geotraverse, Lhasa-Golmud (1985) and Lhasa to Kathmandu (1986). *Phil. Trans. R. Soc. Lond.* A327:215–38

Pierce JA, Mei H. 1988. Volcanic rocks of the 1985 Tibet Geotraverse Lhasa to Golmud. *Phil. Trans. R. Soc. Lond.* A327:203–13

Pinet C, Jaupart C. 1987. A thermal model for the distribution in space and time of the Himalayan granites. *Earth Planet. Sci. Lett.* 84:87–99

Powell CM, Conaghan PG. 1973. Plate tectonics and the Himalayas. *Earth Planet. Sci. Lett.* 20:1–12

Powell RE. 1993. Balanced palinspastic reconstruction of pre-Late Cenozoic paleogeology, southern Californa: geologic and kinematic constraints on evolution of the San Andreas fault system. In *The San Andreas Fault System: Displacement, Palinspastic Reconstruction, and Geologic Evolution*, ed. RE Powell, RJ Weldon II, JC Matti. *Geol. Soc. Am. Mem.* 178:1–106

Price RA. 1981. The Cordilleran foreland thrust and fold belt in the southern Canadian Rocky Mountains. In *Thrust and Nappe Tectonics*, ed. MP Coward, KR McClay. *Geol. Soc. Lond. Spec. Publ.* 9:427–48

Qinghai BGMR (Qinghai Bureau of Geology and Mineral Resources). 1991. *Regional Geology of Qinghai Province.* Beijing: Geological Publishing House. 662 pp.

Quade J, Cater JLM, Ojha TP, Adam J, Harrison TM. 1995. Late Miocene environmental change in Nepal and the northern Indian subcontinent: stable isotope evidence from paleosols. *Geol. Soc. Am. Bull.* 107:1381–97

Quidelleur X, Grove M, Lovera OM, Harrison TM, Yin A, Ryerson FJ. 1997. The thermal evolution and slip history of the Renbu Zedong Thrust, southeastern Tibet. *J. Geophys. Res.* 102:2659–79

Ramstein G, Fluteau FF, Besse J, Joussaume S. 1997. Effect of orogeny, plate motion, and land-sea distribution on Eurasian climate change over the past 30 million years. *Nature* 286:788–95

Rao R, Xu J, Chen Y, Zou D. 1987. *The Triassic System of the Qianghai-Xizang Plateau.* Beijing: Geological Publishing House. 239 pp.

Ratschbacher L, Frisch W, Chen C, Pan G. 1996. Cenozoic deformation, rotation, and stress patterns in eastern Tibet and western Sichuan, China. In *The Tectonic Evolution of Asia*, ed. A Yin, TM Harrison, pp. 227–49. New York: Cambridge Univ. Press

Ratschbacher L, Frisch W, Lui G, Chen C. 1994. Distributed deformation in southern and western Tibet during and after the India-Asia collision. *J. Geophys. Res.* 99:19817–945

Rowley DB. 1996. Age of collision between India and Asia: a review of the stratigraphic data. *Earth Planet. Sci. Lett.* 145:1–13

Rowley DB. 1998. Minimum age of initiation of collision between India and Asia north of Everest based on the subsidence history of the Zhepure Mountain section. *J. Geol.* 106:229–35

Richter FM, Lovera OM, Harrison TM, Copeland P. 1991. Tibetan tectonics from a single feldspar sample: an application of the $^{40}Ar/^{39}Ar$ method. *Earth Planet. Sci. Lett.* 105:266–76

Rothery DA, Drury SA. 1984. The neotectonics of the Tibetan Plateau. *Tectonics* 3:19–26

Royden L. 1996. Coupling and decoupling of crust and mantle in convergent orogens: implications for strain partitioning in the crust. *J. Geophys. Res.* 101:17679–705

Royden LH. 1993. The steady state thermal structure of eroding orogenic belts and accretionary prisms. *J. Geophys. Res.* 98:4487–507

Royden LH, Burchfiel BC, King RW, Wang E, Chen Z, et al. 1997. Surface deformation and lower crustal flow in eastern Tibet. *Science* 276:788–90

Ruddiman WF, Kutzbach JE. 1989. Forcing of Late Cenozoic northern hemisphere climate by plateau uplift in southern Asia and the American west. *J. Geophys. Res.* 94: 18409–27

Rumelhart P, Yin A, Butler R, Cowgill E, Zhang Q, Wang X. 1999. Cenozoic vertical-axis rotation of southern Tarim: constraints on the tectonic evolution of the Altyn Tagh fault system. *Geology* 27:819–22

Rumelhart PA. 1998. *Cenozoic basin evolution of southern Tarim, northwestern China: implications for the uplift history of the Tibetan Plateau.* Ph.D thesis. Univ. Calif., Los Angeles

Rupple C, Kogan MG, McNutt MK. 1993. Implications of new gravity data for Baikal rift zone structure. *Geophys. Res. Lett.* 20:1635–38

Ryerson FJ, Peltzer G, Tapponnier P, Finkel RC, Meriaux A, Caffee MW. 1999. Slip-rates on the Karakax valley segment of the Altyn Tagh fault: constraints from surface dating. In *14th Himalaya-Karakorum-Tibet Workshop*, Abstract volume, pp. 185–86. Germany: Kloster Ettal

Sandvol E, Ni J, Kind R, Zhao W. 1997. Seismic anistropy beneath the southern Himalayas-Tibet collision zone. *J. Geophys. Res.* 102:17813–23

Schärer U, Xu RH, Allègre CJ. 1984. U-Pb geochronology of the Gangdese (Transhimalaya) plutonism in the Lhasa-Xigaze region, Tibet. *Earth Planet. Sci. Lett.* 69:311–20

Schärer U, Xu RH, Allègre CJ. 1986. U-(Th)-Pb systematics and ages of Himalayan leucogranites, South Tibet. *Earth Planet. Sci. Lett.* 77:35–48

Schelling D. 1992. The tectonostratigraphy and structure of the eastern Nepal Himalaya. *Tectonics* 11925–43

Schelling D, Arita K. 1991. Thrust tectonics, crustal shortening, and the structure of the far-eastern Nepal, Himalaya. *Tectonics* 10:851–62

Searle MP. 1991. *Geology and Tectonics of the Karakoram Mountains.* New York: Wiley. 358 pp.

Searle MP. 1996. Cooling history, erosion, exhumation, and kinematics of the Himalaya-Karakoram-Tibet orogenic belt. In *The Tectonic Evolution of Asia*, ed. A Yin, TM Harrison, pp. 110–37. New York: Cambridge Univ. Press

Searle MP, Cooper DJW, Rex AJ. 1988. Collision tectonics of the Ladakh-Zanskar Himalaya. *Phil. Trans. R. Soc. Lond.* A326:117–50

Searle MP, Parrish RR, Hodges KV, Hurford A, Ayres MW, Whitehouse MJ. 1997. Shisha Pangma leucogranite, south Tibetan Himalaya: field relations, geochemistry, age, origin, and emplacement. *J. Geol.* 105:295–317

Searle MP, Weinberg RF, Dunlap WJ. 1998. Transpressional tectonics along the Karakoram fault zone, northern Ladakh: constraints on Tibetan extrusion. In *Continental Transpressional and Transtensional Tectonics*, ed. RE Holdsworth, RA Strachan, JF Dewey. *Geol. Soc. Lond. Spec. Publ.* 135:307–26

Sengor AMC. 1984. The Cimmeride orogenic system and the tectonics of Eurasia. *Geol. Soc. Am. Spec. Pap.* 195:1–82

Sengor AMC. 1990. Plate tectonics and orogenic research after 25 years: a Tethyan perspective. *Earth Sci. Rev.* 27:1–201

Sengor AMC, Natal'in BA. 1996. Paleotectonics of Asia: fragments of a synthesis. In *The Tectonics of Asia*, ed. A Yin, TM Harrison, pp. 486–640. New York: Cambridge Univ. Press

Sengor AMC, Okurogullari AH. 1991. The role of accretionary wedge in the growth of continents: Asiatic examples from Argand to plate tectonics. *Ecol. Geol. Helv.* 84:535–97

Shen Z, Zhao C, Yin A, Li C, Jackson DD, et al. 1999. Contemporary crustal deformation in east Asia constrained by Global Posi-

tioning Measurements. *J. Geophys. Res.* In press

Shi X, Yin J, Jia C. 1996. Mesozoic to Cenozoic sequence stratigraphy and sea-level changes in the Northern Himalayas, southern Tibet, China. *Newsl. Stratigr.* 33:15–61

Silver PG. 1996. Seismic anisotropy beneath the continents: probing the depths of geology. *Annu. Rev. Earth Planet. Sci.* 24:385–432

Smith AB, Xu J. 1988. Palaeontology of the 1985 Tibet Geotraverse, Lhasa to Golmud. *Phil Trans. R. Soc. Lond.* A327:53–105

Song T, Wang X. 1993. Structural styles and stratigraphic patterns of syndepositional faults in a contractional setting: example from Quaidam basin, northwestern China. *Am. Assoc. Pet. Geol. Bull.* 77:102–17

Srivastava P, Mitra G. 1994. Thrust geometries and deep structure of the outer and lesser Himalaya, Kumaon and Garwal (India): implications for evolution of the Himalayan fold-and-thrust belt. *Tectonics* 13:89–109

Strecker MR, Frisch W, Hamburger MW, Ratschbacher L, Semiletkin S, et al. 1995. Quaternary deformation in the eastern Pamirs, Tadzhikistan and Kyrgyzstan, *Tectonics* 14:1061–79

Sullivan MA, Windley BF, Saunders AD, Haynes JR, Rex DC. 1993. A palaeogeographic reconstruction of the Dir Group: evidence for magmatic arc migration within Kohistan, N. Pakistan. In *Himalayan Tectonics*, ed. PJ Treloar, MP Searle. *Geol. Soc. Spec. Publ.* 74:139–60

Sylvester AG. 1988. Strike-slip fault. *Geol. Soc. Am. Bull.* 100:1666–703

Tapponnier P, Lacassin R, Leloup PH, Schärer U, Zhong D, et al. 1990. The Ailao Shan/Red River metamorphic belt: Tertiary left-lateral shear between Indochina and South China. *Nature* 343:431–37

Tapponnier P, Mercier JL, Armijo R, Han T, Zhao TJ. 1981. Field evidence for active normal faulting in Tibet. *Nature* 294:410–14

Tapponnier P, Molnar PJ. 1976. Slip-line field theory and large-scale continental tectonics. *Nature* 264:319–24

Tapponnier P, Molnar PJ. 1977. Active faulting and tectonics of China. *J. Geophys. Res.* 82:2905–30

Tapponnier P, Molnar P. 1979. Active faulting and Cenozoic tectonics of Tien Shan, Mongolia, and Baikal regions. *J. Geophys. Res.* 84:3425–59

Tapponnier P, Peltzer G, Armijo R. 1986. On the mechanics of the collision between India and Asia. In *Collision Tectonics*, ed. MP Coward, AC Ries. *Geol. Soc. Lond. Spec. Publ.* 19:115–57

Tapponnier P, Peltzer G, Le Dain AY, Armijo R, Cobbold P. 1982. Propagating extrusion tectonics in Asia: new insights from simple experiments with plasticine. *Geology* 10:611–16

Tonarini S, Villa I, Oberli F, Meier M, Spencer DA, et al. 1993. Eocene age of eclogite metamorphism in Pakistan Himalaya: implications for India-Eurasia collision. *Terra Nova* 5:13–20

Turner S, Arnaud N, Liu J, Rogers N, Hawkesworth CJ, et al. 1996. Post-collision, shoeshonitic volcanism on the Tibetan plateau: implications for convective thinning of the lithosphere and the source of ocean island basalts. *J. Petrol.* 37:45–71

Turner S, Hawkesworth CJ, Liu J, Rogers N, Kelley S, van Calsteren P. 1993. Timing of Tibetan uplift constrained by analysis of volcanic rocks. *Nature* 364:50–53

Vance D, Harris N. 1999. The timing of prograde metamorphism in the Zanskar Himalaya. *Geology* 27:395–98

van der Beek P. 1997. Flank uplift and topography at the central Baikal Rift (SE Siberia): a test of kinematic models for continental extension. *Tectonics* 16:122–36

Van der Woerd J, Ryerson FJ, Tapponnier P, Gaudemer Y, Finkel R, et al. 1998. Holocene left-slip rate determined by cosmogenic surface dating on the Xidatan segment of the Kunlun fault (Qinghai, China). *Geology* 26:695–98

Wang C, Hu C, Wu R. 1987. Discovery and geologic significance of the Casang-Cabu rift in northern Xizang. *Bull. Chengdu Coll. Geol. Sci.* 14:33–46

Wang E. 1997. Displacement and timing along the northern strand of the Altyn Tagh fault zone, northern Tibet. *Earth Planet. Sci. Lett.* 150:55–64

Wang E, Burchfiel BC. 1997. Interpretation of Cenozoic tectonics in the right-lateral accommodation zone between the Ailao Shan shear zone and the eastern Himalayan syntaxis. *Int. Geol. Rev.* 39:191–219

Wang E, Burchfiel BC, Royden LH, Chen Z, Chen J, et al. 1998. Late Cenozoic Xiangshuihe-Xiaojiang, Red River, and Dali fault systems of southwestern Sichuan and central Yunnan, China. *Geol. Soc. Am. Spec. Pap.* 327:1–108

Wang N, Yang J, Xia Z, Me D, Li Y, Pan M. 1996. *Cenozoic Sedimentation and Tectonic Geomorphology of the Shanxi Graben.* Beijing: Chinese Science Publishing House. 400 pp.

Wang S, Li Z, Qiangba X. 1983. Unpublished geologic map (1:1,000,000) and geologic report of the Xigaze area, Xizang Bureau of Geology and Mineral Resources, 568 pp.

Wang T. 1996. Characteristics of sedimentary rocks and their environmental evolution. In *Geological Evolution of the Karakorum and Kunlun Mountains,* ed. P Yusheng, pp. 22–50. Beijing: Seismological Press

Willems H, Zhou Z, Zhang B, Grafe K-U. 1996. Stratigraphy of the Upper Cretaceous and Lower Tertiary strata in the Tethyan Himalayas of Tibet (Tingri area, China). *Geol. Rundsch.* 85:723–54

Willett SD, Beaumont C. 1994. Subduction of Asian lithospheric mantle beneath Tibet inferred from models of continental collision. *Nature* 369:642–45

Wittlinger G, Tapponnier P, Poupinet G, Jiang M, Shi D, et al. 1998. Tomographic evidence for localized lithospheric shear along the Altyn Tagh fault. *Science* 282:74–76

Worley B, Powell R, Wilson CJL. 1997. Crenulation cleavage formation: evolving diffusion, deformation and equilibration mechanisms with increasing metamorphic grade. *J. Struct. Geol.* 19:1121–35

Worley BA, Wilson CJL. 1996. Deformation partitioning and foliation reactivation during transpressional orogenesis, an example from the Central Longmen Shan, China. *J. Struct. Geol.* 18:395–411

Wu C, Nelson KD, Wortman G, Samson S, Yue Y, et al. 1998. Yadong cross structure and South Tibetan detachment in the east central Himalaya (89°–90°E). *Tectonics* 17:28–45

Xia L, Xia Z, Xu X. 1996. *Origin of the Oceanic Island Arc System in the Northern Qilian Shan.* Beijing: Geological Publishing House. 153 pp.

Xiao X, Chen G, Zhu Z. 1978. Geological and tectonic significance of paleo-ophiolite zone of the Qilian Mountains. *Acta Geol. Sin.* 52:281–95

Xie G, Liu C, Zheng T. 1992. Geochemical characteristics of Cenozoic volcanic rocks along the rim of the Tibetan plateau—evidence for ancient enriched mantle. In *Mesozoic and Cenozoic Volcanic Rocks and Their Geochemical Characteristics,* ed. Liu Rouxing, pp. 100–27. Beijing: Seismological Press

Xinjiang BGMR (Xinjiang Bureau of Geology and Mineral Resources). 1989. *Regional Geology of the Xinjiang Uygur Autonomous Region.* Beijing: Geological Publishing House

Xizang BGMR (Xizang Bureau of Geology and Mineral Resources). 1992. *Regional Geology of the Xizang Autonomous Region.* Beijing: Geological Publishing House

Xu R, Zhang Y, Xie Y, Vidal Ph, Arnaud N, et al. 1996. Isotopic geochemistry of plutonic rocks. In *Geological Evolution of the Karakorum and Kunlun Mountains,* ed. P Yusheng, pp. 137–86. Beijing: Seismological Press

Xu RH. 1990. Age and geochemistry of granites and metamorphic rocks in south-central Xizang (Tibet). In *Igneous and Metamorphic Rocks of the Tibetan Plateau,* ed. Chinese Academy of Geological Sciences, pp. 287–302. Beijing: Science Press

Xu RH, Schärer U, Allègre CJ. 1985. Magmatism and metamorphism in the Lhasa

block (Tibet): a geochronological study. *J. Geol.* 93:41–57

Xu Z, Mei J, Yang J, Zhao G, Cui J, et al. 1998. Mantle diapir and inward intracontinental subduction: a discussion on the mechanism of uplift of the Qinghai-Tibet Plateau. In *Himalaya and Tibet: Mountain Roots to Mountain Tops*, ed. A Macfarlane, RB Sorkhabi, J Quade. *Geol. Soc. Am. Spec. Pap.* 328:19–31

Yin A. 1999. Mode of Cenozoic east-west extension in Tibet suggests a common origin of rifts in Asia during the Indo-Asian collision. *J. Geophys. Res.* In review

Yin A, Harrison TM, Murphy MA, Grove M, Nie S, et al. 1999a. Tertiary deformation history of southeastern and southwestern Tibet during the Indo-Asian collision. *Geol. Soc. Am. Bull.* 111:1644–64

Yin A, Harrison TM, Ryerson FJ, Chen W, Kidd WSF, Copeland P. 1994. Tertiary structural evolution of the Gangdese thrust system, southeastern Tibet. *J. Geophys. Res.* 99:18175–201

Yin A, Kapp P, Manning CE, Harrison TM, Din L, Deng X. 1998a. Extensive exposure of Mesozoic melange in Qiangtang and its role in the Cenozoic development of the Tibetan plateau. *Eos* 79:816

Yin A, Kapp PA, Murphy MA, Manning CE, Harrison TM, et al. 1999c. Evidence for significant Late Cenozoic E-W extension in North Tibet. *Geology* 17:787–90

Yin A, Kapp PA, Murphy M, Manning C, Harrison TM. 1998b. Evidence for large scale underthrusting (>250 km) of Lhasa beneath Qiangtang during the Indo-Asian collision: implications for the deep-crustal structures in Tibet and uplift mechanisms. *Geol. Soc. Am. Abstr. Progr.* 30:A353

Yin A, Kong X. 1997. Spacing of N-S rifts in Tibet implies lithospheric extension. *Eos* 78:F173

Yin A, Murphy MA, Harrison TM, Ryerson FJ, Chen Z, et al. 1996. Miocene evolution of the Kailas thrust and Gurla Mandhata detachment fault, western Tibet: implications for the displacement history of the Karakorum fault. In *11th Himalaya-Karakorum-Tibet Workshop*, Abstract volume, Flagstaff, Arizona, pp. 173–74

Yin A, Nie S. 1993. An indentation model for North and South China collision and the development of the Tanlu and Honam fault systems, eastern Asia. *Tectonics* 12:801–13

Yin A, Nie S. 1996. A Phanerozoic palinspastic reconstruction of China and its neighboring regions. In *The Tectonics of Asia*, ed. A Yin, TM Harrison, pp. 442–85. New York: Cambridge Univ. Press

Yin A, Wang X, Harrison TM, Cowgill E, Rumelhart P, et al. 1999b. Preliminary results from a collaborative geologic investigation of the Altyn Tagh Fault, North Tibet. In *14th Himalaya-Karakorum-Tibet Workshop*, Abstract volume, pp. 185–86. Germany: Kloster Ettal

Yin J. 1997. *Stratigraphic Geology of Gandwanan Facies of Qinghai-Xiang (Tibet) Plateau and Adjacent Areas.* Beijing: Geologic Publishing House. 206 pp.

Yin J, Bian Q. 1992. *Geologic Map of the Karakorum-Western Kunlun and Adjacent Regions (1:2M).* Beijing: Science Press

Yin J, Xu J, Liu C, Li H. 1988. The Tibetan plateau: regional stratigraphic context and previous work. *Phil. Trans. R. Soc. Lond.* A327:5–52

Yu Z, Zheng A-Z. 1979. *Unpublished geologic map of the Lhasa region at a scale of 1:1,000,000 and geologic report*, Xizang Bureau of Geology and Mineral Resources, p. 284 (in Chinese)

Yuan X, Ni J, Kind R, Mechie, J, Sandvol E. 1997. Lithospheric and upper mantle structure of southern Tibet from a seismological passive source experiment. *J. Geophys. Res.* 102:27491–500

Zhang G, Li J. 1998. Triassic flysch trace fossils and their geological significance from east Karakorum mountains, China. *Sci. Geol. Sin.* 33:257–66

Zhang J, Xu Z, Xu H, Li H. 1998. Framework of North Qilian Caledonian subduction-

accretionary wedge and its deformation dynamics. *Sci. Geol. Sin.* 33:290–99

Zhang M, Hu C, Wu R. 1985. Geochemical characteristics and tectonic setting of the Xiangqiong-Casang mafic volcanic belt. In *Geologic Research on the Qinghai-Xizang Plateau Publication no. 9*, pp. 57–68. Beijing: Geological Publishing House

Zhang Y, Zheng J. 1994. *Geologic Overview in Kokshili, Qinghai and Adjacent Areas.* Beijing: Seismological Publishing House. 177 pp.

Zhang YQ, Mercier JL, Vergely P. 1998. Extension in the graben system around the Ordos (China), and its contribution to the extrusion tectonics of south China with respect to Gobi-Mongolia. *Tectonophys.* 285:41–75

Zhao W, Morgan WJ. 1987. Injection of Indian crust into Tibetan lower crust: a two-dimensional finite element model study. *Tectonics* 6:489–504

Zhao W, Nelson KD, Project INDEPTH. 1993. Deep seismic reflection evidence for continental underthrusting beneath southern Tibet. *Nature* 366:557–59

Zhong D. 1998. *Paleotethyan Orogenic Belts in Yunan and Western Sichuan.* Beijing: Science Publishing House. 230 pp.

Zhou D, Graham SA. 1993. Songpan-Ganzi Triassic flysch complex as a remnant-ocean-basin along diachronous collision orogen, central China. *Geol. Soc. Am. Abstr. with Programs* 25:A118

Zhou D, Graham SA. 1996. The Songpan-Ganzi complex of the western Qinling Shan as a Triassic remnant ocean basin. In *The Tectonic Evolution of Asia*, ed. A Yin, TM Harrison. pp. 281–99. Cambridge, UK: Cambridge Univ. Press

Annual Review of Earth and Planetary Science
Volume 28, 2000

CONTENTS